Instrument Design in UV Polarised Spectroscopy

Daniel Waldron

Submitted in partial fulfilment of the requirements for the degree of Doctor of Philosophy

Chemistry Department, University of Warwick

July, 2011

Contents (Outline)

Contents (Detailed)

List of figures

Figure 1.9: Difference in electron redistribution upon excitation between a chiral and non- chiral system. Electron movement in a chiral system will always be of a helical nature, whilst in an achiral system movement is always planar. Image taken from 'Circular Dichroism and Linear Dichroism'[13]. Figure used with permission.

Figure 1.10: CD spectra of the major secondary structure types. Solid line, α-helix; long dashed line, anti-parallel β-sheet; dotted line, type I β-turn; cross dashed line, poly proline II helix; short dashed line irregular structure. It is important to note that whilst termed 'random coil', is used the structure of such molecules is still highly ordered, hence the generation of a reproducible CD spectrum. Figure taken from the paper 'How to study Proteins by Circular Dichroism' by Kelly *et al*.

Figure 1.11: Diagram of the optical bench within a J-800 series CD spectrophotometer. Light of all wavelengths is generated from the xenon lamp, before being manoeuvred through two monochromators (the 1st being between S1 & S2, the 2nd between S2 & S3). These two monochromators (more commonly referred to as a double monochromator) is very effective at reducing stray light within an optical system. The prisms within each monochromator, in addition to selecting a wavelength of light are also axially orientated, generating linearly polarised light that is easier to modulate. All reflection within the system is achieved using aluminium mirrors. Figure from Model J-800 CD spectrometer Hardware/Function manual (2006) by Jasco. Figure used with permission of Jasco UK.

Figure 1.12: Experimental set-up for linear and circular dichroism (image taken from Hinds Instruments application note on photoelastic modulators, by T.C. Oakberg (an excellent source, free download of the application note at http://www.hindsinstruments.com/wp-content/uploads/LinearCircular_Dichroism.pdf).

Figure 1.13: Top-down view of the microvolume Couette LD cell. To the left of the image you can see the quartz rod insert that is placed inside the capillary of the LD cell proper. Note the rod that can be placed with the capillary to create the required angular gap. It is in the gap

between the rod and capillary that the sample is contained within. Image taken from www.kromatek.co.uk.

Figure 2.1: The focusing lens of the caCDRM instrument. Note that the lens is positioned precisely in the centre of the capillary.

Figure 2.2: caCDRM image showing the slide-way of the instrument. The base-plate features a groove, where various optical components can slot into.

Figure 2.3: Na [Co (Edds)].H_2O at 0.55 mM spectra acquired through both cuvette CD and caCD. The caCD spectra were acquired using the Marrington design of caCD base plate. The path-length of the capillary was 1.12 mm, determined through analysis with potassium dichromate. Capillary spectra scaled using a 0.892 correction factor to allow for differences in path-length. The path-length of the cuvette was 1 mm, verified via analysis with potassium dichromate.

Figure 2.4: 'Many faces of light: As Newton Saw it, With Some Magic Tricks' lecture given by Prof. U. Mallik 14/02/05.

Figure 2.5: Capillary Optics. Blue lines represent light that passes through the internal diameter of the capillary. Pink lines represent light that interacts with the internal bore of the capillary but is still optically net divergent. Yellow lines represent light that does not interact at all with the internal bore of the capillary, creating a high degree of divergence. Image used with permission of Paraytec Ltd.

Figure 2.6: Graph showing the relationship between slit-width and wavelength for a J-800 series spectrophotometer (data plotted from Jasco technical notes for the J800 series spectrophotometer).

Figure 2.7: The alignment caCD cell, including lens holder. The design for this cell was simple and very cost effective. However, difficulties with data reproducibility marred the cell design.

Figure 2.8: Diagram showing the effect on the light beam as it interacts with the capillary.

Figure 2.9: Na [Co (Edds)].H_2O 0.55 mM spectra acquired through both cuvette CD and caCD. The caCD spectra were acquired using the alignment cell design of caCD base plate. The path-length of the capillary was 1.12 mm, determined via analysis with potassium dichromate. Spectra

Figure 3.5: The etching rig female component, before (left) and after (right) the etching process. It should be highlighted that after etching, two of the heads of the screws had been so undermined by acid attack that they disintegrated upon removal from the HF solution.

Figure 3.6: (a) Bottom face, (b) top face and (c) side view of the etching rig machined on a lathe in black nylon. The recess in the centre of the bottom was been machined to create a push-fit for a 1 inch diameter cylindrical quartz flats.

Figure 3.7: Interference pattern of an etched flat. Note the band pattern on both sides of the channel, where optical flatness has been retained.

Figure 3.8: WYKO image of a 6.5 μm etched flat channel / plain surface. The surface finish of both the etched and non-etched components is of exceptional quality, in terms of surface roughness and sharpness of interface. There is very little evidence of undercutting or smoothing at the interface, proving the efficacy of the acid mask.

Figure 3.9: Assembled etched cuvette inside the sample cell holder. The interference pattern of the two flats can be clearly seen, identifying the surfaces of the two pieces of quartz as being optically flat.

Figure 3.10: UV / Visible spectrum absorbance spectrum of the etched cell. The spectrum was acquired under the following conditions: Bandwidth 1 nm, data pitch 0.2 nm, scan speed 100 nm/min.

Figure 3.11: UV/Vis K_2CrO_4 path-length determination. A 0.2 M solution was used to test the micron path-length cuvettes, whilst a 0.002 M solution was used for the 1 mm path-length cuvette. Parameters for the UV/Vis analysis were: bandwidth 1 nm, data pitch 0.5 nm, speed 100 nm/min.

Figure 3.12: Etched cuvette holder assembly side view schematic. An aperture has been machined through the centre to allow light into the cuvette. The diameter of the aperture running through the middle of the holder is 12 mm.

Figure 5.1: LD spectra of Bacillus Subtilis in Luria Broth. Final LD signal is shown in blue. Figure taken from the thesis of Dr. Adair Richards 'Taking the fight to the Superbugs: Interactions of Synthetic DNA-binding Metallomolecules with Biological Systems'. Figure used with permission.

Figure 5.2: LD spectrum of *B. Subtilis* at an A280 concentration of 1.5 OD (baseline subtracted). The phosphate buffer baseline is included here to facilitate comparison. The bacteria were buffered in pH 7, 0.1 M phosphate solution. Orientation of the sample was achieved using a Couette LD cell under standard conditions.

Figure 5.3: E.M. image of *B.Subtilis*. The sample was taken from a solution of LB media, rather than agar to properly reflect the number of flagella present per bacterium as measured by other methods. The large black object towards the bottom left of the image is a *B.Subtilis* bacterium, whilst its flagella can be most clearly seen centre left and centre right, protruding from the rear of the bacterium

Figure 5.4: E.M. image of cell extract post homogenisation. The sample was taken from the suspension of the homogenised solution after centrifugation. This fraction contains cell debris, as well as individual flagella (the long thin objects within the image, the best example being in the top right hand corner of the E.M. image).

Figure 5.5: E.M. image of purified flagella, taken from a re-suspension of the pellet produced via ultra-centrifugation.

Figure 5.6: LD spectrum of 0.25 OD Flagella.

Figure 5.7: LD spectrum of *B. Subtilis* under different flow conditions. All B. Subtilis spectra were acquired at an Å280 concentration of 1.5 OD The LD spectra of A 0.25 OD couette aligned purified flagella and the original Couette LD B. Subtilis have been added to the figure for comparison.

Figure 5.8: LD as a function of time for 0.5OD flagella (as calculated by A280). Under constant laminar flow, the LD signal increases over time. The LD spectra were acquired in a standard 3 mm O.D. extruded quartz capillary with a 1.1 mm quartz rod.

List of tables

Acknowledgements

This project has been completed over several years thanks to the help and support of many individuals, some of which are listed below. Warwick has been a good home to me for the last few years, but an institution is not just a geographical position but rather a gathering of people, all of which work on the common goal of making the world around them a better place. I consider myself privileged to have worked in such a rich environment and with such talented individuals.

I would first like to thank my supervisors Alison Rodger and Timothy Dafforn, who have provided me with scientific expertise, guidance and advice as and when I required it. I would also like to thank my industrial supervisors, Rhoderick Mortimore (Crystal Precision Optics) and Richard Taylor (Jasco UK) for their support throughout my project. I would also like to thank Matt Hicks, for his excellent advice and practical expertise that helped boost the entire project.

I would particularly like to thank William Mortimore of Dioptica Ltd (Engineering and Machining) and Charles Penn (Electron Microscopy). Both people gave freely of their time and expertise, for which I am very grateful. I would also like to thank Emma Gilroy (Light Scattering), Angeliki Damianoglou (CD), Rosemary Parslow (Molecular Biology) and Andy Beavers (HPLC) for their aid.

Special thanks go to Paul Taylor (advisory committee) and Ross Hatton (advisory committee) for their assistance throughout this project. Additionally I would like to take this opportunity to thank Gemma Warren and Isobel McKenzie for their invaluable comments on the different version of this manuscript.

I would also like to thank everyone in the Rodger group and at MOAC, in particular Richard Snowdon, Patrycja Kowalska, Jarek Kowalski, Xi Cheng and Nigel Dyer. I am also grateful to the EPSRC for their funding of this project.

Finally, I would like to express my deepest thanks to my mother, my father and my brother Ben. All of you have been fantastic throughout this process. Lastly, I want to thank Laura, my wonderful wife who has continued to support and believe in me.

Dedication

To my parents, for being the finest teachers I have ever had.

Thank you.

Declaration

The work presented in this thesis is original (except where otherwise stated). No portion of the work submitted in this thesis has been submitted in support of an application for another degree or qualification at this or any other University or institute of learning.

Abstract

Biological macromolecules are becoming increasingly important as a target for pharmaceutical research. Structural examination of this class of compounds is vital, both in terms of understanding the three-dimensional structures these molecules form as well as for quality control of bio-pharmaceutical products. UV polarised spectroscopy, such as circular dichroism (CD) is a powerful tool for this form of analysis, rapidly providing the user with structural information on the sample. The ease of data analysis combined with its non-destructive nature make UV polarised spectroscopy an ideal tool for this purpose. However, limitations in the current instrumentation, especially in terms of sample handling have placed significant barriers in the way of fully realising the potential of these techniques.

To address the weaknesses of the currently available UV polarised spectroscopy accessories, new devices have been designed and tested to increase the utility of such techniques. A low volume capillary sample holder has been developed which significantly reduces the sample requirements for circular dichroism without loss of signal quality. This advance has been coupled with an HPLC auto-sampler to create a device that can process 96-well and in some cases 384-well plates. This device opens up a host of new applications for polarised UV spectroscopy, including refolding screening as well as freeing up user time.

Additionally, a high precision demountable micro scale cuvette has been developed that reproducibly assembles to the same path length every time. The percentage error of path-length for this new cuvette is of the same order as currently commercially available 1 mm cuvettes. This new accessory should prove highly advantageous for the bio-pharmaceutical industry, as it allows accurate path-length CD analysis for high concentration samples.

Additionally, the first confirmed linear dichroism (LD) spectrum of a bacterium and flagella are reported, opening up the potential for real time UV spectroscopic analysis of living bacteria.

By using the work contained within this thesis, it should be possible to construct a new form of high path-length accuracy, low volume, multiple-sample UV polarised spectroscopy accessory that could be used for both CD and LD analysis.

Abbreviations

A	Adenine
A	Absorbance
α	Alpha
Å	Angstrom
ACS	Ammonium camphorsulphonate
ABTS	2,2'-azino-bis(3-ethylbenzothiazoline-6-sulphonic acid)
AMS	Automated multi-sample
ASTRID	Aarhus storage ring in Denmark
β	Beta
c	Concentration
C	Cytosine
caCD	Capillary circular dichroism
CD	Circular dichroism
DCX	Double-convex
DMSO	Dimethyl sulfoxide
DNA	Deoxyribonucleic acid
DUV	Deep ultraviolet
ε	Extinction coefficient
EDDs	Ethylenediamine-*N*,*N'*-disuccinic acid
ELISA	Enzyme-linked immunosorbent assay (ELISA)
EM	Electromagnetic
E.M.	Electron Microscopy
Flat	Noun used to describe a surface that has been polished to optical flatness.
G	Guanine
HPLC	High performance liquid chromatography
HRP	Horse radish peroxidase
HT	High tension voltage
I	Intensity of transmitted light
ID	Internal diameter
ISA	Institute for Storage ring facilities in Aarhus

$I_{\circ}$	Intensity of incident light
l	Path-length
L	Levorotatory
LB	Luria Broth
mg	Milligram
MS	Mass spectrometry
Nm	Nanometre
NMR	Nuclear Magnetic Resonance
LD	Linear dichroism
O.D.	Outer diameter
OD	Optical density
PCX	Plano-convex
PE	Polyethylene
PEEK	Polyetheretherketone
PEM	Photoelastic modulator
PTFE	Polytetrafluoroethylene
PVA	Polyvinyl alcohol
PVC	Polyvinyl chloride
QF	Queued flow
QS	Queued sample
Ra	Surface flatness
Rt	Difference between the highest and lowest point on a surface
Rz	Surface roughness
SRCD	Synchrotron radiation circular dichroism
SSI	Single sample injection
T	Thymine
μ	Micro
UV	Ultraviolet
YOYO	Oxazole yellow dimer
π	Pi
λ	Wavelength

CHAPTER ONE

Introduction

Potentilla anserina L. in both visible colour and UV.

CHAPTER 1: Introduction

Summary

Biological macromolecules are becoming increasingly important in scientific research, both as targets for therapies and as therapies themselves. Key to understanding and utilising these molecules is elucidating the structures that they can form, especially for proteins. Polarised UV spectroscopy is a potent technique for probing biological macromolecules that is used worldwide, but increasingly the available instrumentation is not sufficient for the applications that are of interest to scientists today. The aim of this project was to develop new technologies and applications for UV polarised spectrophotometers that will prove valuable to life science researchers in the future.

This introductory chapter describes the core structures encountered in the cell, before going into more detail about UV polarised spectroscopy and how it can be used to prove these structures in more detail.

1.1 Chemical basis of biological systems

Prior to the evolution[1] of biological life, there was a period of chemical evolution[2], creating as an end product the building blocks of life on Earth as we know them. Composed primarily of carbon, hydrogen and oxygen, with smaller but significant amounts of nitrogen, phosphorus and other elements those simple compounds are the same material upon which life today is predominately based[2].

DNA, the molecule which carries the genetic information that defines an organism had its structure first postulated in the famous 1958 paper by Watson and Crick. However, the full implications of its biological function were only realised in the publication of what is now known as the central dogma of molecular biology, first presented in a Nature paper in 1970[3]. The central dogma states that for general processes in the cell, information from DNA is used to code RNA in a process called *transcription*; the RNA produced then being *translated* at a ribosome to produce proteins. As a result, the two factors that influence the structure of proteins are the amino acid sequence coded originally by the DNA and the environment that those particular chemical groups are placed within.

In order to carry out their roles effectively, the three dimensional structure formed by biological molecules is of great importance, as molecular binding is of great importance between difference substrates within the cell. Natural systems take advantage of the potential chirality of the carbon atom to form highly specific structures- amino acids can form into D or L isomers but for the majority of proteins only L isomers are used during translation of RNA at the ribosome (although some D isomers can be found in proteins that have undergone posttranslational modification. Additionally, proteins such as Gramicidin contain both D and L amino acids; although in the case of Gramicidin it is not formed at the ribosome, but rather by non-ribosomal peptide synthetaes). This creates a highly ordered chemical system of internal structural consistency with only a single isomer being present for the vast majority of protein systems. Indeed, this predominant use of a single isomer allows for further complexity in protein structure when selective L amino acids in the protein backbone are substituted for D isomers, adding the potential for further complexity in protein structure.

Amino acids, lipids and carbohydrates, whilst being chemically relatively simple in structure can, when combined appropriately create an array of macromolecules, form

very strong and light materials such as keratin[4], to synapse ion channels that allow exceptionally fast cellular communication. Indeed, all the different forms of life on Earth are formed from the same types of molecule. If we are to understand fully how life works, it is important that we have a greater understanding of the forms these classes of biological molecules take when associating with one another to form their macromolecular equivalents.

1.1.1 DNA

DNA, or deoxyribonucleic acid is the biological macromolecule that holds all the genetic information about the organism. Through the gene sequence of a given organism, all the required information for the growth, maintenance and reproduction of that organism is available. Changes in the genetic code of an organism, via either random mutation or environmental factors can lead to disease such as cancer[5]. Located in the chromosomes of virtually every organism, each cell contains the complete genetic code of the organism.

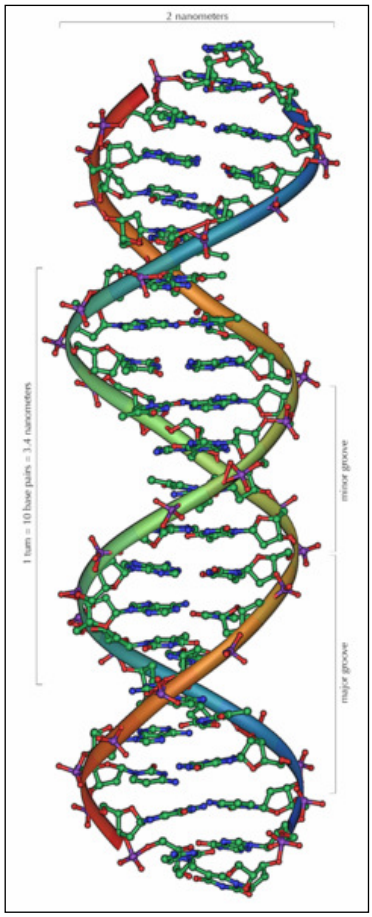

Figure 1.1: DNA double Helix. Image by Michael Ströck, under the GNU Free Documentation License, availible at http://commons.wikimedia.org.

DNA was first isolated by Miescher[6] in 1868 where, when isolating cell nuclei from pus he noticed the presence of a phosphorous containing compound. However, it was only in 1953 that the structure of DNA as we understand it today was first postulated, in the famous paper of Watson and Crick[7]. In this paper, the structure of DNA (shown figure 1.1) was postulated to be that of two negatively charged sugar-phosphate chains that individually had formed into a helix. The individual helices were then bound to one another, forming a double helix that was bonded together via arrays of hydrogen bonds. These hydrogen bonds were generated by the bases associated with each nucleotide. There are four dominant types of base in DNA, the purines adenine (A) and guanine (G) and the pyrimidines thymine (T) and cytosine (C). These bases form into the two pairs of AT and GC. The AT pair forms only two H-bonds per base pair whilst GC forms three per base pair, resulting in a stronger association between the nucleotide chains for DNA rich in GC content.

The double helix formed by the bonding between the two nucleotide chains can vary greatly in terms of diameter, number of bases per 360º turn and length depending on environmental factors. There are three broad types of DNA based on these factors, A-B, and Z-DNA (figure 1.2).

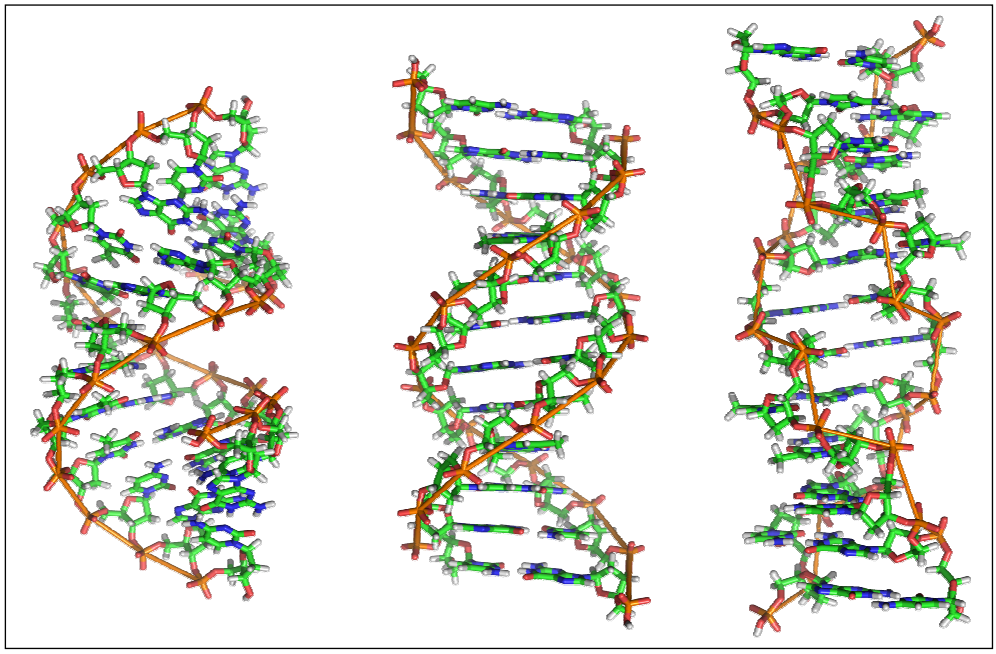

Figure 1.2: Different types of DNA. From left to right: A-DNA, B-DNA and Z-DNA. Note how the structures, whilst all being helical, vary widely with A and B forming a wider, shorter double helix than is observed in Z-DNA. Image created by Richard Wheeler, available at http://commons.wikimedia.org.

Of these three types, it is the right handed B-DNA helix that is predominately found in biological systems. The base pairs within a B-DNA structure are perpendicular to the axis of the helix, where there are typically 10 base pairs per 360º turn. The structure of B-DNA allows for three different forms of binding by drug or other molecules.

- Binding through electrostatic interactions (taking advantage of the anionically charged phosphate backbone of a nucleotide strand).
- Intercalation of a molecule between base pairs (especially if the intercalating molecule is planar with π bonding orbitals).
- Groove binding interactions.

Due to the double helical nature of DNA, the macromolecule has two groove binding sites, one bigger than the other. The large recess in the B-DNA helix is called the major groove, whilst the smaller recess is called the minor groove. There are many DNA binding agents that bind to the DNA via one of these grooves.

1.1.2 RNA

RNA, or ribonucleic acid is the intermediate molecule in the vital process of transferring biological information from DNA to encode proteins. Chemically similar to DNA (RNA differs from DNA through its use of ribose rather than deoxyribose and changes in its nucleobases as discussed below), RNA is structurally very different as it exists only as a single strand of bio-polymer, unlike DNA which forms a double helix structure. Additionally, RNA uses the nucleobase uracil rather than thymine, which allows the binding of adenine and guanine in vivo. RNA tends to form very complicated structures in the cell, hydrogen bonding into a wide range of structures.

Messenger RNA (mRNA) is used in all cells to carry information from DNA to encode a polypeptide chain. However, there are far more applications for RNA recorded in nature, from being used in viruses as their genetic material, to transfer RNA (tRNA) which carries amino acids to the ribosome during protein synthesis.

1.1.3 Proteins

All forms of life are fundamentally based upon a single building block – the cell. This versatile unit can be both the entirety of the organism in the case of bacteria or

archaea, or the subunit by which more complex organisms are made *e.g.* a collection of cells forming tissues in eukaryotes.

As vital components of the cell, proteins are the class of macromolecules that are assembled from amino acids. They perform a wide variety of roles within the cell and within biological systems as a whole. These roles include structural and perhaps most importantly, enzymatic roles. Due to the precision and flexibility in which proteins can be folded (into virtually any shape or size) proteins play a vital role in cellular metabolism and function by mediating chemical reactions within the cell as enzymes (proteins that catalyse biochemical reactions in the cell).

The composition and shape of proteins is defined by the chain of amino acids that the protein is made from (usually called a polypeptide chain), which is ultimately defined by the DNA gene sequence of the organism. Any changes in the genetic code of the organism (through mutation or damage) can result in a change in the amino acid sequence of the protein, potentially leading to protein mis-folding and loss of enzymatic function[5]. This loss of function in many instances results in disease.

Protein organisation and structure

Depending on their role within the organism, proteins can be organised into three broad types of structure:

- Globular
- Fibrous
- Membrane-bound

Of these three broad categories, the majority of proteins are globular, with their structures composed of alpha helices, beta sheets and a range of other forms. These have also proven by far the easiest proteins to isolate and purify. Globular proteins usually function as enzymes, and as such are very often soluble in water.

Fibrous proteins tend to be used in structural roles, forming connective tissues such as muscle fibres, tendons and collagen. They are not as sensitive to chemical and temperature changes as globular proteins and as such tend to be much harder to denature.

The last of the broad categories of proteins are membrane proteins. Existing within the hydrophobic interior of cell membranes, membrane proteins perform many vital functions for the cell, acting as mediators between the interior of the cell and its environment, as well as having a very important role to play in inter-cellular

signalling. The structure of a membrane protein is typically alpha-helical to enable better insertion into the cell membrane for the protein, although β-barrel structures are also observed. In the past this important category of protein received little academic attention due to the difficulty of expressing, purifying and refolding such proteins but in recent years research has gathered pace in this area.

Individual proteins are ordered on several levels, as simple polypeptide chains are formed into complicated three dimensional structures.

There are four levels of protein structure, each increasing in both size and complexity.

Primary Structure: the sequence of amino acids in the polypeptide chain. This is the simplest level of protein organisation, consisting of only a chain of amino acids.

Secondary Structure: the arrangement of polypeptide chains into a three dimensional spatial structure. These structures are typically stabilised by arrays of hydrogen bonds formed between amine and carboxyl groups close to each other in a polypeptide chain. The manner of the hydrogen bond arrays determines the structural motif of the secondary structure; these motifs include helical, sheet and turn-based molecular arrays.

Tertiary Structure: the interactions and spatial arrangement of amino acid residues that are folded into close physical proximity, but are not close along the polypeptide chain. Tertiary structure involves a wide variety of inter-molecular forces to control the conformation of the protein. These include covalent bonds, dipole-dipole interactions, hydrophobicity and ionic bonding. Virtually all enzymes are organised to at least the level of tertiary structure.

Quaternary Structure: The structure generated when more than one polypeptide chain is used to form a protein. Typically only the largest and most complex proteins exhibit quaternary structure.

Secondary structure bonding motifs

The hydrogen bonding between the amine and carboxyl group of each amino acid residue dominates the formation of secondary structure with a polypeptide chain. In the case of amino acids, the amine acts as an H-bond donor whilst the carboxyl group acts as an H-bond acceptor. (Note that in terms of electron density, the lone pair on the oxygen is partly shared with the de-shielded H atom. The term H-bond acceptor applies to the direction of the H-bond, rather than to the movement of electron density across the bond).

Secondary structure has three main types:

- Alpha-helices
- Beta-sheets
- Beta-turns

In addition, there is random coil that is strictly used to refer to unstructured polypeptide chains within the confines of a protein, but often used to describe 'other' motifs that are not alpha helices, beta-sheets or beta-turns. This list is a general rule of thumb for secondary structure, structures such as that of poly-proline II do not necessarily 'fit' into this organisation.

Alpha helix

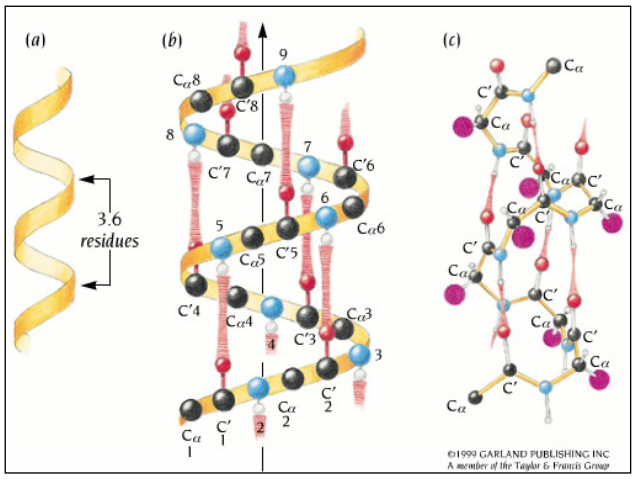

Figure 1.3: Molecular Structure of an α-helix. Image (a) shows the overall structure of the helix, whilst image (b) shows which residues associate with each other to form the helix. Image (c) shows the helix from a covalent bond perspective, highlighting the orientation of various chemical groups within. (Image taken from C. I. Branden,J. Tooze, Introduction to Protein Structure[8]).

The α-helix is the most common of all secondary structure motifs, creating a long, thin, spring-like structure. This shape is created by H-bonding occurring between amino acid residues that are close to one another in the polypeptide sequence (figure 1.3). This causes the sequence to twist in on itself, creating the characteristic spiral of the α-helix. First postulated by William Astbury in the 1930's, the structure was only finally resolved in 1951 by Pauling and Corey[10]. The length of an α-helix ranges from four or five amino acid residues to over forty and in some cases (such as tropomysosin[11]) two hundred and eighty four, varying from protein to protein. Within an α-helix there are 3.6 residues per turn of the spiral (i.e. how many amino acid subunits it takes to turn 360º) and a rise of 1.5 Å per residue, resulting in an

overall length of 5.41 Å per complete turn of helix. The diameter of the helix is 4.6 Å in total.

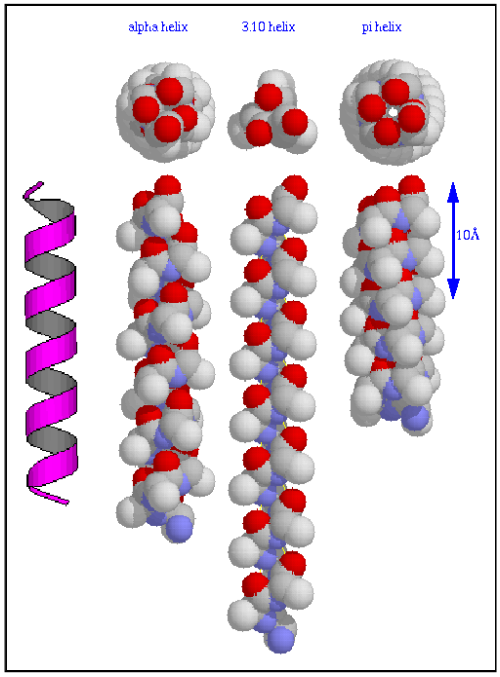

Figure 1.4: Different types of helix; the α-helix, 3_{10} helix and π-helix. The different types of helical structure are formed from a change in the number of residues that comprise each turn. Image taken from http://www.cryst.bbk.ac.uk/PPS2/course/section8/ss-960531_5.html.

In addition to α-helices, there are also two rarer but well-defined types of helical motif, 3_{10} helices and π-helices (figure 1.4). The difference between these helices and a traditional α-helix are the number of residues per turn, creating a difference in the shape and dipole of the helix (for a polypeptide chain of the same length, 3_{10} helices are thinner and longer than the traditional α-helix whilst pi helices are shorter and fatter). Due to the use of L amino acids in its construction, α-helices are right handed helices. Poly-proline, whilst not an alpha helix structure also forms helices. Comprised solely of proline residues, it adopts left-handed helices when bonding in a *trans* fashion between the proline residues, or a right-handed helix when bonding in a *cis* fashion.

Beta-sheet

β-strands are formed when a polypeptide chain lies flat rather than associating with itself. β-sheets (figure 1.5) are formed when β-strands lie adjacent to one another, forming a sheet-like structure bound together through hydrogen bonding. If the

strands run in the same direction this forms a parallel β-sheet, if they run in opposite directions then an anti-parallel β-sheet is formed. This structure is stabilised by H-bonds forming between N-H and C=O groups on different β-strands, allowing for H-bonding between any residue on a given amino acid residue (unlike in α-helices where proximity in the polypeptide chain has the predominant role in H-bond formation). The structure of β-sheets was, in much the same way as the α-helix first postulated by William Astbury but finally resolved by Pauling *et al.* in 1951[12].

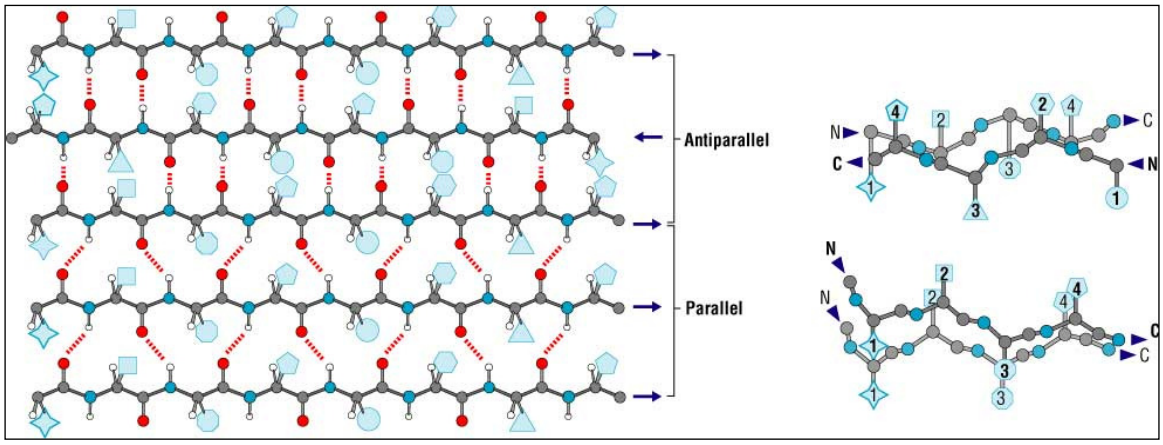

Figure 1.5: Parallel and anti-parallel β-sheet structures. (Image taken from http://wiz2.pharm.wayne.edu/biochem/prot.html)

β-strands are typically formed from two to six residues each and have several available binding modes *in vivo*, being capable of binding with α-helices and other β-strands (in some cases a line of β-strands loop around to bind with themselves, forming what is known as a β-barrel). Additionally, they can easily form hydrogen bonds with water or another polar solvent.

β-sheets, in addition to being a vital unit involved in protein construction are also used to create what is termed a β-turn. A β-turn is where two adjacent anti-parallel β-strands are connected, allowing the polypeptide chain to loop back on itself, changing the direction of the protein. This ability to form loops is a vital one in shaping the three dimensional structures of proteins, which are highly complex and need to be assembled to a high degree of precision in order to fulfil their biological functions. A wide variety of turns are included under the label β-turn, where the flexible nature of the protein makes it an excellent coupling unit.

1.1.4 Lipids, membranes and bilayers

Lipids are a very important class of biological molecule, with their functions varying from energy storage to being vital structural molecules. One of the most biologically important uses of lipids is as part of phospholipid bilayers. These molecules form the majority of the cell membrane of cells across the natural world, making it possible for the contents inside of the cell to be chemically different from the outside of the cell.

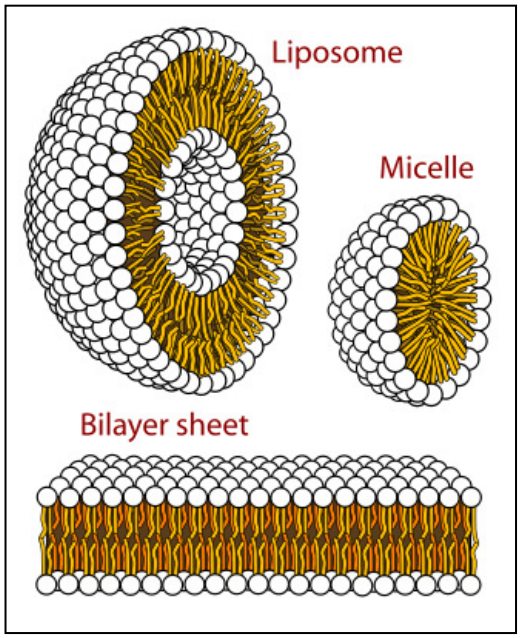

Figure 1.6: Different cellular forms of phospholipid layers. Image used with permission of Mariana Ruiz Villarreal from http://commons.wikimedia.org

The structure of phospholipids bilayers (figure 1.6) allows the creation of a hydrophobic barrier between the aqueous solution inside the cell and the external environment. This barrier is not permeable to water via osmosis and will not let through charged ions. The movement of polar molecules is facilitated by membrane proteins which act as channels through the membrane. This can be activated or deactivated when needed, allowing the cell a high degree of control to maintain cellular homeostasis.

In addition to bilayers, lipids are also used in the construction of vesicles and of micelles. Vesicles are used to partition a chemical solution from the main contents of the cell and thus are used to transport undesirable molecules such as waste products or to create a low pH environment for enzymes to work in as with lysosomes.

1.1.5 Methods for determining the structure of biological macromolecules

The overall structure of biological macromolecules can be determined through the use of many different techniques in conjunction with one another. For proteins, methods such as nuclear magnetic resonance (NMR) spectroscopy and X-ray crystallography have proven potent methods of determining detailed structural information at atomic resolution. Biophysical methods that are commonly used include electron microscopy, fluorescence spectroscopy, gel electrophoresis, isothermal titration calorimetery, neutron diffraction, small angle x-ray scattering and many others, all of which yield information about biological macromolecular structure.

The use of polarised light as a means of analysing biological molecules is now well established, with circular dichroism (CD) and linear dichroism (LD) becoming increasingly important as a means of structure determination. The research represented in this thesis has concentrated particularly on methods of biological macromolecule structure elucidation using polarised spectroscopy, allowing quick, accurate analysis of samples without damaging the sample.

1.2 Spectroscopy

Spectroscopy can be defined as 'the branch of science concerned with the investigation and measurement of spectra produced when matter interacts with or gives out electromagnetic radiation'[12]. Spectroscopy as a discipline was made possible through the discovery of optical dispersion of white light into its composite wavelengths using a prism. Prisms are still used extensively today for this very purpose. Data generated from a spectroscopic technique is referred to as a spectrum (plural spectra), whilst an instrument used to generate spectra is commonly known as a spectrometer or spectrophotometer.

The most basic form of spectroscopy is that of direct absorbance, or how much light of a given wavelength is absorbed by a sample. By knowing exactly how much light is being shone through a sample and then measuring afterwards how much light is left over after passing through the sample, one can calculate how much of the light the sample is absorbing at a given wavelength of light.

The absorbance of a sample can be calculated using the Beer Lambert law:-

$$A = \log\left(\frac{I_\circ}{I}\right) = \varepsilon c l \qquad \text{Equation 1.1}$$

where

A is the absorbance of the sample at a given frequency

$I\circ$ is the intensity of incident light

I is the intensity of transmitted light

ε is the molar absorptivity or extinction coefficient of the sample ($mol^{-1}dm^3cm^{-1}$)

c is the concentration of the sample ($mol^{-1}dm^3$)

l is the path length of the sample (cm)

This equation readily relates the absorptive qualities of the sample and the optical characteristics of the system. The Beer-Lambert law is used extensively across spectroscopic applications. In CD and LD spectroscopy it is particularly important, especially when analysing biological samples of unknown concentration. Note that the ε of a system is dependent on the wavelength of light as well as the molecule's environment. Different parts within a molecular assembly will be excited at different wavelengths.

Depending on the energy of the EM radiation, absorbance of light can lead to electronic, vibration or rotational transitions (summarized by the Born-Oppenheimer approximation) within the target molecule. The ability to absorb EM radiation of a given energy is defined by the chemical character of the molecular system, where different bonds and geometries affect both the wavelength of light that the system can interact with and if a type of transition is allowed.

If of the correct energy, photons of light can be absorbed by electrons within a chemical bond. This photo-excitation propels the electrons from the highest occupied molecular orbital, to an unoccupied orbital of higher energy. This elevated electronic state can facilitate an electronic transition. The movement of an electron at a given energy level into a higher energy level is termed a molecular electronic transition. The direction in which the electron density changes during this transition is called its polarisation. To fully describe an electronic transition, by knowing the intensity of the transition and its direction of polarisation one can create a vector property known as a transition dipole moment. These potential electronic transitions occur when the photon is of the same energy as the energy difference between the ground state and the excited state. The energy of the EM radiation defines what types of transition it can generate. Visible and UV radiation can induce electronic transitions whilst lower energy IR radiation can induce vibrational transitions. It is therefore vitally important to select the correct wavelength of light to investigate your matter property of interest.

1.2.1 UV spectroscopy

Spectroscopy in the UV region of the EM spectrum is particularly effective in the study of biological molecules, due to the nature of the chemical bonds found in such compounds. The majority of transitions found within proteins absorb in the region 300 nm and below, covering the whole of the UV region. Of the UV active chemical groups within proteins, amide bonds within the polypeptide chains that comprise all proteins are the most active. Additionally, the amino acids that incorporate aromatic groups are also UV active, due to the presence of the delocalised π system present in such molecules.

The UV region for proteins is by convention spilt up into two areas, the near UV (300 – 250 nm) and the far UV (250 – 180 nm). In proteins, the near UV is dominated by the signal of aromatic residues from trpytophan ($\varepsilon_{280\ nm}$ = 5500 $mol^{-1}dm^3cm^{-1}$)[13], tyrosine ($\varepsilon_{280\ nm}$ = 1490 $mol^{-1}dm^3cm^{-1}$)[12] and phenylalanine ($\varepsilon_{258\ nm}$ ~ 190 $mol^{-1}dm^3cm^{-1}$)[14]. Figure 1.7 illustrates the aromatic absorption in the near UV of these aromatic resides. With its strong signal, tryptophan tends to dominate any other signal from aromatic resides due to its relatively high extinction co-efficient in the near UV when compared to the other aromatic resides (who contribute more at lower wavelengths i.e. at approximately 220 nm).

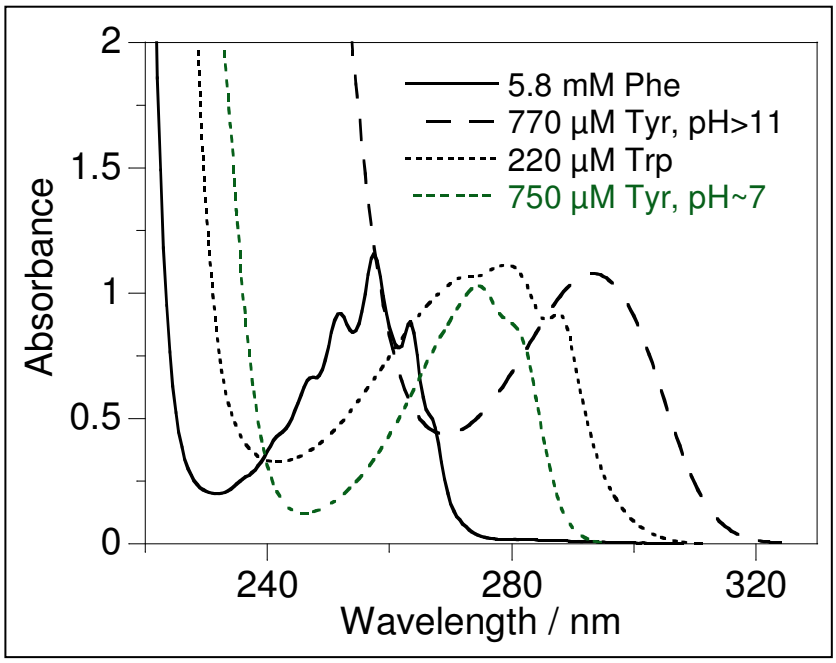

Figure 1.7: Aromatic absorption spectrum of tryptophan, tyrosine and phenylalanine. Figure from Circular Dichroism and Linear Dichroism (Rodger and Nordén, 1997)[13].

In the far UV the $\pi \rightarrow \pi^*$ transition of the amide carbonyl bond within the protein backbone has an absorption peak at 195 nm, with an extinction coefficient of approximately 7000 $mol^{-1}dm^3cm^{-1}$ [9].

For DNA, planar $\pi \rightarrow \pi^*$ transitions occurring in the purine and pyrimidine bases give rise to its UV absorbance. The backbone begins to contribute at about 190 nm.

Transitions in the UV are dominated by the carbonyl group within the protein backbone. At 230 – 210 nm the $n \rightarrow \pi^*$ transition is most important, with the polarisation of the transition occurring predominantly along the carbonyl bond. This transition can also couple with the π system of the amide. Typically the ε of this transition is approximately 100 $mol^{-1}dm^3cm^{-1}$.

The data produced by UV absorbance spectroscopy is very useful for giving information about what type of molecules and groups are present in a solution and in what concentration, but it does not give us much information on how those molecules are ordered. An example of this is π-π stacking, which leads to hypochromism in nucleotides[14]. For that information, we need to look at other forms of UV spectroscopy that take advantage of different chemical properties within our samples.

1.2.2 Circular Dichroism

Circular dichroism is a form of UV / visible spectroscopy that measures the differential absorbance between left and right handed circularly polarised light to probe the structure and bond types within a given sample. This difference in absorbance is created by chiral molecules that preferentially absorb one polarisation of circularly polarised light over another. Different optical stereo-isomers will absorb left or right handed circularly polarised light to a different degree. This difference in absorbance between the two types of circularly polarised is the recorded CD signal. The difference in absorption between left and right handed polarised light is very small, with the strength of the CD signal being several orders of magnitude smaller than that of linear dichroism (section 1.2.3).

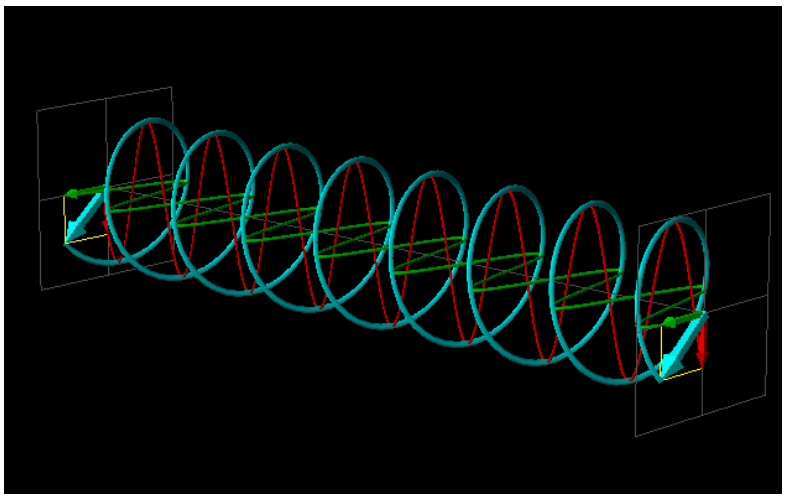

Figure 1.8: Circularly polarised light creation using wave interference. Image created using the wave modelling program EMANIM, developed by András Szilágyi (program available free at http://www.enzim.hu/~szia/emanim/emanim.htm).

Circularly polarised light is produced when two waveforms of light constructively interfere with one another when out of phase by precisely one quarter of a wavelength, as illustrated in figure 1.8. This creates the characteristic 'corkscrew' shape of the now circularly polarised light. For left-handed light the direction of the corkscrew is anti-clockwise, for right handed light it is clockwise when viewed down the direction of propagation.

CD signal is calculated from the following equation:

$$\Delta A = CD = A_L - A_R \qquad \text{Equation (1.2)}^{13}$$

Where

A_L is the absorbance of left handed circularly polarised light.

A_R is the absorbance of left handed circularly polarised light.

Physical basis for circular dichroism spectroscopy

A CD active electronic transition must have both electrical and magnetic character. In practical terms it means that the excitation process must move the electron density within the target molecule in such a way as to generate helical motion (illustrated in figure 1.9).

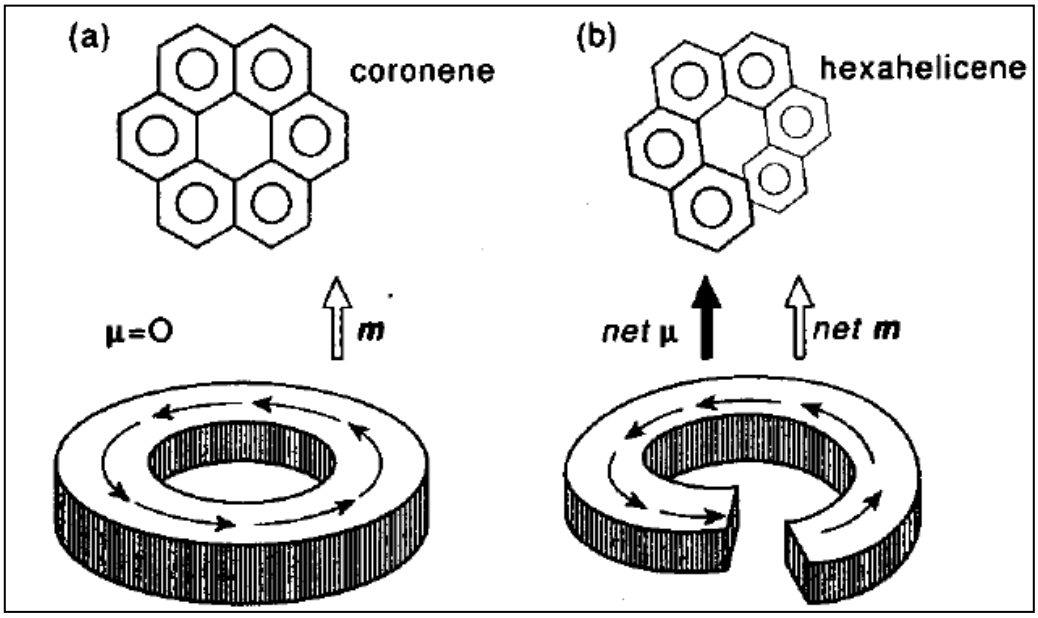

Figure 1.9: Difference in electron redistribution upon excitation between a chiral and non- chiral system. Electron movement in a chiral system will always be of a helical nature, whilst in an achiral system movement is always planar. Image taken from 'Circular Dichroism and Linear Dichroism'[13]. Figure used with permission.

Due to the chemical bonds contained within their structures, bio-macromolecules are typically chiral in nature. It is these chiral groups (in the case of proteins, amide bonds) with their asymmetric structures that cause the helical turning of charge within a molecule as it undergoes photo-excitation. Planar movement of charge could not distinguish between left and right circularly polarised light as both forms of circularly polarised light would be absorbed by the molecule equally.

Any molecule that exhibits the ability to distinguish between one handedness of circularly polarised light over another is said to be circularly birefringent. This property is essential in samples that are being analysed using CD spectroscopy, but for sample holders and other transmission materials its absence (or minimisation) is critical. CD has in the past been measured in terms of ellipticity, with units in millidegrees (an indication of the small the differences in absorption are in this technique). This was to indicate the degree of deviation from circularity for a given circular polarisation of light, as modified when passed through a sample. Modern methods of CD spectroscopy have allowed for the development of a new unit of CD, molar absorbance units, which are a measure of the intensity differences in absorption of light.

The equation below allows for the ready interconversion between molar absorbance units and molar ellipticity.

$[\theta] = 3298.2\ \Delta\varepsilon$

DNA Circular Dichroism

Circular dichroism as a technique is routinely used as a means of detecting secondary structure in proteins and as a means of distinguishing between different conformations of DNA. In DNA the ribose sugar units are responsible for its chirality. The CD signal for these backbone sugars is unfortunately beneath 190 nm, limiting how effectively these signal can be measured. On only the most advanced bench-top CD spectrophotometers or synchrontron beam lines can an effective signal be generated at these wavelengths, limiting the overall utility of CD as a technique for analysing DNA structure. However, the spectrum obtained between 190 and 300 nm is more useful, containing pi-pi* transitions that are of great value to the spectroscopist, as the helical conformation of the DNA strand defines the stacking of bases, whose spectrum can be used to distinguish between the B and Z forms of DNA[1]. The sugar units of the DNA backbone induce the bases to adopt a helical arrangement – these effects dominate the electronic coupling, creating the observed DNA CD signal.

DNA ligand binding can also be followed using CD, as even if the ligand itself does not exhibit chirality (and therefore is a valid target molecule for CD), then the CD it gains on binding the DNA molecule can be monitored (this technique is called induced CD, or abbreviated to ICD).

Whilst the uses of CD for DNA analysis are well regarded and well known, CD is also used for the rapid analysis of protein structure.

Protein Circular Dichroism

The abundance of chiral backbone molecules and many varied structural forms of these polypeptide backbones within proteins makes them an almost perfect class of molecules to analyse using CD. The information generated by CD for proteins tends to focus around the secondary structure, although very low wavelength work has been carried out that suggests the possibility of tertiary structure elucidation[17].

Protein secondary structures generate excellent CD signals, due to the high number of chiral groups within each sample. However, as the recorded CD spectrum will measure the difference in absorption of left and right circularly polarised light at a

given wavelength for the whole sample, CD as a technique cannot distinguish between different types of chemical environment within the same sample. Additionally, any CD data generated from a protein sample will be an average of all secondary protein structures present. Deconvolution software exists for CD spectra, which can identify the different types of secondary structure within a given protein based on a database of CD spectra recorded for a wide variety of proteins whose structures are known. There are several programs available for this purpose, a number of which can be accessed at http://dichroweb.cryst.bbk.ac.uk/, a website run by the Wallace group at Birkbeck College. Each type of secondary structure gives rise to a different type of CD spectrum (as shown in figure 1.10), but these are all a form of approximation.

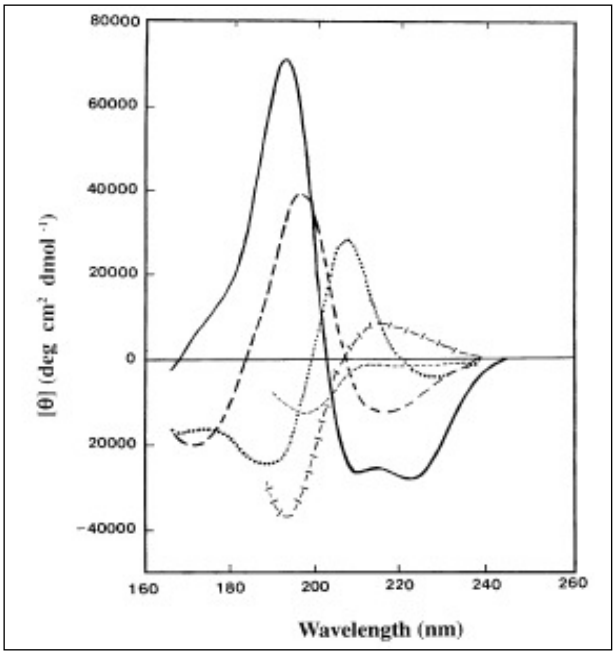

Figure 1.10: CD spectra of the major secondary structure types. Solid line, α-helix; long dashed line, anti-parallel β-sheet; dotted line, type I β-turn; cross dashed line, poly proline II helix; short dashed line irregular structure. Figure taken from the paper 'How to study Proteins by Circular Dichroism' by Kelly *et al*[18].

α-helix

Showing the strongest CD signal of any secondary structure motif, the distinctive shape of the CD spectrum of an α-helix is one of the most commonly found in CD protein spectroscopy. Dominating the spectrum are negative peaks at 208 and 222 nm (formed from the $\pi \rightarrow \pi^*$ transition and the $n \rightarrow \pi^*$ respectively), whilst a positive peak is observed at 192 nm (formed from another part of the $\pi \rightarrow \pi^*$

transition). The separation of the positive 208 nm band and negative 192 nm band is due to exciton coupling, which causes the $\pi \rightarrow \pi^*$ transition to split into two separate transitions. The origin of this effect is from the interaction of the transition dipole moments of amide bonds along the protein backbone – when one transition dipole of a chromophore is excited, there is a possibility of an interaction with the transition dipole of a neighbouring unexcited molecule. In the case of an ordered array of molecules, such as in a polypeptide, the transition dipole of one of the chromophores will be split into two transitions, one at higher energy and one at lower energy than that of the original transition, thus broadening the absorption/emission range of the $\pi \rightarrow \pi^*$ transition. The 208 nm band is only observed in the spectrum of an α-helix, with the intensity of signal being greater for a longer helix.

β-sheet

The CD spectrum of β-sheets can change depending on whether or not the sheet is arranged parallel or anti-parallel. This orientation parameter, in addition to the relative size of the sheet has an impact on the relative size and shape of the spectrum. However, there has yet to be a definitive assignment of different β-sheet peaks in a CD spectrum aside from a positive band at 195 nm and a negative band at 218 nm Whilst CD spectroscopy can identify the presence of β-sheet secondary structure, it is not trivial to say precisely what kind of β-sheet structure is present in the sample.

β-turn

Traditionally formed between β-sheet sub units, the CD spectrum of a β-turn is not well defined. However, there is typically a positive band at between 200 – 205 nm from $\pi \rightarrow \pi^*$ transitions, as well as a negative 225 nm band from $n \rightarrow \pi^*$ transitions.
If instrumentation allows it, at between 180 – 190 nm an intense negative band can be observed in the CD spectrum.

Random coil

Defined more by what is absent than by what is present, random coil CD spectra usually consist solely of a negative band at 200 nm. Unfortunately poly-proline II and βII have a very similar spectrum to random coil.

Flexibility of circular dichroism as an analysis method

Some of the advantages that CD grants over other means of biological macromolecular structure elucidation include rapidity of data acquisition, sensitivity to the creation of new chiral molecules within a system and its flexibility in looking at samples in the liquid phase. Proteins that are difficult to isolate and crystallise *e.g.* membrane proteins, are notoriously difficult to analyse by standard means. CD allows us to look at biological molecules that would otherwise be closed off to study.

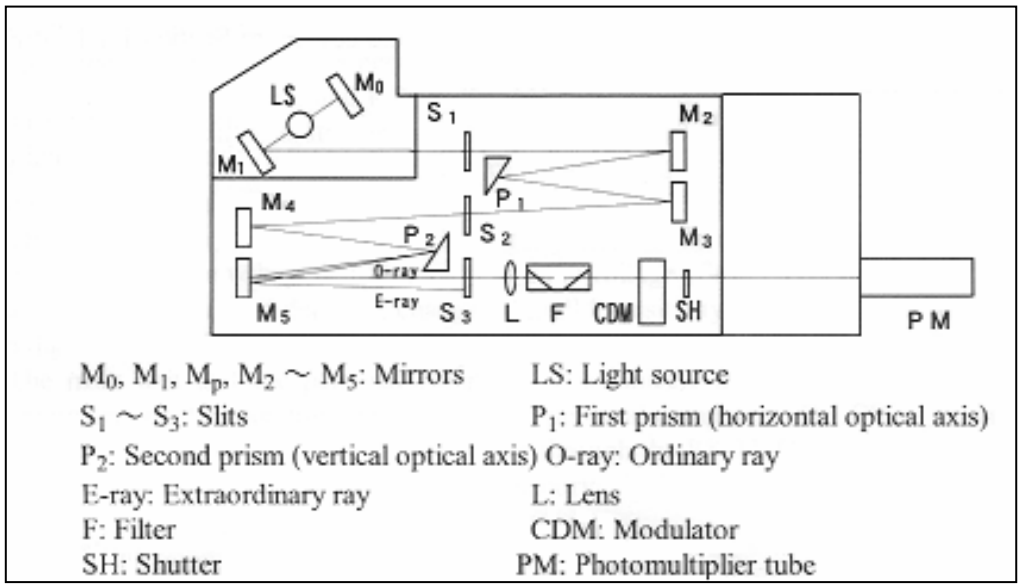

Figure 1.11: Diagram of the optical bench within a J-800 series CD spectrophotometer. Light of all wavelengths is generated from the xenon lamp, before being manoeuvred through two monochromators (the 1st being between S1 & S2, the 2nd between S2 & S3). These two monochromators (more commonly referred to as a double monochromator) is very effective at reducing stray light within an optical system. The prisms within each monochromator, in addition to selecting a wavelength of light are also axially orientated, generating linearly polarised light that is easier to modulate. All reflection within the system is achieved using aluminium mirrors. Figure from Model J-800 CD spectrometer Hardware/Function manual (2006) by Jasco. Figure used with permission of Jasco UK[19].

Instrumentation

The most challenging aspect of CD spectrophotometer design is creating an instrument that reliably produces both left and right handed polarised light in equal quantities and for an equal duration. Any deviation from this will cause the CD spectrum to go awry, as the actual differences detected by CD spectroscopy are very small indeed. Figure 1.11 details the optical design of a Jasco J800 series spectrophotometer. This has the effect of selecting a specific wavelength of light

(with more obtuse angles giving rise to UV wavelengths). In combination with masking of the light beam by the beam slits, light after the prism is to a reasonable approximation monochromatic and collimated.

A xenon arc lamp is used to produce the light used by the spectrophotometer, producing both UV and visible light in most bench-top machines. In order to select a single wavelength of light, the light beam produced by the lamp is focused onto a prism, which is moved to select specific wavelengths. Alternatively a grating may be employed to block out the unwanted wavelengths of light. As the angle of incidence is changed for the oncoming light beam, the prism changes the wavelengths of light reflected and absorbed.

The main advance that allowed the development of CD spectroscopy was the development of the photoelastic modulator (PEM). An example of how this device is employed is shown in figure 1.11. This device takes advantage of the photoelastic effect to change the birefringence of an optical element (usually formed from silica for UV-visible CD). This changing of the birefringence of the optical element is created by sending a current that is set to the resonance frequency of the material, through the crystal, causing it to 'flip' its birefringence. This flipping is used to switch between left and right circularly polarised light by sending the light through two quarter-wave-plates. The additional 'flipping' of the PEM allows one of the plates to be nullified optically, creating the required ¼ wave constructive interference that is required to make circularly polarised light.

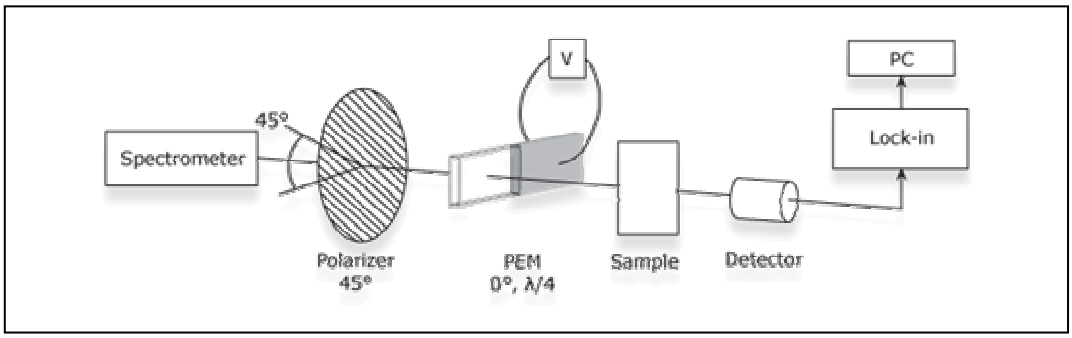

Figure 1.12: Experimental set-up for linear and circular dichroism (image taken from Hinds Instruments application note on photoelastic modulators, by T.C. Oakberg (an excellent source, free download of the application note at http://www.hindsinstruments.com/wp-content/uploads/LinearCircular_Dichroism.pdf).

The experimental set-up shown in figure 1.12 can also be used to generate linearly polarised light. One of the key changes in the processing of the light beam to create

linearly polarised light or circularly polarised light involves changing the peak retardation of the modulator, to create two orthogonal polarisation states that are required for both techniques[20]. Additionally, the orientation of the sample must also be changed. For linear dichroism, the sample should be aligned at 45º to the modulator axis (so PEM altered light become parallel and perpendicular to the sample). Additionally, as linear dichroism involves a half wave retardation (rather than a quarter for circular dichroism), the measurement of the spectrum has to take account of this in order to generate data. A common method used to address this is to alter the AC output of the spectrophotometer to be at twice the frequency of the modulator[21].

Instrument parameters

There are several parameters[18] that can be changed when collecting a CD spectrum that can be used to improve the quality of collected data.
These are:

- Bandwidth

  Bandwidth is a measurement of the degree of precision used by a monochromator to select light of a given wavelength. As you increase bandwidth, more light is let through the system (especially important at low wavelength where photon flux is reduced), but at the cost of less resolution of spectral bands. In order to resolve fine structure the bandwidth should ideally be as small as possible.

- Accumulations

  This is a measure of how many full spectrum scans are taken and averaged out to produce the final data set. As you increase the number of accumulations you decrease the background noise in the final spectrum (the signal/noise ratio is proportional to the square root of the number of scans), but at the cost of increasing the acquisition time.

- Scan rate and response

  These two parameters are closely linked and are vital for the collection of meaningful data. The response time is a measure of the time over which the CD data are averaged whilst the scan rate is the speed of collection over a given wavelength range e.g. 100nm/min. A faster scan rate can be balanced by a more

rapid response time, but in all cases efforts should be made when altering these parameters that distortion does not occur in the collected CD spectrum.

- Data pitch

Data pitch is simply how often data points are collected i.e. a value of 0.5 nm would collect a data point every 0.5 nm.

1.2.3 Linear Dichroism

Linear Dichroism (LD), like circular dichroism is a form of UV spectroscopy that uses polarised light to probe the structure of molecules, especially biological macromolecules. However, as the name implies linear dichroism uses linearly polarised light rather than circularly polarised light as a means of gathering spectral information. A sample that is to be analysed using LD needs to be orientated, either through the application of force or by having a degree of intrinsic orientation as a molecule.

Linear Dichroism can be defined as:-

$$LD = A_{//} - A_{\perp} \qquad \text{Equation (1.3)}$$

where

$A_{//}$ = Absorbance of light parallel to the orientation direction

$A_{\perp}$ = Absorbance of light perpendicular to the orientation direction.

The greater the degree of orientation of a molecule, the greater the magnitude of its LD signal. This is because there are correspondingly more aligned molecules and therefore more total electronic transitions within the sample system that can be detected. This allows LD to be used as a means of analysing classes of molecules that can be orientated, as well as being able to assay the orientation of a chromophore bearing molecule embedded in another surface.

LD alignment methods

Some of the first LD experiments on organic molecules were done using a stretched film as the orientation method. The analyte molecules were placed upon a thin

polymer film – these molecules would be absorbed into the polymer. Once the sample is present inside the polymer film the film in question would then be stretched, causing the embedded analyte molecules to become orientated in the direction of the stretch. The polymer used for the stretching would typically be comprised of polyethylene (PE), polyvinyl alcohol (PVA), or polyvinyl chloride (PVC). Provided that the direction of orientation is known, this alignment method can be used to acquire high quality LD spectra.

One of the issues with the stretched film approach to LD alignment is that solution phase molecules cannot be analysed in their native state when suspended on a film. In order to address this, the Couette LD system was developed by Wada and later by Nordén, Rodger and others[22] to address this problem (figure 1.13).

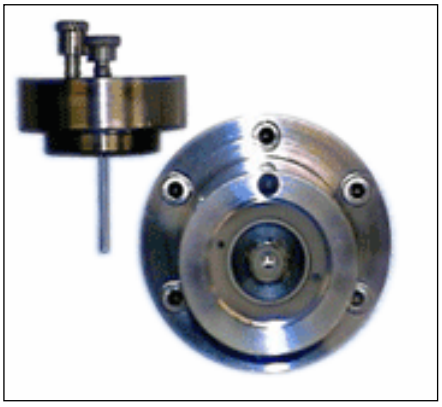

Figure 1.13: Top-down view of the microvolume Couette LD cell. To the left of the image you can see the quartz rod insert that is placed inside the capillary of the LD cell proper. Note the rod that can be placed with the capillary to create the required angular gap. It is in the gap between the rod and capillary that the sample is contained within. Image taken from www.kromatek.co.uk.

The Couette system of sample orientation places the sample in the gap between two cylindrical objects (usually a capillary tube for the outer layer and a rod for the inner). One of the cylinders then rotates on its axis; the turning force generated causing the molecules within the sample to align (figure 1.13). The key to the success of the technique is keeping the flow within the system laminar. This design of LD cell has vastly increased the versatility and user take-up of LD spectroscopy as a whole.

1.3 References

1: C. Darwin, The Origin of Species (1859), Penguin Books, ISBN-13: 978-0-140-43205-3

2: A.I. Oparin, The Origin of Life (1924), Dover Publications, ISBN-13: 978-0486495224

3: F. Crick, Central dogma of molecular biology, 1970, Vol. 227, 561-563, Nature

4: R.D.B. Fraser, T.P. MacRae, A. Miller, The coiled-coil model of α-keratin structure, 1964, Vol. 10, Issue 1, 147 – 156, Journal of Molecular Biology

5: D.E. Brash, J.A. Rudolph, J.A Simon, A. Lin, G.J. McKenna, H.P. Baden, A.J.Halperin, J. Ponten, A role for sunlight in skin cancer: UV-induced p53 mutations in squamous cell carcinoma, 1991, Volume 88 no. 22, 10124 – 10128, PNAS.

6: J.D. Watson and F.H.C. Crick, A Structure for Deoxyribose Nucleic Acid, 1953, 171, 737 – 738, Nature

7: Colour Oxford English Dictionary, (2011), Oxford University Press, ISBN-10: 0199607915

8: C. I. Branden,J. Tooze, Introduction to Protein Structure, (1998), Garland Science, ISBN-13: 978-0815323051

9: L. Pauling, R. B. Corey, H.R. Branson, The structure of Proteins: Two Hydrogen-Bonded Helical Configurations of the Polypeptide Chain, 1951, Volume 37, Issue 4, 205 – 211, Proceedings of the National Academy of Science in Washington

10: F.G. Whitby, G.N. Phillips Jr., Crystal structure of tropomyosin at 7 Angstroms resolution, 2000, 38(1):49 - 59, Proteins

11: L. Pauling, R.B. Corey, The Pleated Sheet, A New Layer Configuration of Polypeptide Chains, 1951, Volume 37, 251 – 211, Proceedings of the National Academy of Science in Washington

12: R. Dahm, Discovering DNA: Friedrich Miescher and the early years of nucleic acid research, 2007, 122:565–581, Human Genetics

13: N. Page, F. Vajdos, L.Fee, G. Grimsley, T.Gray, How to measure and predict the molar absorption coefficient of a protein, 1995, 4, 2411 – 2423, Protein Science

14: Alison Rodger and Bengt Norden, Circular Dichroism and Linear Dichroism (1997) Oxford University Press, ISBN - 019855897X

15: I.Tinoco Jr, Hypochromism in Polynucleotides, 1959, vol 82 4785 – 4790, Journal of the American Chemical Society

16: J.C. Sutherland, K. Pietruszka Griffin, P.C. Keck and P.Z. Takacs, Z-DNA: Vacuum ultraviolet circular dichroism, 1981, 78(8), 4801–4804, PNAS

17: B.A. Wallace, R.W. Janes, Synchrotron radiation circular dichroism spectroscopy of proteins: secondary structure, fold recognition and structural genomics, 2001, 5:567-571, Current Opinion in Chemical Biology

18: S. Kelly, T.J. Jess, N.C. Price, How to study proteins by Circular Dichroism, 2005, Vol 1751, 119 – 139, Biochimica et Biophysica Acta

19: Jasco, Model J-800 CD spectrophotometer hardware/function manual, 2006, P/N:0302-7511B.

20: T. C. Oakberg, Application note– Linear and Circular Dichroism, Hinds Instruments, Inc. (1991). http://www.hindsinstruments.com/applications/polarization/dichroism/circular-dichroism/

21: A.F. Drake, Polarisation modulation - the measurement of linear and circular dichroism, 1986, vol 19, 170- 181, J. Phys. E: Sci. Instrum.

22: R. Marrington, T.R. Dafforn, D.J. Hasall, J.I., MacDonald, M. Hicks, A. Rodger, Validation of new micro volume Couette flow linear dichroism cells, 2005, 130, 1608 – 1616, The Analyst

CHAPTER TWO

Development of capillary circular dichroism spectroscopy

Arnica angustifolia in both visible colour and UV.

THIS WORK HAS BEEN PUBLISHED IN *CHIRALITY* AND PRESENTED AT THE 12TH INTERNATIONAL CONFERENCE ON CIRCULAR DICHROISM, 2009, BRESCIA, ITALY

CHAPTER TWO: Development of capillary circular dichroism spectroscopy

Summary

Circular dichroism (CD) has become an increasingly important tool in the study of biological molecules as it enables structural information to be obtained non-destructively on solution-phase samples. However, sample requirements for CD are often seen as being too high with protein backbone measurements in standard cuvettes typically requiring ~100–300 μL of 0.1 mg/ml protein. To address this issue, we have designed a new form of CD sample holder, which reduces the sample requirements of the technique by up to two orders of magnitude, with a sample requirement of less than 3 μl. This sample saving has been achieved through the use of extruded quartz capillaries, the sample being held within the internal diameter of the quartz capillary through capillary action. The extruded quartz capillaries exhibit remarkably little birefringence whilst still transmitting high energy UV circularly polarised light. The optics associated with capillaries were investigated, with the light beam of the spectrophotometer being precisely and accurately focused through the centre of the capillary using a double convex lens. The focusing is vital to the low wavelength performance of the cell, where we have acquired reliable data down to 181 nm using a Jasco J-815 spectrophotometer.

2.1 Introduction

Circular Dichroism (CD) is a form of spectroscopy that uses circularly polarised light to probe the structure of molecules. Solution phase circular dichroism requires analyte molecules that have absorption bands in the wavelength range of interest and exhibit a degree of chirality in order to generate a CD signal [1]. In terms of automation and sample requirements, CD spectroscopy is not as developed as other structural methods such as NMR [2] and X-ray crystallography [3], both of which are potent methods of obtaining detailed structural information on the secondary, tertiary and in some cases quaternary level structure of proteins and nucleic acids. Synchrotron radiation circular dichroism (SRCD) [4] allows the use of the deep UV (DUV) region, probing the structure of the analyte molecules using light of far higher energy than that available from most bench-top instruments. The light created at a synchrotron light source covers a far greater range of wavelengths than a bench-top inst*r*ument at a continuous high photon flux and produces a far greater amount of photons This expansion of the examined spectral range helps generate far more information about the molecule, potentially allowing the probing of tertiary structural fold information for protein molecules, which dramatically increases the scope of the technique [5]. However, the sample requirements for CD are a barrier to its greater uptake and use, both in academic research and industry.

Uses of CD include the analysis of DNA [6,7] and use in the analysis of pharmaceutical solutions of proteins. Reduction of sample volume would allow less sample waste and reduced risk of sample contamination in reclaimed sample. An additional benefit of reducing sample volumes would be the ability to analyse expensive or difficult to produce samples such as supra-molecular assemblies[8], cyclical DNA[9,] RNA and synthetic assemblies of amino acids [10] – the association of these molecules with both themselves and other molecules can be easily observed using CD spectroscopy but sample requirements have put barriers in place to the utilization of CD for analysis of these types of sample.

2.1.1 Cuvette circular dichroism

In the past, circular dichroism data has been collected using flat-faced, circular or rectangular quartz cuvettes as the sample holder, or in certain instances CaF_2 cuvettes[11]. The design of the cuvette has many aspects in its favour. Firstly, the optical qualities of a cuvette are very simple and easy to control. There are only four flat interfaces for the light to pass through (air – solid (quartz) – liquid (sample) – solid (quartz) – air). Optics of this simplicity minimise refraction of the light beam, leading to a well-defined optical path for the light beam. Secondly, the size of the aperture for most cuvettes allows easy sample recovery, taking advantage of the fact that CD is a non-destructive technique. Finally, the standard quartz cuvette can be made to a large variety of specifications, including dramatically increasing or reducing the path-length of the cuvette. This variability of path-length allows CD spectroscopy to be used to collect spectra of samples with protein concentrations ranging from 0.001 mg / ml protein solution right up to 10 mg / ml protein solution. In addition to this, the face of the cuvette can be manufactured to be larger than the light beam from the spectrometer, optimising the amount of light passing through the sample.

However, there are a number of issues with currently used cuvettes for CD which sometimes make~~s~~ them non-ideal for use by the experimentalist:

(i) Sample size—A typical rectangular cell of path length 1 mm requires (with care) ~150 µl of 0.1 mg/ml protein (*i.e.* 15 µg) in order to generate a good quality CD spectrum. This issue with sample size reduces the efficacy of CD for biological use, where often the amount of protein generated will not be sufficient to make such a solution.

(ii) Baseline accumulation—In order to generate a CD spectrum it is necessary to generate a spectrum of not only the analyte molecule, but also of the carrier solvent in the same cuvette, be it buffered, saline or organic. This is so any CD generated by the solvent and cuvette can be compensated for in the final recorded spectrum, where only the analyte molecule's absorbance is plotted. Currently, the same cuvette must be cleaned and dried between baseline and analyte samples. This is a very time-consuming process which places strict limitations on how many samples can be

analysed in a given time frame, and precludes any option of high throughput data collection since perfectly matched CD cuvettes are hard to source.

(iii) Sample contamination— whilst correct experimental procedure can reduce this possibility, bio-macromolecular samples can adhere to quartz, enhancing the risk that a previous sample remains in the cuvette even after cleaning.

These issues, but predominantly the large sample requirements, pose serious limitations on the application of CD spectroscopy in the field of biological research.

2.1.2 Capillary circular dichroism

We therefore proposed quartz capillaries as an alternative method of holding the sample in the path of the light beam. We have found quartz capillaries to be well-suited to such an application, exhibiting remarkably little intrinsic birefringence [11]. The capillaries are formed from high-purity fused silica, which is heated until molten and then extruded. The resultant capillary has a very good uniformity (deviation of the outer diameter is a maximum of 50 μm) as well as excellent optical qualities, being generally free from imperfections. Capillary CD (caCD) offers the potential to use smaller sample volumes whilst obtaining good quality data. If we replace a 1 mm rectangular cuvette with a 1 mm internal diameter capillary, the required sample volume has the potential to be reduced. However, to be of any use, this requires the light beam to be tightly focused so as to pass directly through the sample. Assuming this can be achieved, the volume required for a 1 mm path length CD spectrum can be reduced from 200 μl to 3 μl of sample.

The work outlined in this chapter describes how a Jasco J-815 spectrometer was adapted to address these issues through the incorporation of a caCD base-plate, and how the resulting set-up can be used to collect high quality CD data.

2.2 Instrument development

2.2.1 Initial design

Work carried out by Rachel Marrington (a previous PhD student within the Rodger group) acted as the initial basis for this investigation. Her investigation proved the concept of using capillaries for polarised spectroscopic applications, which ultimately bore fruit in the Couette LD cell design [11].

The initial caCD cell (caCDRM) (figure 2.1) was made by a company called Dioptica Scientific Limited for researcher Rachel Marrington. Aluminium was used for the construction of the cell, with the lens holders, capillary holder and the base-plate itself all fabricated from that material. The slide-way was also constructed from aluminium, with a series of holes for securing the optical component holders in place. For the optical elements themselves (*i.e.* the lens holders and the capillary holder) a further step of anodising the aluminium was taken, in order to minimise any scattering effects that may take place should any stray light hit the metal of the optical component holders.

The original design for the caCD cell consisted of two double convex (DCX) lenses, produced by optical suppliers Edmund Optics in series, with a holder for the capillary placed between them. The light path enters the first lens (seen here furthest from the camera) which is then focused on to the capillary. This first lens is named the *focusing* lens (Figure 2.1). This takes the slightly diverging light beam of the spectrophotometer and focuses it onto a central point in the capillary. Once the light beam has passed through the capillary the now significantly divergent light passes through the second lens, named the *collecting* lens. This lens takes the light and limits the degree of divergence experienced by the light beam, so that it enters the detector.

This cell design worked on the principle that the focusing lens would ensure the light beam went through the sample held in the capillary. After leaving the capillary, the now divergent light beam would be harvested by the collecting lens. The light beam would remain within the confines of the optical system due to the parallelism of the optical components (Figure 2.2). This method of caCD had many advantages. First and foremost, light passed through the capillary in a manner which would generate CD data. In addition to this, the use of the collecting lens meant that the photon flux was reasonably high for the system (photon flux is the number of photons over a time period, with SI units of s^{-1}, see http://goldbook.iupac.org/P04636.html for more information). For a polarised spectrophotometer, this term is shown by the HT (or more formally known as the high tension voltage), which is proportional to the absorbance of the sample.

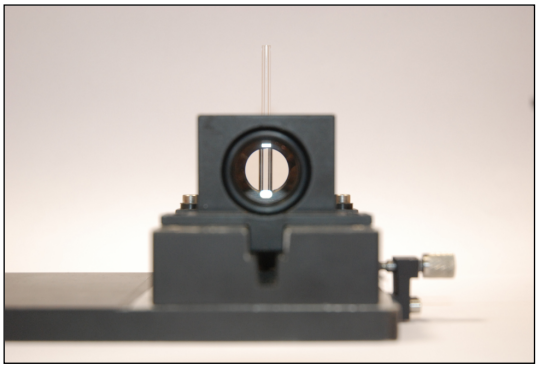

Figure 2.1: The focusing lens of the caCDRM instrument. Note that the lens is positioned precisely in the centre of the capillary.

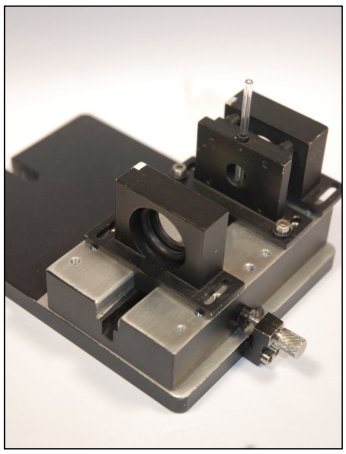

Figure 2.2: caCDRM image showing the slide-way of the instrument. The groove permits the addition of different optical components into the light path.

As the photon flux of a CD instrument decreases, the voltage passed through the detector increases to compensate. An HT reading higher than 600 V does not produce reliable CD data on a bench-top instrument, as the photon flux reaching the photomultiplier tube is too low to be accurately 'multiplied'. This creates a non-linear relationship between CD signal recorded and the actual sample absorbance. Keeping the HT as low as possible is important to ensure the widest possible wavelength range for data collection: as wavelength decreases, the amount of information accessible for the structure of the biological macromolecules contained within the sample increases. For this reason, the design of the caCD cell should maximise photon flux whilst retaining spectral shape and quality.

In order to test the instrument, Na [Co (Edds).H_2O] [12] spectra were gathered to ensure the suitability of the caCDRM cell. This standard, developed by the Scott group in collaboration with the Rodger group at Warwick University, allows CD spectroscopists to test the effectiveness of a CD instrument across a wide wavelength range (160 – 750 nm). The standard consists of solutions of independent R,R

enantiomers and a S,S enantiomers, which give an equal but opposite spectrum to one another. Used in conjunction, the two enantiomers can show any errors with the performance of either the CD instrument or, critically for this application, any optical systems accessories placed within the light path of the spectrophotometer. In this case, we wished to compare the data quality between a standard CD cuvette and the prototype caCD cell. If the cell design worked then there should have been no difference between the caCD and the cuvette spectra, after differences in path-length had been accounted for.

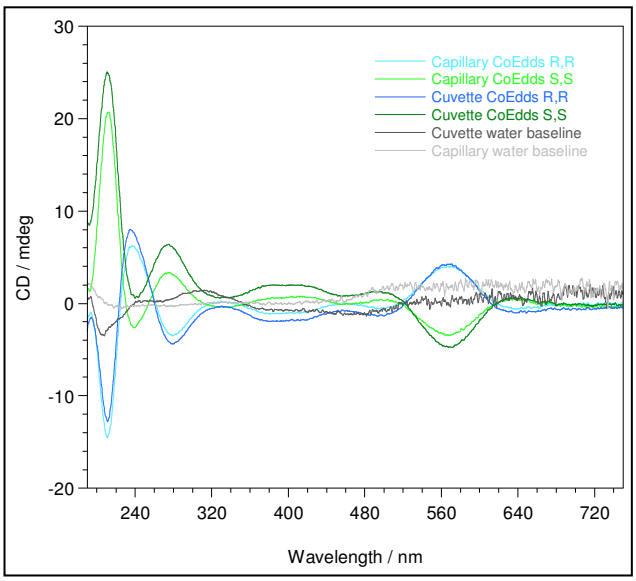

Figure 2.3: Na [Co (Edds)].H_2O at 0.55 mM spectra acquired through both cuvette CD and caCD.
The caCD spectra were acquired using the Marrington design of caCD base plate.
The path-length of the capillary was 1.12 mm, determined through analysis with potassium dichromate. Capillary spectra scaled using a 0.892 correction factor to allow for differences in path-length.
The path-length of the cuvette was 1 mm, verified via analysis with potassium dichromate.

As can be seen from figure 2.3, the caCDRM cell did not produce sufficiently high quality CD spectra in terms of data correlation between the capillary cell and the cuvette. The low-energy data values are in fairly good agreement, but the wildly varying magnitude and shape of the CD signal at lower wavelength shows a poor correlation between the cuvette spectrum and the capillary spectrum of the S,S CoEdds stereoisomer (the R,R data by contrast was in reasonable agreement). Whilst the concentrations of the two enantiomers were not the same (hence the difference in spectral magnitude between the R, R and S, S forms), the caCD data does not overlay

the cuvette data with any single scaling factor, showing that there was an issue with the design of the caCDRM cell.

After investigating the optical setup of the caCDRM, it became apparent that the amount of light hitting the detector after it had passed through the caCDRM was not sufficient to generate a high-quality CD spectrum. The relatively short focal length of the focusing lens resulted in a highly divergent beam once it had passed beyond the capillary. The collecting lens was therefore not sufficient to ensure all the light reached the detector. The problem with the system was that the capillary itself was exerting a lensing effect upon the light beam. The approach taken in the design of the caCDRM would be effective in a system where the only optical changes experienced by the system were from that of the lenses – this was clearly not the case here.

As a result, it was decided that this cell design would be abandoned in favour of a first principles approach to caCD, based upon an investigation into the optical behaviour of a capillary cross-section.

2.2.2 Capillary optics

The optical qualities associated with the cross section of a capillary are surprisingly complicated. Cuvette CD uses flat optical components to ensure the light beam does not deviate significantly from the normal – if there is any deviation recorded from the normal then it will be by a very small margin, typically induced by a curvature in the flat transmitting face created by the thermal annealing of the quartz within the cuvette.

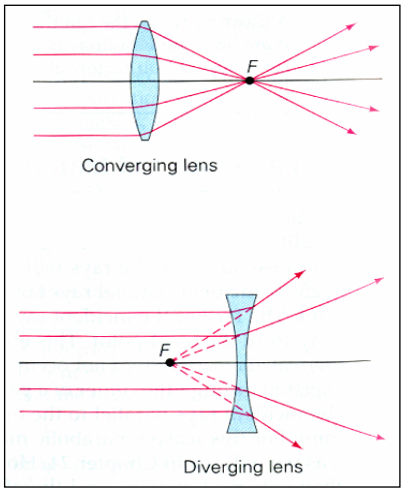

Figure 2.4: 'Many faces of light: As Newton Saw it, With Some Magic Tricks' lecture given by Prof. U. Mallik 14/02/05.

Capillaries, by way of contrast, are optically more complex. The route experienced by the light as it passes through the capillary is the same as the cuvette in terms of phase changes, but radically different in terms of focusing. Due to the curved shape of its sides, the capillary has a 'lens-like' effect on the light beam. Figure 2.4 shows the effect different types of lens have upon an incident light beam. Lens effects arise from the interaction of light between different densities of transmission media and different angles at which the transmission occurs. As light travels between different media the light beam can become refracted, distorted away from the normal. The difference between the lenses is therefore determined by the phase change they sit at - a lens focuses when light moves from a less dense to more dense media via a convex interface, whilst a lens that causes light to diverge is convex at a more dense to less dense media interface.

Assuming that the light beam is perfectly collimated (i.e. the composite rays of light in the light beam are all parallel), a convex (bulging or curving outwards) lens will cause the light beam to converge to a point (i.e. focusing the light beam) whilst a concave (curving inwards) lens will cause the light to diverge (i.e. defocusing the light beam). As shown in figure 2.5, the capillary has a combination of these effects, leading to a very interesting array of outcomes for a light beam entering the capillary.

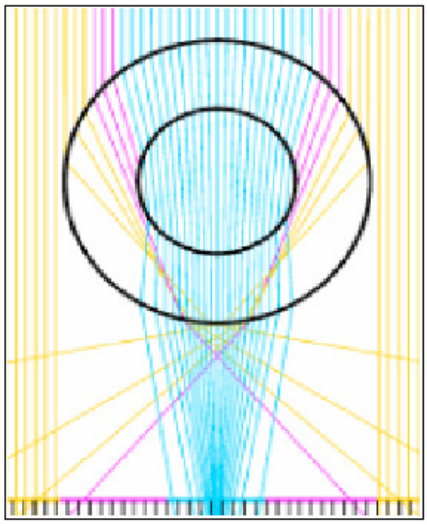

Figure 2.5: Capillary Optics

Blue lines represent light that passes through the internal diameter of the capillary. Pink lines represent light that interacts with the internal bore of the capillary but is still optically net divergent. Yellow lines represent light that does not interact at all with the internal bore of the capillary, creating a high degree of divergence. Image used with permission of Paraytec Ltd.

The optical properties of a capillary can be effectively thought of as being comprised of a pair of lenses, one focusing the light whilst the other causes the light to diverge. The normal optics for such an arrangement would cause the light beam leaving the capillary to be more or less the same as when it entered it. However, the capillary has an additional complication — the internal diameter of the capillary stands at 1.1 mm, whilst the external diameter is 3 mm. This results in the curvature of the outer lens being far less pronounced than the inner lens. Were the light beam perfectly centred on the capillary, minimal light would be lost since if the light entered the capillary in a straight line then divergent effects would be countered by the final phase change (quartz-air) which is focusing in nature. This light path is denoted by the blue light in figure 2.5. Therefore a *collimated* light beam results in a *convergent* light beam when passed through the centre of the capillary. However, the light beam from a standard CD spectrophotometer is neither collimated nor sufficiently focused for caCD spectroscopy. In order to focus the light into a sufficiently small area (such as that of a 3 mm O.D. quartz capillary) it is necessary to employ a double convex lens – taking the incident light beam and focusing it to a pin-point onto the capillary itself. This act of focusing the light loses its collimation. Failure to use such a device will result in a complete lack of recorded CD spectrum–simply not enough light will enter the capillary to generate a signal without focusing optics.

The importance of proper focusing onto the capillary for this technology to work cannot be overemphasised. When the light beam is *wider* than the internal diameter of the capillary, the curvature of the capillary ensures that the internal divergent lenses are far more potent at altering the light path than the external convergent lenses, resulting in a net *divergent* effect on the light beam (as denoted by the yellow light in figure 2.5). This is because the more pronounced the curvature of a lens, the stronger effect it has upon the exit light beam. These two main problems—the initial focusing of the light beam and the collecting of the light once it has passed through the capillary—have been addressed in several ways in this work, as discussed below. However, two core principles were identified that had to be satisfied within the design of any caCD cell. Firstly, the entire apparatus had to be mounted with each optical component parallel to one another.

Wavelength / nm	**Slit size / µm**
1000	10
900	11
800	13
700	19
600	27
500	53
400	104
300	278
250	538
200	1344

Table 2.1: Table displaying the change in slit size with wavelength in a J-800 spectrophotometer over a consistent 1 nm bandwidth (data from Jasco technical notes for the J800 series spectrophotometer).

The axis of this apparatus would then need to be, in turn, perfectly parallel to the instrument light beam. The linear alignment of the optical components within the system is of vital importance for its proper functioning, for should any component deviate from a central alignment it would lead to a propagation of errors throughout the system, resulting in the collection of a poor-quality spectrum. It should be noted that an initial problem with this project was that the light beam of the CD spectrophotometer itself was not centred. This needs to be confirmed after every instrument service, for such errors impact on all applications of the spectrophotometer. Secondly, in order to ensure that data quality would be of the highest standard, the caCD cell required the employment

of a 'light mask'. This mask would block all light that comes into contact with it, stopping divergent light from reaching the detector, so that only light which had passed directly through the sample would be collected. Masking does, however, have a cost when recording CD spectra. When a mask blocks a ray of light the number of photons reaching the detector is lowered, resulting in a correspondingly higher HT value than that observed by a non-masked sample holder. When designing a mask for an optical system, there is a fine balance between blocking out any divergent/scattered light which could potentially damage the quality of the recorded spectrum and maximising the amount of light travelling through the sample.

2.2.3 Spectrophotometer design– a case for precision optical engineering in CD applications

As mentioned above, one of the major issues with the caCD design was the successful focusing of the light beam. This focusing was made more difficult by the current design of light beam for the J-815 spectrophotometers from Jasco. The demands placed upon the spectrophotometers for standard CD are such that the current design is more than adequate to address its needs. However, caCD, being of far smaller volume, requires a light beam of uniform shape and size for ease of focusing.

Typically, J-815 spectrophotometers create a rectangular light beam, which has a degree of divergence as it moves from the light source to the detector. This is very awkward for any potential application of CD that requires precise focusing, as the 'raw' light beam is itself diverging, propagating errors throughout the optical system. The shape of the light beam is quite close to that of the standard CD cuvette. However, this shape necessitates a large sample volume to fill such a cuvette. If sample volumes are to be lowered, as with this technique, then the target area of the sample will be smaller by necessity. Obtaining a CD spectrum using such a sample holder would ideally involve a better-quality light beam entering the sample compartment, with a high degree of collimation. If further improvements to low volume CD are undertaken, these optical problems of the spectrophotometers need to be addressed. The caCD device is currently located just before the entrance to the detector, within the sample compartment, but due

to the quality of the light beam significant modification of the light beam is required to acquire meaningful caCD data. A potential route for improving the current spectrophotometer design would be to change the shape of the incident light beam from rectangular to circular. By using a circular light beam in place of a rectangular one, optical devices such as irises and lenses can be more easily used to manipulate the light beam, giving the user far more control of the optics of the system than exists presently. This issue is especially important with regards to low wavelength CD work, due to the change of slit-size as the wavelength decreases in some prism-based instruments (including the J800 JASCO series of spectrometers). Simply put, as the spectrophotometer moves down in wavelength the size of the light beam increases in order to compensate for the lower amount of photons produced by the light source at higher energy wavelengths. This effect arises from the use of double prism monochromators to select the different wavelengths of light –at present all Jasco instruments use double prism monochromators in this manner.

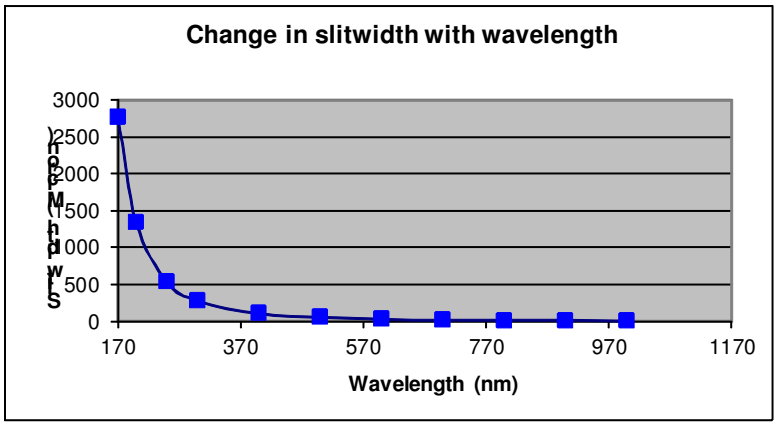

Figure 2.6: Graph showing the relationship between slit-width and wavelength for a J-800 series spectrophotometer (data plotted from Jasco technical notes for the J800 series spectrophotometer).

In order to generate a consistent 1 nm bandwidth, the slit-size of the instrument must be increased (figure 2.6), leading to an increase in the size of the light beam entering the sample chamber of the spectrophotometer as the wavelength decreases. The slit-width is increased to compensate for lower photon flux at lower wavelengths, allowing more light through but at a loss of spectral resolution. The effect that the slit opening has upon the functioning of the capillary is profound. The difficulty in focusing the light is greater in a more diffuse system, where the entry beam is far larger. Optical focusing has less of

an effect on this diffuse beam. Only with successive optical components can the beam shape and alignment be maintained. For this reason, the optics of the capillary make low wavelength spectroscopy, (where a low photon flux and high absorption of both air and sample / sample buffer already provide a great number of problems) more of a challenge.

2.2.4 Multiple optical elements reduce photon flux

When designing an optical system it is important to remember that each successive optical component induces two changes in the transmitted light beam. The first of these is the intended optical effect, be it focusing in the case of a lens or transmitive in the case of a cuvette. The second, smaller effect is in the reflection losses incurred. No material is 100% transmitting of a beam of light – some of the energy in the light beam will be transferred to an intervening media. Typically, optical components comprised of quartz incur a 10% loss of photon flux in any light beam that passes through it, due to reflection losses. In addition, the natural absorbance of the quartz will also mean that thicker quartz windows absorb more than thin quartz windows, although this rarely becomes an issue until the light beam reaches very high energy. Therefore a standard cuvette cell, with two quartz windows through which the light must pass through, incurs a minimum 19% loss of total transmitted light (10% for the first interface, followed by 10% of 90% for the second interface). This loss of photon flux has no appreciable effect on the spectra when in the near UV/visible region of the EM spectrum – the amount of photons being produced by the spectrophotometer at these wavelengths allows a high quality spectrum to be easily collected. Light at lower (i.e. higher-energy) wavelengths is more difficult to harness. Firstly, higher-energy light is inherently more difficult to produce, especially in the DUV. Secondly, a large number of compounds absorb in this region, including most notably $O_{2\,(g)}$. The ubiquitous nature of this gas in the atmosphere results in a high absorbance of any photons in this region. The high energy involved in the light beam also catalyses the production of ozone ($O_{3\,(g)}$), which is a fiercely strong absorptive media for UV light. Only under a nitrogen atmosphere can effective transmission of DUV light take place, and then only with a correct light source (such as that obtained

from a synchrotron light source). Under vacuum, and at a synchrotron, UV light of wavelength down to 125 nm can be produced.

2.2.5 caCD 'alignment' cell

With these principles in mind, the second generation of the caCD cell was designed and fabricated. Using a modified Jasco base-plate, this cell was built around the principle of minimising optical components-whilst taking advantage of the unique capillary optics to refocus the light beam.

The initial work on this new design was to test the suitability of a single focusing lens as a means of aligning the light beam effectively. Through the use of Blu-tack™, different lenses were substituted into the light path to test their effectiveness. However, in order for the caCD cell to be used as a routine spectroscopic method, a more user-friendly design was required. To this end, a Teflon lens holder was designed which could both accommodate the lens and fit well inside the slide-way of the Jasco base-plate. This design was both simple and inexpensive (figure 2.7).

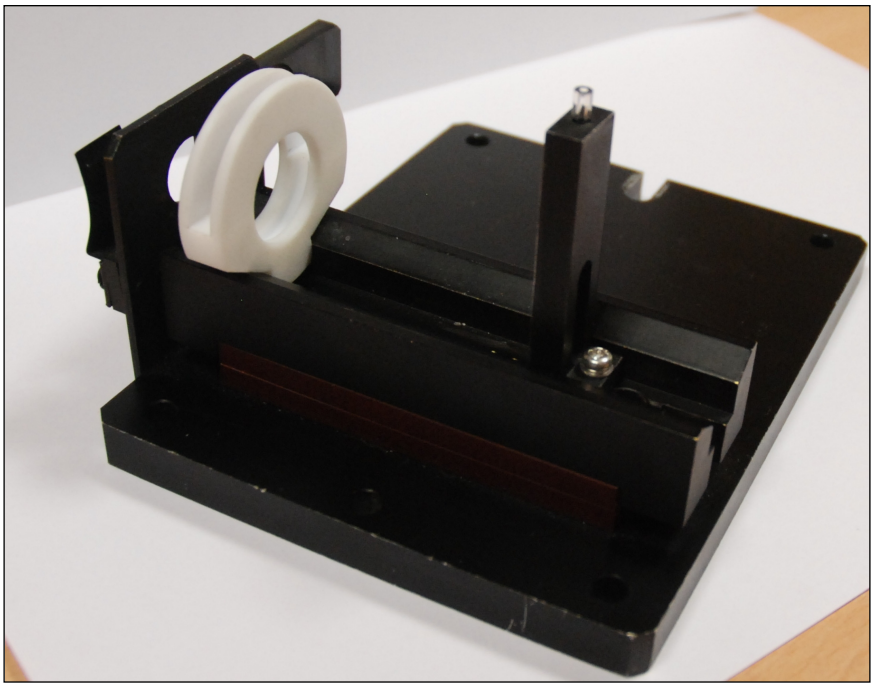

Figure 2.7: The alignment caCD cell, including lens holder. The design for this cell was simple and very cost effective. However, difficulties with data reproducibility marred the cell design.

After several experiments using different lenses at different focal lengths, it became clear that a DCX lens of focal length 100 mm was ideal for the caCD application. A lens of this focal length brings several advantages. Firstly, the level of light focusing

is to a good standard, the beam creating a band 200 µm wide at the focal point of the lens. This is within the sample region of the capillary, enabling the majority of the light produced by the spectrophotometer to pass directly through the sample, rather than the quartz walls of the capillary.

The greatest advantage of the 100 mm focal length lens, however, is the low level of divergence that the lens creates in the light beam after it has passed the focal point of the lens. By placing the focal point of the lens 2 mm before the capillary, the light ray becomes slightly divergent (figure 2.8). However, due to the long focal length, this does not create a large light beam – in reality the light beam remains small enough to enter the sample area of the capillary. The capillary then refocuses the light beam, generating a light beam that exhibits a high degree of collimation after the capillary. It then enters the detector.

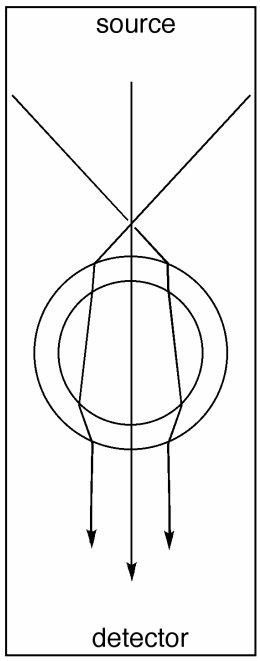

Figure 2.8: Diagram showing the effect on the light beam as it interacts with the capillary.

This design was then tested using Na [Co (Edds).H_2O] to see what effect these changes had upon the spectra.

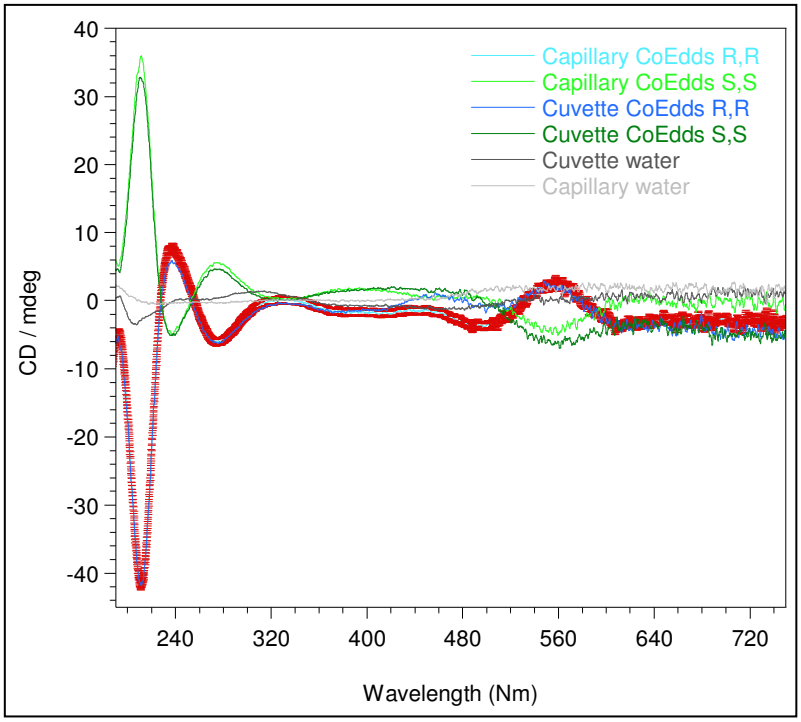

Figure 2.9: Na [Co (Edds)].H_2O 0.55 mM spectra acquired through both cuvette CD and caCD. The caCD spectra were acquired using the alignment cell design of caCD base plate. The path-length of the capillary was 1.12 mm, determined via analysis with potassium dichromate. Spectra scaled using a 0.892 correction factor to facilitate comparison between the spectra. The path-length of the cuvette was 1 mm, verified with potassium dichromate.

In figure 2.9, the spectra overlay fairly well, but the longer wavelength light suffers from a poor baseline. We believe this is due to the effect of chromatic aberration on the focusing lens. Chromatic aberration (illustrated figure 2.10) can be defined as 'the failure of a lens to focus different wavelengths of light to the same convergence point'. In the case of UV light, the chromatic aberration of the lens occurs in a *longitudinal* manner, i.e. the focal point moves at different distances away from the lens. (*Transverse* chromatic aberration, i.e. the movement of the convergence point to different positions within the focal plane, was not observed within the caCD setup). Chromatic aberration has been a known cause of difficulty in optical applications since the 17th century, where it was traditionally minimised by increasing the focal length of lenses within an optical system. This approach proved quite effective, as the focusing 'gradient' of the lens would be significantly reduced in a longer path-length lens.

Wavelength /nm	Focal Point** of 10 cm DCX lens/cm
700	10
650	10
600	10
550	10
500	10
450	10
400	10
375	9.75
350	9.5
325	9.25
300	9
275	9
250	8.5
225	8

Table 2.2: Table and graph showing the effect of chromatic aberration on the focal length of a 100 mm DCX lens. A J-600 spectropolarimeter was used as the light source for these measurements. Focal point determined using white fluorescent paper.

** As wavelength decreases, the width of the light beam increases. This is very closely related to the slit size of the spectrophotometer at that wavelength. It must also be noted that as wavelength decreases, the light beam becomes more diffuse and may scatter more. Masking of the capillary is therefore vitally important to ensure spectral quality.*

*** Taken as a midpoint of the focusing/diverging light cone*

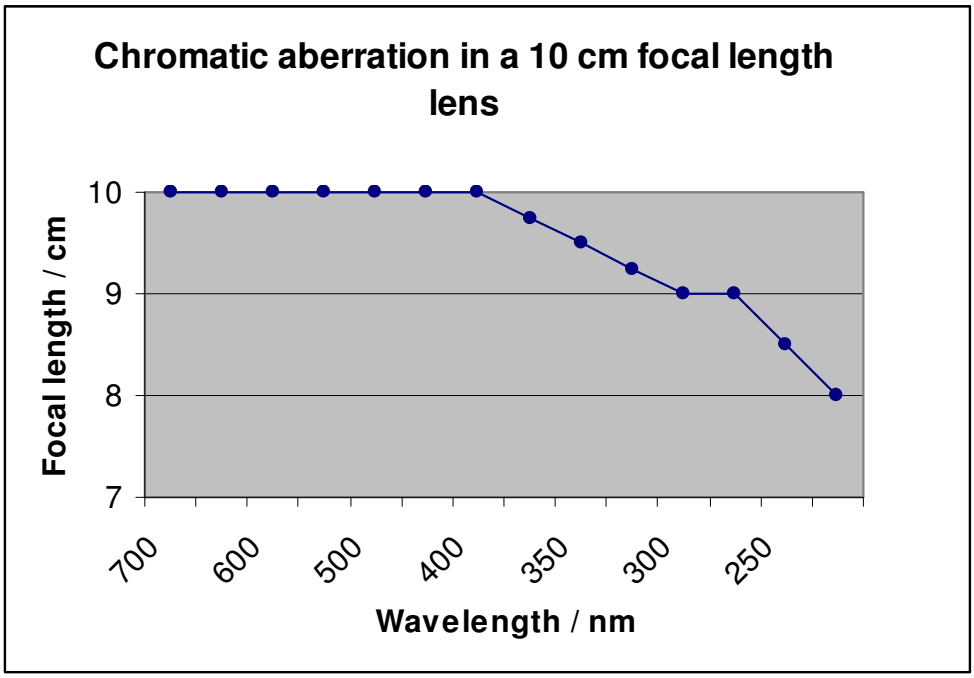

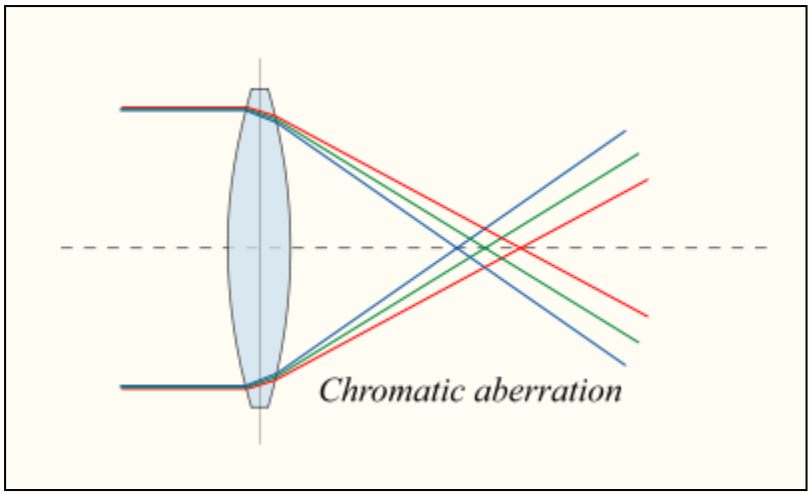

Figure 2.10: Diagram to illustrate the effect of longitudinal chromatic aberration on a light beam. (Image taken from http://en.wikipedia.org/wiki/File:Lens6a.svg)

Some optical applications do not allow for a simple increase in the focal length of lenses used and so a number of specialist lenses have been developed to counter this problem throughout the history of optics. Achromatic lenses were first developed in the 1750's, followed by the invention of the superior apochromatic lens in 1763. Current lenses devised to reduce chromatic aberration are based on the superachromatic design, invented by Max Herzberger in 1963 [13]. However, these lenses are only available in the IR and visible light regions. A UV superapochromatic lens has unfortunately not yet been developed. This is due in part to the difficulty of developing a composite UV lens with the very limited materials available that can successfully transmit UV light, but also because the applications of such a lens are a lot more limited than for visible region applications. Chromatic aberration in UV applications therefore remains an issue to be addressed.

In the case of caCD, the change in wavelength has a big impact on the focal length of the lens, shifting the convergence point by as much as 20% at the lowest observable wavelength (data shown in table 2.2). As the spectrophotometer moves into the UV region, the focal length decreases as the focusing effect of the lens becomes less pronounced. As a result, less light reaches the detector overall since the light beam diverges more as the energy of the light beam increases.

In this instance, the interesting optics of the capillary has proven advantageous. Taking advantage of the net focusing effect of the capillary, the lensing effect observed can help refocus the light – the greater the chromatic aberration, the greater the focusing effect of the capillary.

The issue with the alignment cell was found to be the lack of reproducibility and reliability of the method when compared to a 'fixed' optical path. We postulate that the movement of the lens itself was generating a degree of transverse aberration at a given wavelength, resulting in data that were not of sufficient quality.
This meant that the data were neither repeatable nor reliable, both of which are absolutely essential in a scientific quantitative instrument. Therefore a new design was made, building on the successes of the previous design whilst improving upon its weaknesses.

2.2.6 caCD cell final design

The caCD alignment cell design had been successful in a large number of areas, with the number of optical components in the cell minimised. However, the optics of the caCD device were still not user-friendly, with many of the components easy to accidentally move from their aligned state. To this end, a fixed placement for focusing lens was constructed, to ensure proper focusing onto the capillary itself (figure 2.11). The focusing lens was placed in close proximity to the light beam's entrance to the sample chamber with a minimum of masking, allowing the light to be collected by the lens before any real divergence could occur. This fixed-position cell proved very effective– the data generated were highly reproducible, with very good spectral shape and magnitude. However, the spectra recorded were not perfect. There were still differences between the cuvette spectrum and the capillary spectrum of any given compound, with certain regions of the spectrum suffering more significantly in quality.

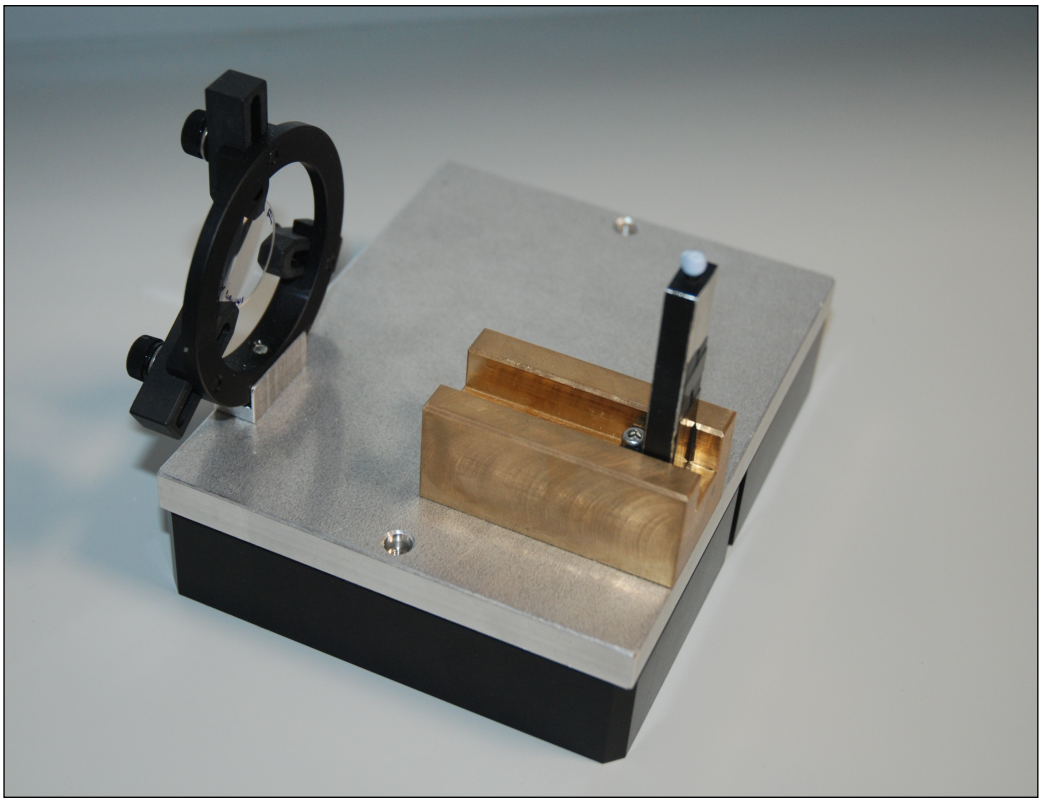

Figure 2.11: Final design for the caCD cell. Building on the concepts of the alignment cell, this cell locks all the optical components in place to consistently generate high quality spectra.

The optical arrangement of the caCD cell at this point was well-aligned and reproducible – the entirety of the exit light beam entered the detector. However, when looking at the HT trace for the capillary spectra, a curious spectral artefact was discovered. As a CD spectrum moves downwards in wavelength, the CD absorbance of the system increases, from the solvent, analyte molecule and the quartz of the cuvette. For the vast majority of CD spectra the meaningful data that can be extracted from the sample is limited by the transmission of the quartz that comprises the sample holder. When the transmission limit of the quartz holder is reached, the HT trace for the spectrum shoots upward. Often referred to as the absorbance 'cut-off', this is typically what happens when the absorbance limit of the spectrophotometer is reached. However, in the case of the capillary cell, the HT trace rose steadily, increasing incrementally as wavelength decreased. This incremental, rather than sharp HT increase is indicative of scattered light entering the detector of the spectrophotometer. After investigation it became apparent that this effect was created through light scattering from the capillary itself as the light beam passed through it.

One of the largest losses of light from quartz is its reflection of light. According to Hereaus (a supplier of optical grade quartz, see http://heraeus-quarzglas.com for more information), 10% of light in the DUV is lost through reflection losses as it passes through a quartz window. This loss is incurred in each phase transition that passes through quartz.

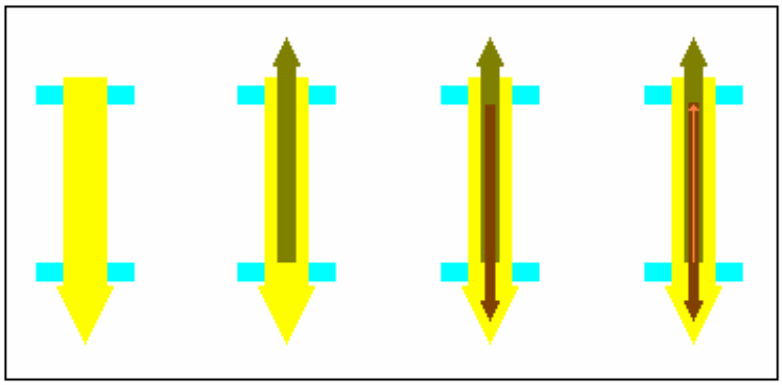

Figure 2.12: Reflected light between two surfaces. From left to right: As the light beam hits a transmitting surface, some of the light is reflected backwards. Part of this light is in turn reflected, creating additional optical changes.

Assuming that 10% of the light is reflected from each surface, then 10% of reflected light is in turn reflected back onto its original direction, i.e. entering the detector. This is a trivial issue when using cuvettes, as the reflected light travels back and forth along the propagation direction of the light beam. However, when using capillaries, the reflections occurring from a curved surface lead to extensive light scattering. In order to counter this, a number of masks for the capillary holder were tested. It was found that masking the horizontal plane was insufficient and so the final mask design was to block out all light from the capillary with the exception of light that was travelling directly along the normal relative to the capillary (i.e. light that passed directly through the centre).

These changes completed, we finally started generating caCD spectra matching those of the cuvette, using only a fraction of the sample required for cuvette CD (figure 2.13).

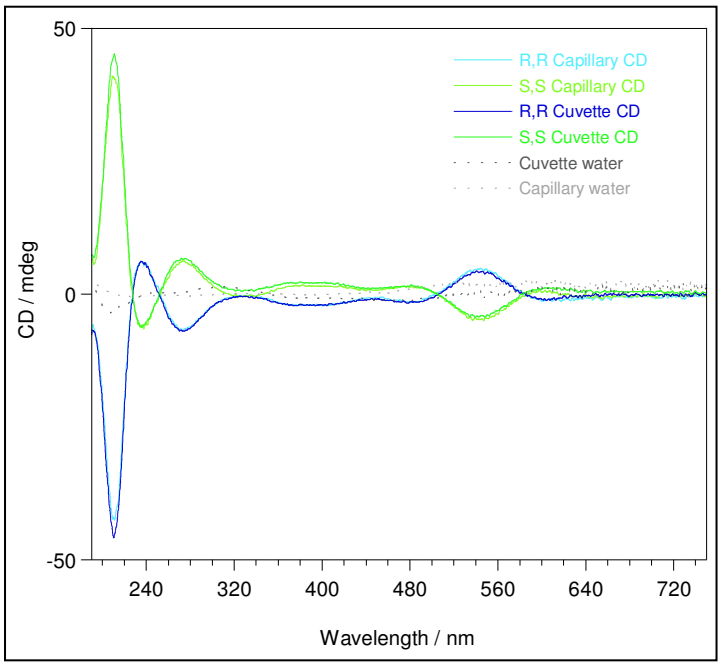

Figure 2.13: Na [Co (Edds)].H_2O 0.55 mM spectra acquired through both cuvette CD and caCD. The caCD spectra were acquired using the final design of caCD base plate. The path-length of the capillary was 1.12 mm, determined using potassium dichromate. Spectra scaled using a 0.892 correction factor to account for path-length differences. The path-length of the cuvette was 1 mm, verified with potassium dichromate.

2.3 Materials and methods

caCD cell design and fabrication

The caCD cell was designed to fit on a standard Jasco CD base-plate. The base-plate was constructed out of aluminium before being anodised.

The lens holder was also constructed out of aluminium, bolted to the base-plate with an internal dowel joint. In addition to this, the capillary holder was also fabricated out of aluminium. Both of these components were also anodised.

Loading the capillary

The key to successful capillary CD once the system was build was designing an effective method of loading the sample into the capillary. The capillary, with its ID (internal diameter) of 1.1 mm, is small indeed compared with standard pipette tips, which proved inadequate to load sample into the capillary. In addition, one aperture

must be closed in order to hold the liquid within the confines of the capillary; failure to do so allowed the sample to slowly flow out of the capillary as soon as it was stood vertically. This is because the liquid inside the capillary is held in place via capillary action – with both apertures open gravity will cause the sample to flow out of the capillary. In order to load the sample into the capillary, a long thin pipette tip capable of fully penetrating the capillary is necessary to position the sample to the correct height. In initial tests, a 5 µl steel syringe was used to load the sample. The syringe was very fine (with a diameter of 0.4 mm) and fitted well inside the capillary. However, it only carried a sample volume of 5 µl. This was problematic as for the majority of capillary CD a sample size of approximately 20 µl was used, allowing greater ease of sample alignment in the light beam. Another issue was the material used in the syringe. Fused silica (a purified version of quartz) has a value of 7 on the Mohr scale of hardness (for comparison, diamond has a value of 10 whilst a human fingernail has a value of 2.5). This value of 7 is very close to the value of stainless steel, 6.5. In practical terms this means that the quartz of the capillary can be quite easily scratched with the syringe, resulting in optical abnormalities within the capillary. These scratches can detrimentally affect the optical performance of the capillary, inducing extensive light scattering and refracting a proportion of the light. However, with due care taken in the handling of the syringe, this can be avoided.

After extensive testing, the syringe concept was dropped in favour of gel-loading tips. Whilst the tips could not be used to probe the entire length of the capillary, they could be used to fill the capillary half-way. By employing a removable seal on the capillary Listed below are the materials required to successfully acquire a caCD spectrum. The materials and equipment list is immediately followed by detailed operational instructions. After extensive testing, the syringe concept was dropped in favour of gel-loading tips. Whilst the tips could not be used to probe the entire length of the capillary, they could be used to fill the capillary half-way. By employing a removable seal on the capillary it is therefore possible to fill a single capillary with both analyte sample and the solvent baseline, with a minimum sample volume required of 3 µl.

The following standard operating procedure was designed to help the capillary CD user to optimise both the loading of the sample into the capillary and the optical alignment of the light beam through the sample.

Capillary Circular Dichroism (caCD)

Standard Operating Procedure:

Materials	Equipment
Distilled water	Fused silica capillary (Crystal Precision Optics)
Ethanol	Anodised Capillary holder (Crystal Precision Optics)
Analysis sample	Two anodised optical lens holders (Crystal Precision Optics)
Analysis buffer	100 mm DCX uncoated fused silica lens (Edmund Optics)
Bingham plastic (e.g. Blu-Tac)	Allen keys (watchmaker size)
White cardboard (e.g. Business ca	Gilson pipettes and tips (Gilson)
	Gel loading tips
	Spectropolarimeter, with a large sample compartment (Jasco
	Anodised base-plate (Crystal Precision Optics)

The caCD cell

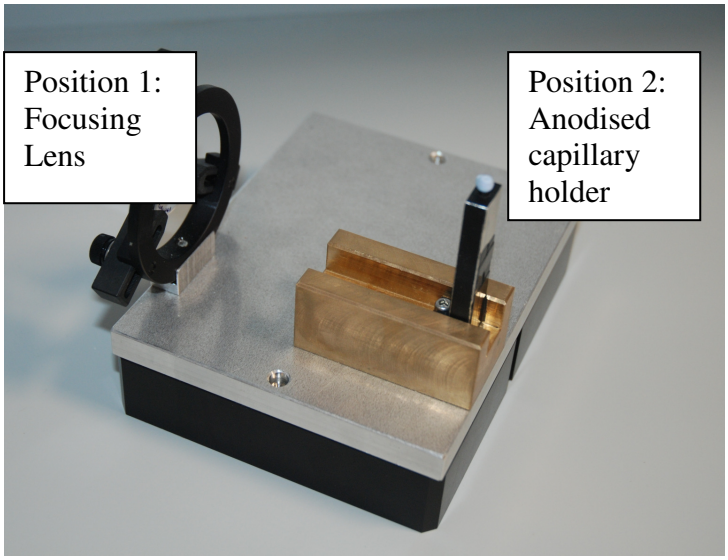

Figure 2.14: The caCD sample cell.

Procedure

Step 1: Alignment of the light beam

1.1 Attach the anodised capillary holder to the anodised base plate at position two on the caCD base plate (see figure 2.14).

1.2 Place the empty fused silica capillary (henceforth referred to as the capillary) into the anodised capillary holder.

1.3 Take the DCX lens and fit it inside the anodised optical lens holder. Take care to not leave any fingerprints on the surface of the lens. Clean with an optical tissue if necessary.

1.4 Attach the lens holder to the anodised base-plate at position 1 so that the lens is positioned within the light path of the spectropolarimeter. The centre of the lens holder should be 105 mm away from the centre of the capillary holder. Errors in the positioning of the focusing lens will result in a poor quality spectrum.

1.5 Remove the capillary from the capillary holder for sample loading.

Step 2: Sample loading

2.1 Place the capillary sideways and flat onto a table, ensuring the capillary does not start to roll around.

2.2 Taking a 2–20 µl pipette, attach a P100 Gilson tip to the end of the device.

2.3 Load the analyte sample into the pipette.

2.4 'Piggyback' a gel loading tip onto the P100 tip, so that the Gilson pipette now has two pipette tips.

2.5 Carefully position the end of the gel loading tip within the confines of the capillary. Leave at least a 5 mm gap between the end of the gel loading tip and the end of the capillary.

2.6 Slowly introduce the analysis sample into the capillary. During injection, ensure that the liquid is brought into contact with both walls of the capillary. The sample is then held in place via capillary action. Push the sample using the pipette to the correct point of the capillary to ensure that light passes through it.

2.7 Take 2 mm^3 of Bingham plastic (e.g. Blu-Tac) and place it over the aperture closest to the analyte sample. During placement the sealant should cover the open surface of the capillary in such a manner as to completely seal the aperture. Ensure that no excess sealant is in contact with the sides of the capillary.

Optional (If user wishes to load the baseline sample and analysis sample at the same time)

It is possible to load both the analysis sample and the baseline sample at the same time in the capillary system. Should you wish to load two samples at a time, in addition to prior instructions follow these guidelines 2.8-2.14.

2.8 Remove both the gel loading and the P100 tips from the pipette.

2.9 Attach a fresh P100 tip to the pipette.

2.10 Take the analysis buffer and load it into the pipette.

2.11 'Piggyback' a gel loading tip onto the P100 tip, so that the Gilson pipette now has two pipette tips on it.

2.12 Carefully place the gel loading tip within the confines of the capillary, using the aperture opposite from that already used to introduce the analyte sample. Leave a 10 mm gap between the end of the gel loading tip and open end of the capillary.

2.13 Slowly introduce the analysis buffer into the capillary. During injection, ensure that the liquid is brought into contact with both walls of the capillary.

2.14 Take 2 mm^3 of Bingham plastic (e.g. Blu-Tac) and place it over the open aperture, i.e. the one not already sealed using Blu-Tac. During placement the sealant should cover the open surface of the capillary in such a manner as to completely seal the aperture. Ensure that no excess sealant is in contact with the sides of the capillary.

Step 3: Optical alignment of the capillary

3.1 Place the loaded capillary into the anodised capillary holder, with the Bingham plastic seal facing upwards.

3.2 Test the optical alignment by moving to a wavelength of 530 nm on the spectrophotometer.

3.3 The light path should hit the centre of the sample inside the capillary. If this is not the case, raise or lower the capillary or sample to bring the solution in line with the light beam.

3.4 The light beam should exit the capillary and enter the aperture which leads to the photomultiplier tube. Place a piece of white card between the capillary and the photomultiplier tube of the spectrometer. This will show the shape of the exit beam as it enters the photomultiplier tube. The entirety of the exit beam should enter the photo-multiplier tube. If this is not the case, check the lens is securely in place, i.e. in a perfect straight line before the centre of the capillary.

Step 4: Acquisition of spectrum

4.1 Check the optical alignment of the sample using the methodology set out in steps 3.2, 3.3 and 3.4.

4.2 Record a spectrum of the analysis sample using the same parameters as those used for the analysis buffer.

Step 5: Cleaning of the capillary

5.1 Upon completion of your CD spectrum, remove the capillary from the anodised capillary holder.

5.2 Gently remove the Bingham plastic seal from the top of the capillary. As you remove the seal, the resultant air flow will cause the swift exit of the sample material from the capillary. Should the sample remain in place, wash the sample out by passing a small volume of distilled water through the capillary.

5.3 Wash the capillary by flowing 20 ml of distilled water through the internal diameter.

5.4 Flow 20 ml of ethanol solution through the capillary.

5.5 Repeat steps 5.3 – 5.4 twice more to ensure vigorous cleaning of the capillary. If protein has still stuck to the surface (as shown by a water spectrum with protein shape) then a more vigorous cleaning agent is required. For more thorough cleaning soak the capillary in 2% Hellmanex solution at 75 ºC for 5 minutes. In extreme cases place the capillary in a 50% nitric acid 50% distilled water solution. This washing mixture should remove any biological molecule which has bound to the surface of the capillary.

5.6 Dry the capillary using a blast of oil free pressurised air or nitrogen to evaporate any remaining liquid residue. The capillary should now be suitable for re-use or storage.

2.4 Results and Discussion

2.4.1 Capillary CD quality compared to Cuvette CD

The sample savings for caCD are immensely useful, but this is of no value if the data produced is of a low quality. In order to confirm the utility of caCD as a spectroscopic technique, we therefore acquired spectra from both cuvette and caCD instruments using the same samples. The CD spectra recorded from such data should therefore be directly comparable to one another, the differences in the recorded spectra negligible.

The data shown for the capillary spectra have been adjusted for path-length. Using a K_2CrO_4 standard at 0.002 M the path-length of the capillary cell was calculated for each capillary using a Jasco V660 UV/vis spectrophotometer. The correction factor used for each set of spectra is shown below the corresponding figure.

Na[Co(EDDS)].H2O

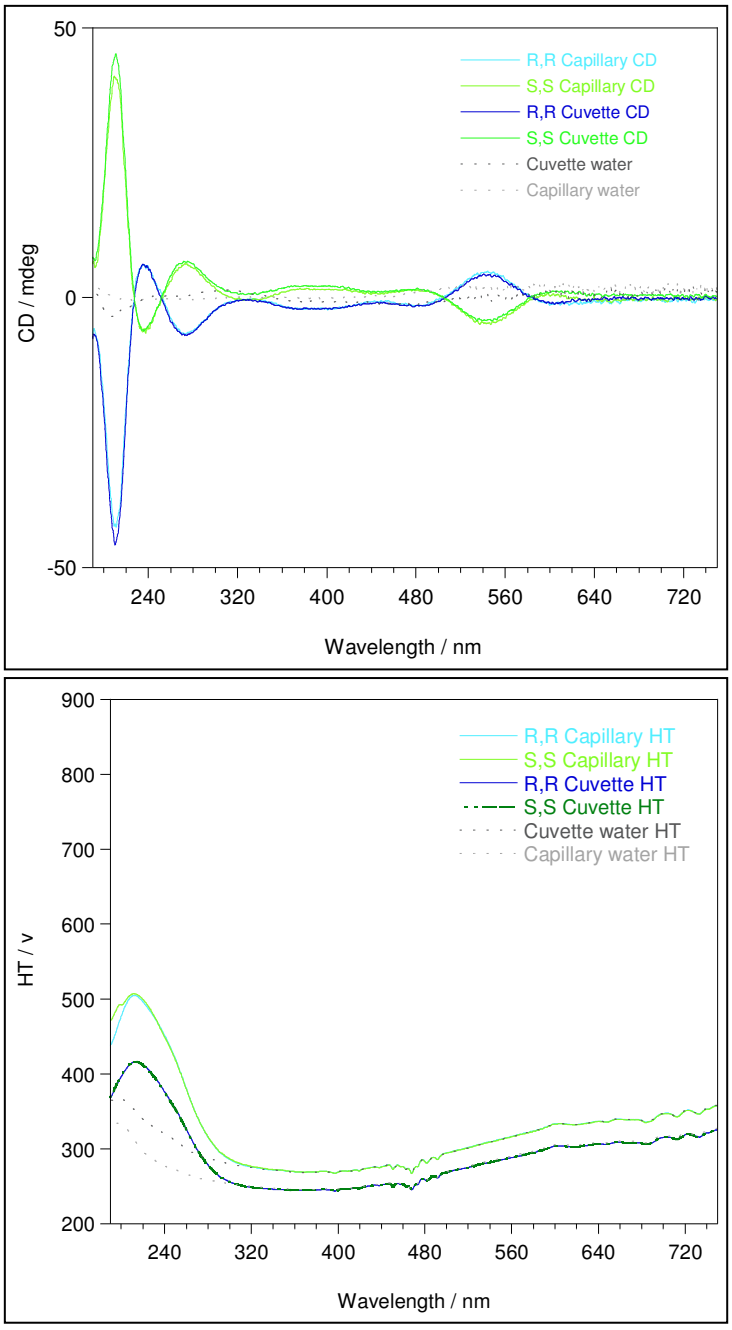

Figure 2.15: CD spectra, with separate HT trace, of Na [Co (EDDS)].H_2O (0.55 mM in water) in a cuvette (1 mm path length) and capillary (1.12 mm path length, data divided by 1.12 to facilitate comparison). The RR spectra have been multiplied by minus 1 for ease of comparison.

Na[Co(EDDS)].H_2O[12] is a new industry standard for the testing of CD spectrophotometers. With several CD peaks across the entire UV/Visible region, CoEDDS allows the researcher to test new instrumentation with a revolutionary

thoroughness which was previously impossible with older standards such as ammonium d-10-camphorsulfonate. Comprised of two separate solutions, the R,R form and the S,S form, CoEDDs allows for the testing not only of the full wavelength range but also for sensitivity to both R and L forms of circularly polarised light. The R,R and S,S forms should generate equal and opposite CD spectra, resulting in highly useful CD spectra. Throughout the caCD project, CoEDDs was used as a spectroscopic test to see if the caCD cell had been optimised. Initial work with the CoEDDs saw the capillary spectrum being different from the spectrum acquired using a cuvette. Several areas of the capillary spectrum failed to correlate with either the cuvette data or the published data. However, in the final design for the caCD cell, the spectra shown in figure 2.15 were generated, showing very close magnitude and spectral shape to that recorded through the use of cuvette CD.

Looking at the HT trace for the various spectra, it is apparent that the HT traces for caCD spectra are once again consistently higher than the HT traces for the cuvette spectra. This said, the HT for the spectrum remains well within the instrument's tolerance (600 V) and so does not impinge upon its performance as a technique. This may become more of an issue were caCD applied to more DUV applications, including the difficulty in securing high quality extruded fused silica capillaries.

Aside from that, the spectra overlay very well indeed, opening the way forward for low-volume CD spectroscopy. It should also be noted that CoEDDs allows the development of new instrumentation to be implemented with revolutionary thoroughness, enabling the designer to identify exactly which parts of the CD spectra need attention.

Lysozyme

In figure 2.16 we wanted to test both the effectiveness of the capillary cell as well as whether or not we had properly controlled the light beam going through the capillary.

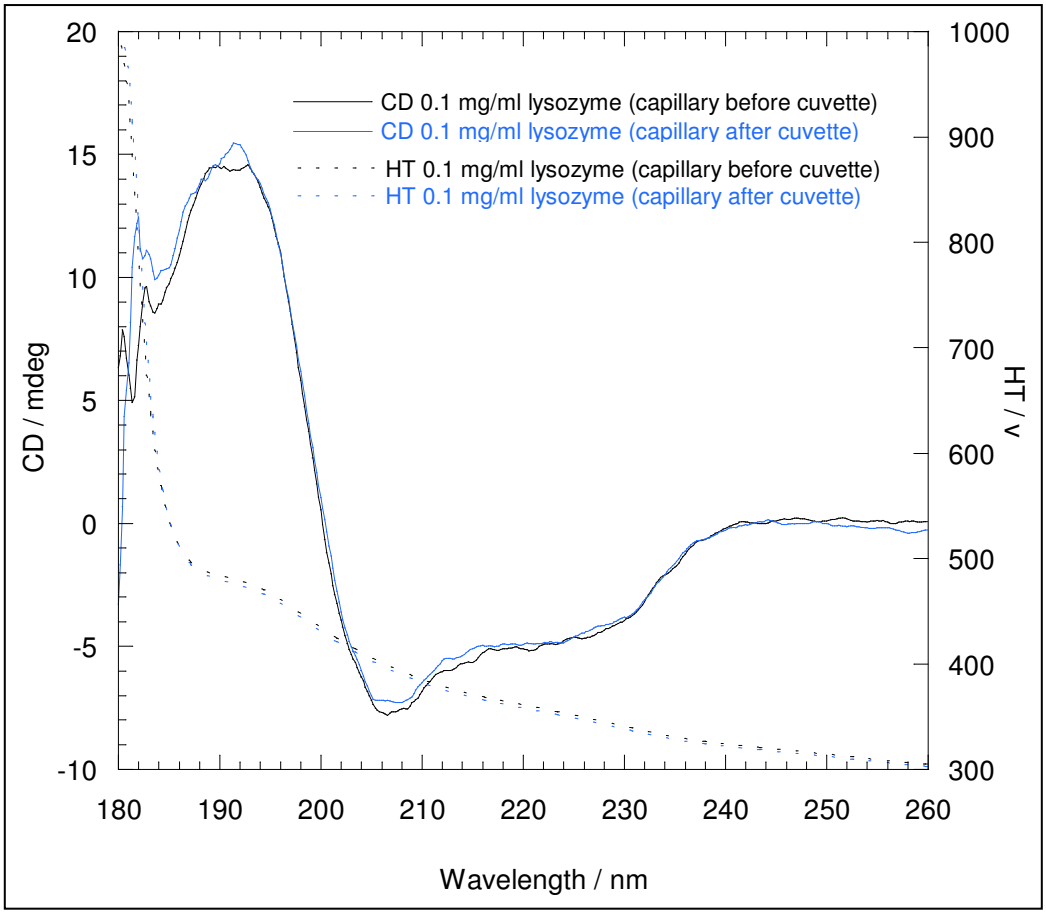

Figure 2.16: CD spectra of lysozyme (0.1 mg/ml) in a cuvette of 1 mm path length). Capillary before cuvette denotes CD measured in a cuvette located before a water-filled capillary. Similarly, capillary after cuvette denotes a spectrum measured in a cuvette placed after the light beam has passed through a water-filled capillary.

In order to fully assess the impact of the capillary on the CD spectra recorded using caCD, we took the CD spectra of lysozyme with a water filled capillary both before and after the sample cuvette. This experiment showed that the spectral shape is broadly similar and that only very small changes can be observed between having a capillary placed before or after the light beam has gone through the sample. This is entirely consistent for an optical system with the sample components but placed in a different order. Whilst not overlaying directly with the caCD/cuvette plots, we believe the small lateral shift can be ascribed to the addition of an optical component. The small UV artefact is still observed in these spectra, forming a consensus with other spectra collected using caCD.

Concanavalin A

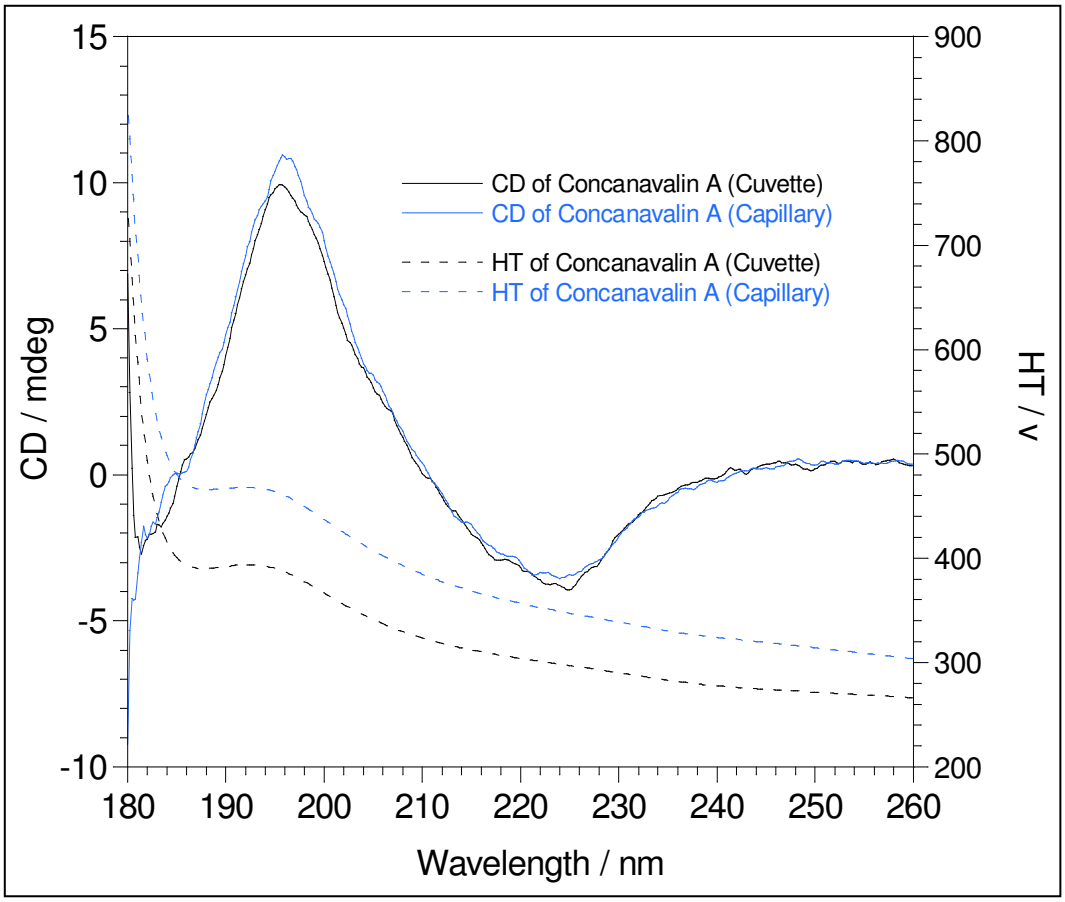

Figure 2.17: CD spectra, with HT traces overlaid, of Concanavalin A (0.1 mg/ml) in a cuvette (1 mm path length) and a capillary (1.19 mm path length, data divided by 1.19 to facilitate comparison).

Figure 2.17 shows a very strong correlation between the capillary spectrum and the cuvette spectrum. Concanavalin A is a protein comprised of predominantly β-sheet secondary structure that can be clearly seen in the above spectra.

Progesterone

The spectra for progesterone in figure 2.18 suggest that the rise in the HT at low wavelength renders the capillary data less reliable. Throughout the wavelength range the HT voltage is higher for the capillary than the cuvette, which reduces the concentration range that can be studied. However, within the range that can be studied, there is once again a very strong correlation between the capillary data and the cuvette data, confirming the reliability and accuracy of the technique.

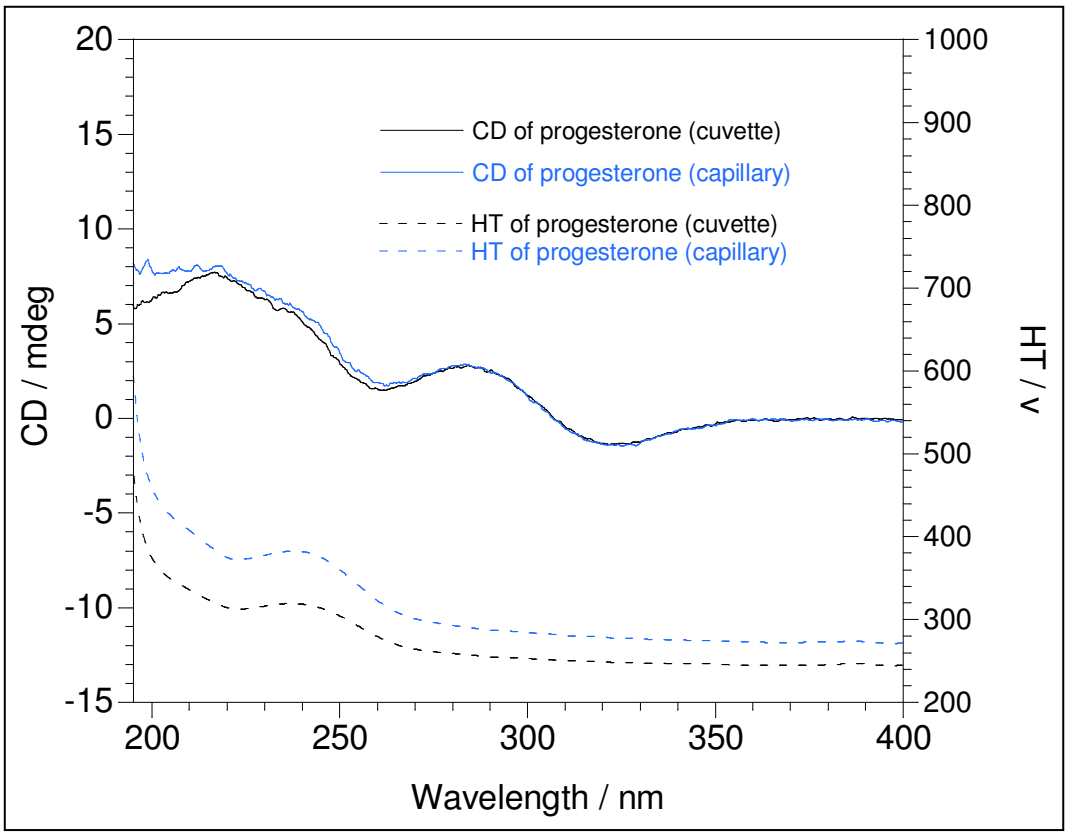

Figure 2.18: CD spectra, with HT traces overlaid, of progesterone (0.1 mg/ml) in a cuvette (1 mm path length) and capillary (1.16 mm path length, data divided by 1.16 to facilitate comparison).

2.4.2 New experiments facilitated by the development of CaCD

The reduction in sample volume offered by caCD is very useful in a number of ways for CD users, most obviously in lowering sample requirements but also in terms of opening up new experiments for study. Many experiments require reagents that are simply too expensive to be feasible using current CD sample sizes, or in certain other cases e.g. when a novel protein supply of the sample is too limited to allow CD analysis. Below we describe two experiments that would have been too expensive to carry out using cuvette CD but have been possible using CaCD.

YOYO-1 DNA binding

YOYO-1 is a bis-intercalating fluorescent dye that exhibits a strong fluorescence enhancement upon binding to double stranded DNA. YOYO-1's use is widespread in the study of DNA, especially its statistical-mechanical properties. While very useful, the cost of the dye is high (£366 for 200 µl from Invitrogen, correct as of January 2011), limiting its use in high-volume applications. In this experiment YOYO-1

Iodide was added to 200 mM calf thymus DNA in a 1:2 and a 1:20 ratio. We also acquired the spectrum of the DNA without any YOYO.

As can be seen from figure 2.19, the addition of YOYO-1 very effectively disrupts the structure of the double stranded DNA. The iodide counter-ion (and presence of DMSO) cut the CD spectrum of the YOYO samples below 230 nm, but the band at 280 is clearly visible.

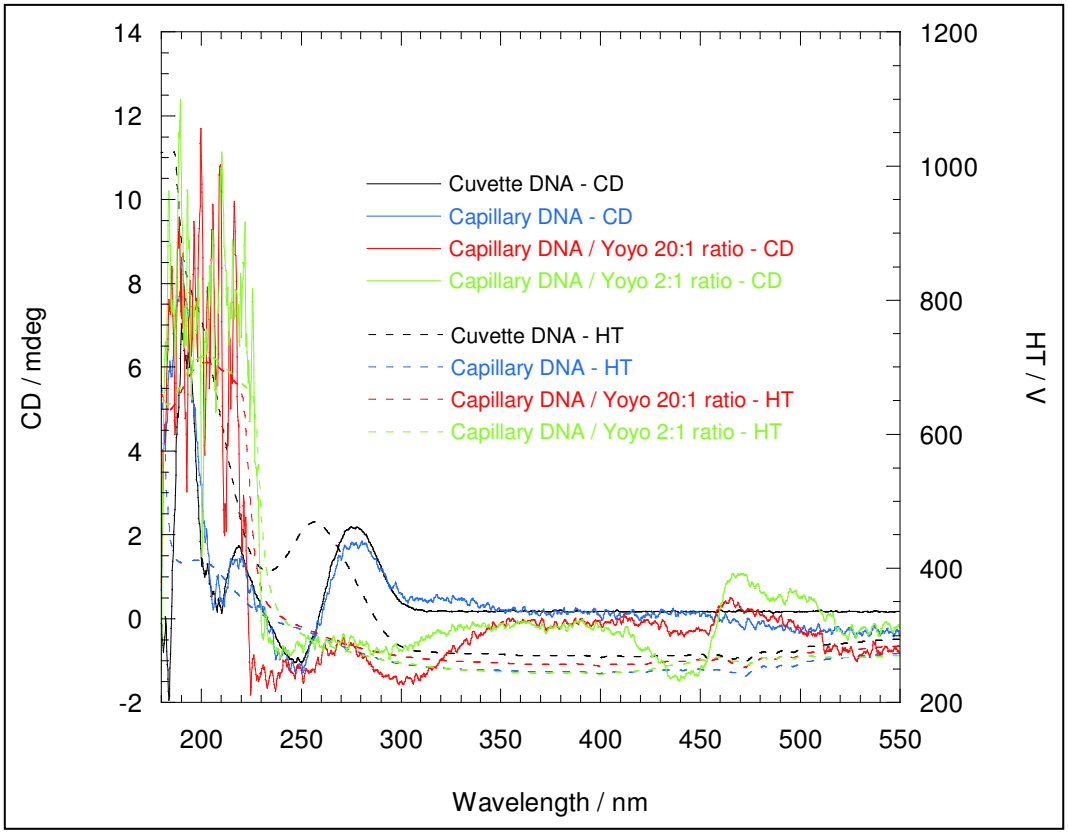

Figure 2.19: CD spectra, with HT traces overlaid, of calf thymus DNA (200 µM) in a cuvette (1 mm path length) and capillary (1.16 mm path length, data divided by 1.16 to facilitate comparison). YOYO-1 was added to the DNA prior to be being placed in the capillary.

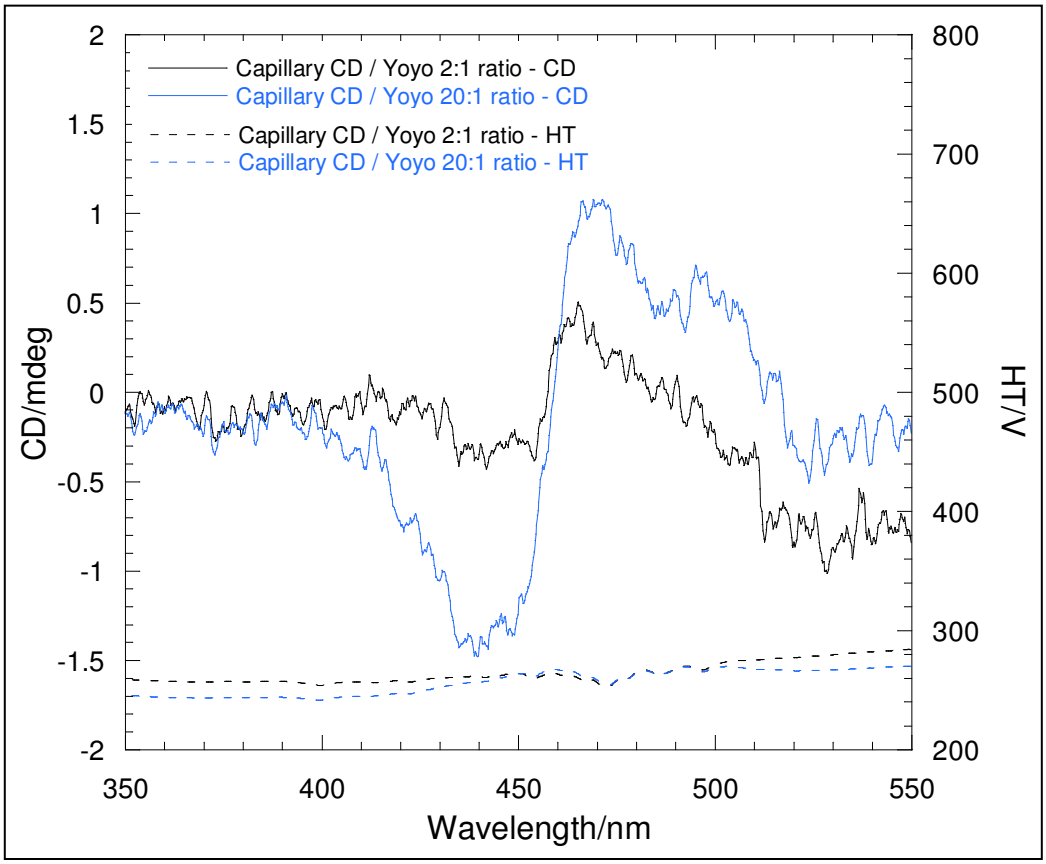

Figure 2.20: YOYO exciton CD spectra, with Ht traces overlaid, of YOYO-1 bound to 200 µM calf thymus DNA in a capillary (1.16 mm path length). YOYO-1 was added to the DNA prior to be being placed in the capillary.In addition to intercalating,

YOYO-1 can also produce an exciton band (figure 2.20). More interestingly, the presence of an exciton band can be quite clearly observed in the YOYO spectra between 400 and 500 nm. This coupling of YOYO molecules at this concentration is almost certainly intra-molecular[15]. The difference in the exciton bands between the 2:1 YOYO and the 20:1 YOYO can be explained in terms of intercalator binding sites. Once all intercalator binding sites have been filled, then external binding between the DNA and YOYO occurs, increasing the likelihood of intra-molecular interactions and by extension the signal of the exciton coupling.

Whilst this experiment was possible[15] using cuvette CD, the cost of a single spectrum CD using that method would have been significantly larger, due to the extra material required to generate a CD spectrum using that sample holder.

CoEDDS scattering experiment

Another experiment that we have often thought to try but could not easily afford was an investigation into the effect of scattering on CD spectra. Light scattering is a constant problem in spectroscopy, reducing both data quality and photon flux. In this instance, we wanted to investigate the consequences of light scattering on the recorded CD spectrum itself. Whilst increased voltage in the HT reading was anticipated, we were unsure about the effect on the shape and magnitude of the CD signal itself.

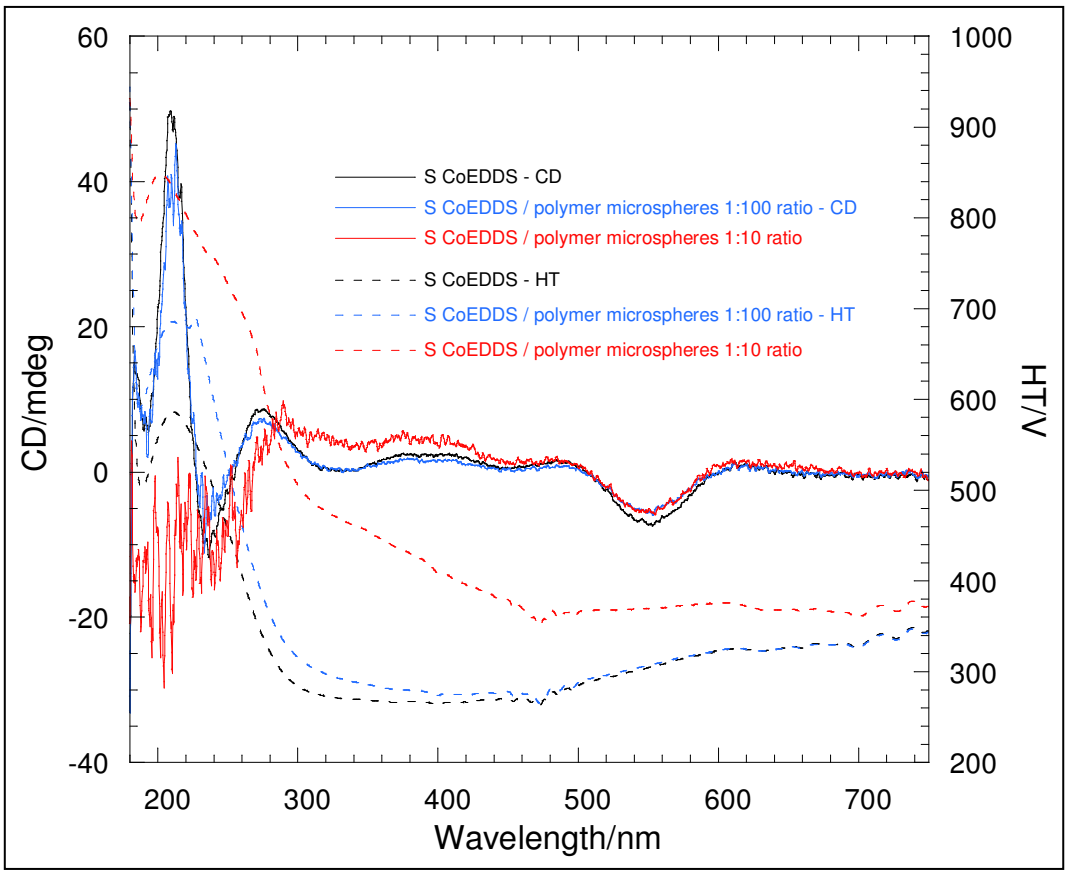

Figure 2.21: CD spectra, with HT traces overlaid, of 0.5 mM S,S COEDDS in the presence of 100 nm polymer spheres.

The R,R form of CoEDDs was also examined, generating a similar result (see figure 2.21).

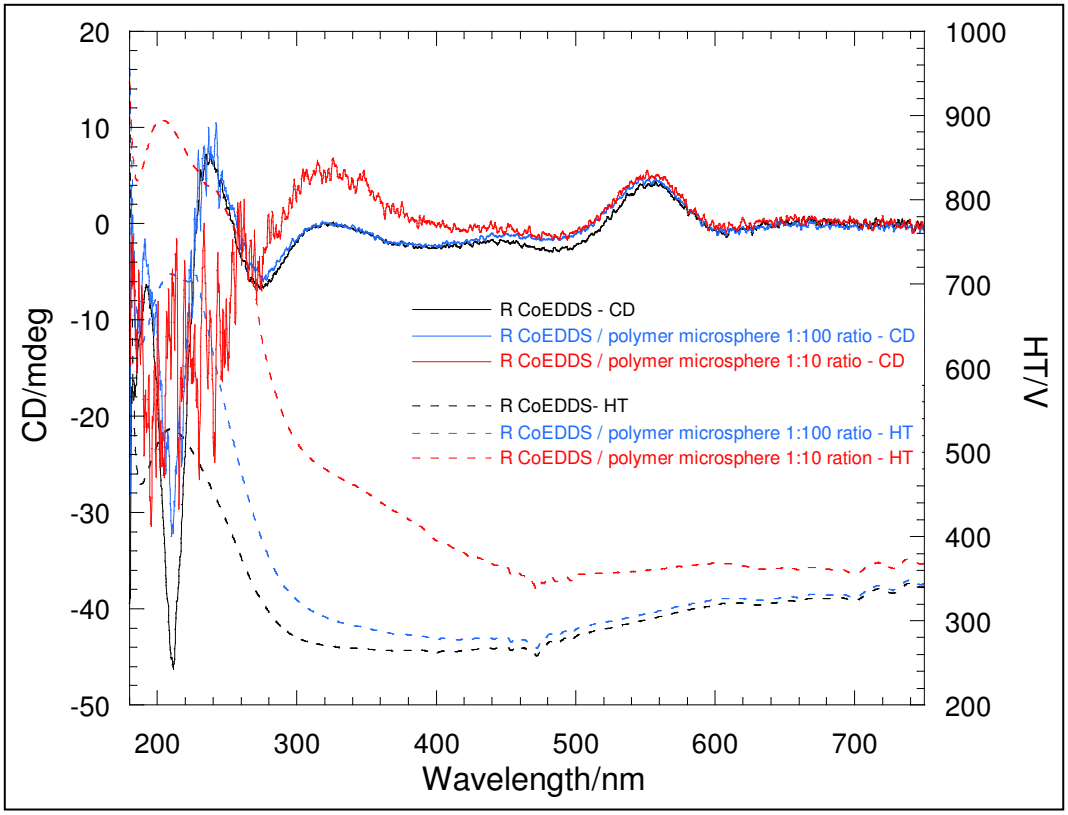

Figure 2.22: CD spectra, with HT traces overlaid, of 0.5 mM R,R COEDDS in the presence of 100 nm polymer spheres.

From figures 2.21 and 2.22, it can be seen that at low polymer concentration the CD signal is not adversely affected. The 600V HT cut-off is understandably at higher wavelength for both 10:1 and 100:1 samples (for both enantiomers), but it is with the 1:10 ratio that we truly see an interesting change in CD spectrum. From the data it can be seen that there is a bias towards left-handed circularly polarised light absorption in both forms of CoEDDs. This starts happening when the characteristic 'hump' begins to form in the HT reading.

On the basis of this experiment, the data suggests that once a high degree of light scattering is observed in the HT reading, all data points must be questioned, not just those data points past the HT cut-off.

2.5 Conclusion

The aim of this project was to expand the utility of circular dichroism spectroscopy through a reduction of the sample volume required. This reduction was achieved through the use of extruded quartz capillaries as a means of holding the sample within the light beam. A DCX lens was employed to ensure the correct focusing of the light onto the centre of the capillary, the entire ensemble being fitted to an aluminum base-plate suitable for use in a Jasco J-815 spectrophotometer.

It has been shown that caCD lowers the sample requirements for CD spectroscopy by a significant margin; that a spectra which previously would have required a minimum of 200 µl of sample now requires only 3 µl to generate a spectrum of the same quality. In addition, the relatively low cost of the quartz capillary opens up the possibility of single-shot applications for hazardous samples.

caCD is a significant development in the field of CD spectroscopy, combining a reduction of sample requirements by two orders of magnitude with a simple and effective means of sample loading, with ease of cleaning reducing instrument 'dead-time' and thus increasing efficiency.

2.6 References

1: Alison Rodger and Bengt Norden, Circular Dichroism and Linear Dichroism (1997) Oxford University Press

2: Peter J. Sadler, Alan Tucker, Proton NMR studies of bovine serum albumin, 2005, volume 205 pg 631 – 643, European Journal of Biochemistry

3: M. Forstner, SAXS, SANS and X-ray crystallography as complementary methods in the study of biological form and function, 2000, 33, 519 – 523, Journal of Applied Crystallography

4: Andrew J. Miles and B.A. Wallace, Synchrotron radiation circular dichroism spectroscopy of proteins and applications in structural and functional genomics, 2006, 35, 39 – 51 Chemical society reviews

5: B.A. Wallace and Robert W. Janes, Synchrotron radiation circular dichroism spectroscopy of proteins: secondary structure, fold recognition and structural genomics, 2001, 5, 567 – 571, Current Opinion in Chemical Biology

5: Reidar Lyng, Alison Rodger, Bengt Norden, The CD of ligand-DNA systems .2. Poly (dA-dt) B-DNA, 1992, 1201 – 1214, Biopolymers

6: D.P. Arya, T.C. Bruice, Triple-helix formation of DNA oligomers with methylthiourea-linked nucleosides (DNmt): A kinetic and thermodynamic analysis, 1999, 4384 – 4389, PNAS

7: Masayuki Endo and Tetsuro Majima, Structural arrangement of two DNA double helices using cross-linked oligonucleotide connectors, 2004, 1308 – 1309, Chemical Communications

8: Nuria Escaja, Enrique Pedroso, Manuel Rico, Carlos Gonzalez, Dimeric Solution Structure of Two Cyclic Octamers: Four-Stranded DNA Structures Stabilized by

A:T:A:T and G:C:G:C Tetrads, 2000, 122, 12732 – 12742, Journal of the American Chemical Society

9: G. Mezo, Z. Majer, E. Vass, M.A. Jimenez, D. Andreu, F. Hudecz, Conformational study of linear and cyclic peptides corresponding to the 276-284 epitope region of HSV gD-1, 2003, 103, 51 – 65, Biophysical Chemistry

10: F.Wien, B.A.Wallace, Calcium Fluoride micro cells for synchrotron radiation circular dichroism spectroscopy, 2005, 58, 1109 – 1113, Applied Spectroscopy

11: R. Marrington, T.R. Dafforn, D.J. Hasall, J.I., MacDonald, M. Hicks, A. Rodger, Validation of new micro volume Couette flow linear dichroism cells, 2005, 130, 1608 – 1616, The Analyst

12: A. Damianoglou, E. J. Crust, M. R. Hicks, S.E. Howson, A.E. Knight, J. Ravi, P. Scott, A. Rodger, A New Reference Material for UV-visible Circular Dichroism Spectroscopy, 2008, 20, 1029 – 1038, Chirality

13: M. Herzberger and N McClure, The design of superachromatic lenses, 1963, 2, 553 – 560, Applied Optics

14. K. Gunther, M. Mertig, R. Seidel, Mechanical and Structural properties of YOYO-1 complexed DNA, 2010, 38 6526 – 6532, Nucleic Acids Research

15. A. Larsson, C. Carlsson, M. Jonsson, B. Albinsson, Characterization of the Binding of the Fluorescent Dye YO and YOYO to DNA by Polarized Light Spectroscopy, 1994, 116, 8459 8465, JACS

CHAPTER THREE

Development of an etched cuvette of well-defined path-length for circular dichroism spectroscopy

Gagea minima in both visible colour and UV.

CHAPTER THREE: Development of an etched cuvette of well-defined path-length for circular dichroism spectroscopy

Summary

In this chapter we report the development, manufacture and validation of a novel small path-length demountable cuvette of high path-length accuracy and reproducibility. This design is based upon the properties of acid etched quartz optical flats that retain their original surface properties. The holder designed to reproducibly insert the cuvette is also described. The etched cuvette has been designed to be loaded after its assembly, affording the device great potential as an optical component of flow systems.

3.1 Introduction

3.1.1 Rationale for precision CD cuvettes

Circular dichroism is currently recognised as a valid technique for assessing the quality of protein molecules in pharmaceutical preparations by the World Health Organisation[1, 2] as well as the US Food and Drug Administration[3]. CD spectroscopy is an attractive choice for pharmaceutical companies[4] as a means of structure validation for protein molecules, especially in batch to batch verification of biopharmaceutical products. There are however several technical challenges in obtaining a cuvette that is truly suitable for such analyses, as the concentration of formulated products is typically in the region of 1 – 100 mg / mL[5]. These extremely high protein concentrations reduce injection volumes when administering such products and allow large quantities of product to be transported in relatively small volumes. Additionally, should a particular solution require cooling (a temperature of 40ºC can easily denature a protein, causing irrevocable damage to the product) lower volumes are more economical to store and transport. However, at the concentrations which pharmaceutical companies work it is necessary for CD to use a path-length of 10-1 µm. The variable quality of the commercially available cells and their implementation in our hands is shown below and led us to develop a method of producing a well-defined micron-scale unit.

3.2 Materials and methods

3.2.1 Materials

Uncoated UV grade quartz flats of a quality 1/20th of a waveband were purchased from Edmund Optics at ½ inch in diameter. HF and HCl solutions were purchased from Sigma Aldrich at a concentration of 40% and 30% wt. in H_2O respectively.

The etching rig and instrument base-plate were produced by Crystal Precision Optics.

3.2.2 Cuvettes

1 mm and 0.01 mm rectangular cuvettes were both purchased from Starna, Hainault, UK.

3.2.3 Quartz flats

Quartz flats or optical flats, as they are more commonly known, are pieces of quartz that have been polished to a high degree of surface flatness. A surface is said to be optically flat when it deviates by no more than λ/4 from a perfect plane[6] (λ is typically 633 nm, the wavelength of light produced from a standard helium/neon lamp). 12.27 mm uncoated UV grade quartz flats of a quality $1/20^{th}$ of a waveband were purchased from Edmund Optics.

3.2.4 Quartz Etching

The etching rig and instrument base-plate described below were produced by Crystal Precision Optics, Rugby, U.K. Quartz flats were etched by placing them into the etching rig, ensuring that they are firmly seated against the rubber insert. The rig was then placed in a 500 ml plastic beaker of the acid solution (i.e. 40% HF and 30% HCL in a 1:1 ratio), which was in turn placed in an oscillating water bath (SS40 water bath from Grant Instruments), set at the required temperature (30 ºC) with a stroke rate of 60 per minute. The rig was left in the acid for the required time (typically 8 minutes 30 seconds) before being transferred to a 0.1 M solution of $Ca(OH)_2$ for 10 minutes.

HF solutions need to be treated with great care as the acid poses significant risks at any concentration, including but not limited to tissue necrosis and degeneration of bones. Additionally HF is a systemic poison, making its treatment potentially difficult. All components were plastic, Teflon or nylon as HF etches glass and metal.

3.2.5 Methods for assessing the flatness of quartz surfaces

Qualitative interferometry is a method that uses a monochromatic light source of known wavelength to investigate the finish of nanoscale surfaces. Typically a 632.6 nm helium/neon light source is used for this purpose. The quartz is placed upon a reference flat of known flatness, with the air gap between the two flats

creating the characteristic 'fringe' pattern. The flatter the surface the more bands will be shown. A perfectly flat surface will have only straight bands, whilst non-flat surfaces will start to show evidence of contours, in much the same manner as a geographical map. The size and shape of these contours give the user information on the type of surface analysed. Figure 3.1 shows the different interference patterns associated with different types of surface finish.

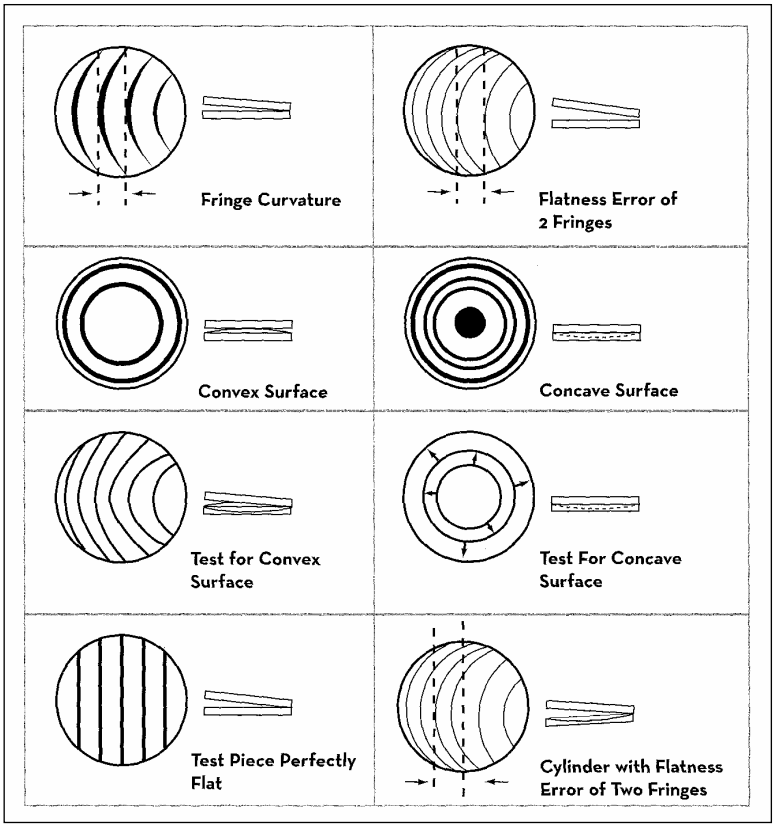

Figure 3.1: Figure illustrating types of interference pattern generated by different surface finishes. Image taken from 'Optical flat manual' Edmund Optics Worldwide.

Quantitative interferometry involves monochromatic light source of known wavelength that shine a concentrated light beam onto a small part of the surface. The light source then traverses across the length of the examined surface, allowing larger areas to be scanned. This allows for measurement of the flatness through interferometry and gives better information about the types of flatness observed on the surface. Nanoscale flatness can be defined in one of two ways. The first, the Ra value can be defined as the average of the peaks and valleys within a surface over 1 micro-inch (μinch) whilst the second measurement, the Rz is the difference between the tallest peak and the deepest valley. The Ra

value is typically a more useful measurement in surface science, although large Rz values can cause a great deal of problems to the surface scientist as particularly large peaks on the surface can cause damage to both instrumentation and to any optically flat surfaces they may come into contact with. In surface science, the Ra value is typically referred to as surface flatness, whilst the Rz value is reffered to as surface roughness.

Quantitative interferometry was carried out using a WYKO NT-1100 Mirau interferometer and a Taylor Hobson Form Talysurf, which uses a Coherence Correlation interferometric measurement method. WYKO interferometry is accurate to 0.1 nm, or a Ra value of 1 Å over 13.1 µm of traverse. Talysurf data is accurate to within 0.1 µm over 20 mm of traverse across a sample.

The spectroscopic interference fringe method *(*Miles *et al*[7]) of path-length determination calculates the size of gap between two pieces of quartz by detecting the interference between the incident light beam and light that has been double reflected between the two surfaces of the cuvette. The interference pattern that is generated in this interaction between the two light beams gives rise to a UV / visible absorbance spectrum that is generated as constructive and destructive interference bands come into view on the cuvette as the wavelength of light changes. The distance between the two surfaces is determined from:

$$\text{Path length } (\mu m) = [(n(\lambda_1 * \lambda_2)/(2(\lambda_2 - \lambda_1))]/1000 \qquad \text{Equation 3.1}$$

Where

n = the number of complete 'fringes' over the wavelength region

λ_1 = is the starting wavelength of the wavelength region

λ_2 = the wavelength of the end of the wavelength region

Chemical absorbance UV spectroscopy using potassium chromate (stabilised with a pellet of KOH) is an industry standard for path-length calculations. This substance can be used to determine the path-length of a filled cell using the absorbance spectrum and the Beer-Lambert law.

$$A = \varepsilon.c.l \qquad \text{Equation 3.2}$$

Where

A = Absorbance

ε = the absorptivity of the chemical species under examination

c = the concentration of the sample

l = path length

3.2.6 Machining

A Colchester Triumph 2000 centre lathe was used to machine circular components, including the hollow nylon tube and parts of the sample cell holder. More complicated components, including the iris holder and base plate were machined using a Toss Universal milling machine. Quartz is a relatively hard material (see appendix two) and so has to be machined using diamond studded cutting surfaces.

3.3 Results and Discussion

3.3.1 Currently available cuvettes

Cuvettes of path-lengths 0.1 mm and upward are typically produced by thermal annealing of five pieces of quartz, of which at least two opposing sides have been polished to a desired flatness.

0.1 mm and shorter path-length cuvettes are made by the assembly of two flat pieces of quartz, into one of which a well for samples has been etched or polished. Typically this well will be curved in shape rather than flat due to the nature of the production process used. The motivation for this work was provided by the interference patterns we measured on a standard 1 mm rectangular CD cuvette (figure 3.2) and a standard nominally 10 micron cuvette (figure 3.3) which we were using to collect CD data on biopharmaceutical products. Figure 3.2 shows evidence of optical flaws, in this instance, a convex arc at the bottom of the cuvette (shown at the top of the picture). The effect is comparatively small in a 1 mm cuvette, but it does mean that the baseline signal will vary across the surface of the sample as does the path length. The imperfections in the 10 µm cuvette are more significant. The ‘saddle’ interference pattern observed in figure 3.3 shows a region of overlapping concave and convex surfaces which will make a significant percentage variation

in path length across the cell as the surface flatness of the quartz varies by several bandwidths of light corresponding to an error greater than 2-3 µm.
A further issue with standard demountable cells is that their path-length depends on how they are assembled including volume of liquid, pressure applied and sample viscosity. It takes significant practice to reduce the error on 10 µm path-lengths to less than 20%.

Figure 3.2: Interferometry pattern of a 1 mm thermally annealed quartz cuvette. The top of the pattern shows evidence of optical flaws (in this instance, a convex surface), reducing the accuracy of the cuvette. This effect is small in a 1 mm cuvette, but can have a big impact when designing cuvettes at the micron level of accuracy.

Figure 3.3: Interferometry pattern of a 'flat' component of a 10 micron path length Starna cuvette. The 'saddle' interference pattern observed here is quite rare, showing a region of overlapping concave and convex surfaces. The errors shown here are well into the micron level of surface error, based on the inference pattern observed here.

The surface error for these two pieces of quartz is significant - the flatness of both surfaces is out by several bandwidths of light. In both instances it is not the quality of the polishing of the material that is remiss- rather, it is in its thickness. Zerodur is a preferred material for the crafting of flats due to its thermal stability. Since there is little to no distortion or expansion of the crystal lattice in Zerodur during the abrasive process of polishing, the polished surface when cool is equally flat as it was during polishing. Quartz is also quite thermally stable, but after polishing it can heat up, distorting the crystal lattice. Whilst being polished, the quartz was likely to have had far better surface flatness, but as soon as the quartz cooled down then the crystal structure would return to its relaxed state, creating these interesting distortion patterns. By using thicker pieces of quartz (no less than 3 mm), it is possible to take advantage of the thermal conductivity of the material, resulting in the creation of a quartz flat after polishing and cooling.

3.3.2 Producing cells of known depth using optical flats

The concept behind a cuvette formed from optical flats is very simple. Our aim was to develop a method to produce a channel that was sufficiently uniform to maintain the original flatness of the surface in the base of the final etched channel. Our target was a rectangular channel/basin within a circular flat. The former to match the light beam geometry and the latter to facilitate assembly of the final cell as described below. Once we had the quartz units, then it was necessary to design a holder that could be used to assemble the cell in exactly the same way every time and enabled us to load the sample after it has been assembled. A schematic of the cross section of the final assembly is illustrated in Figure 3.4.

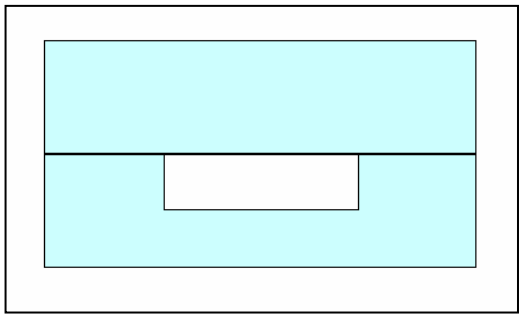

Figure 3.4: An optical flat and an etched optical flat assembled to form a perfectly defined fixed path length cuvette.

The vast majority of methods for producing channels in material involve some form of tooling to machine the required depth. With quartz the very best conventional machining techniques are only able to machine a surface to an accuracy of one twenty thousandth of an inch, or 1.27 micron. For a cell of path length 10 μm, this means an error of 13 %. Additionally, as the surface of channel is not exposed then traditional polishing methods cannot be employed onto the machined material. As a result traditional machining would reduce the optical transmittance of the quartz to a level too low for CD spectroscopy.

We also tried the converse of building up the sides using the epoxy resin SU-8 photoresist which is used extensively in microfludic systems to produce layers from 0.1 micron to 2 mm. Unfortunately, protein samples on occasion adhere to the quartz surface of the cell as such need to be removed using 6 M nitric acid – at this acid concentration the resin was significantly damaged[9]. We therefore chose to etch the quartz by employing methods developed from those found in the literature.

In our initial experiments we established that rapid etching was required otherwise however good the masking (see below), the process undercutting would occur, leading to an etching reaction sideways as well downwards. We first attempted using HF (40% w/v aqueous solution) using the method described above based on the reaction:

$$SiO_2 + 6\ HF \longrightarrow H_2SiF_6 + 2\ H_2O \qquad \text{Equation 3.3}$$

Following the instruction given by Leko et al.[8] it was possible to etch channels of up to 100 micron in ten minutes, whilst maintaining the surface finish. The faster etching rate was achieved using HF and heating up to 50 ºC. As described below the resulting products were flat channels and the depth could be controlled. Unfortunately, the etching rig (figure 3.5) fared less well and was restricted to a single use. Fortunately, we found that if we combined HF (40% w/v) in a 1:1 mixture with HCl (30%) that the rig fared better and the etching was nearly as effective. Table 3.1 summarises the temperature/time combinations with HF/HCl to achieve a given depth channel.

Depth of channel (microns)	Etch time (at 30 ºC)*
10	12 minutes 50 seconds
6.67	8 minutes 30 seconds
5	6 minutes 22 seconds
1	1 minute 16 seconds

Table 3.1 Etch time to depth of channel created.

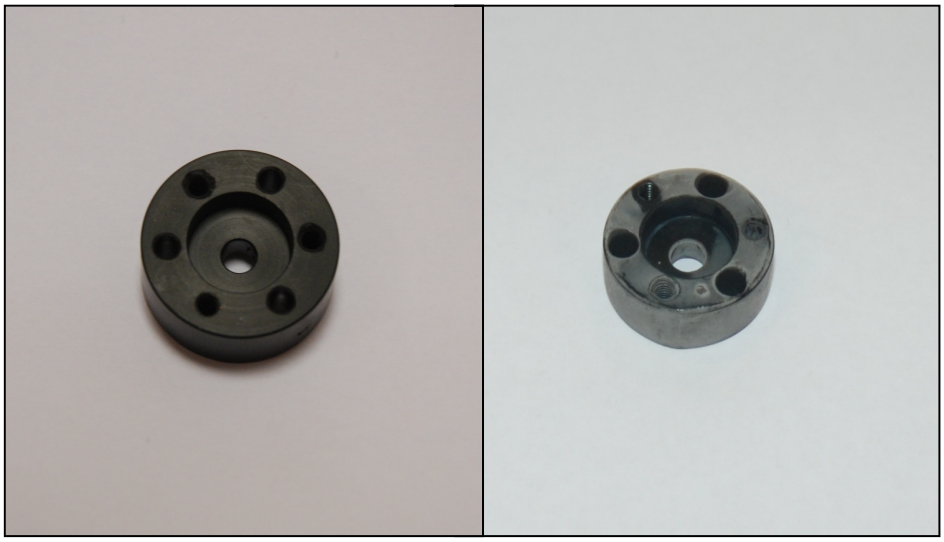

Figure 3.5: The etching rig female component, before (left) and after (right) the etching process. It should be highlighted that after etching, two of the heads of the screws had been so undermined by acid attack that they disintegrated upon removal from the HF solution.

3.3.3 Etching mask

The most important part of this work was the development of an etching rig that could effectively 'mask' the quartz flat to etch the desired shape. Clear nail varnish (ethyl acetate), was tried but led to 'undercutting' during the etching process, with the extreme effect being that the chemical mask often floated away during the etching process. Black nylon is cheap and resistant to acid (though as noted above not completely so to HF).

The etching rig illustrated in Figure 3.6 was fabricated and proved to provide an efficient seal and also readily quenched and cleaned. The quartz flat was a push

fit into the bottom face of the rig; a small hole was drilled in the back of the holder to allow the flat to be 'poked' out. A rubber inset was placed on the side of the flat that was to remain untouched by the acid. The pressure transmitted when the nylon screws were tightened compressed the rubber forming a seal. Three holes were bored into the top face of the rig, to facilitate reclaiming the etching rig from the acid solution once the etching process was complete. The top component was additionally lined with rubber to allow the formation of a proper seal when the rig was fully constructed.

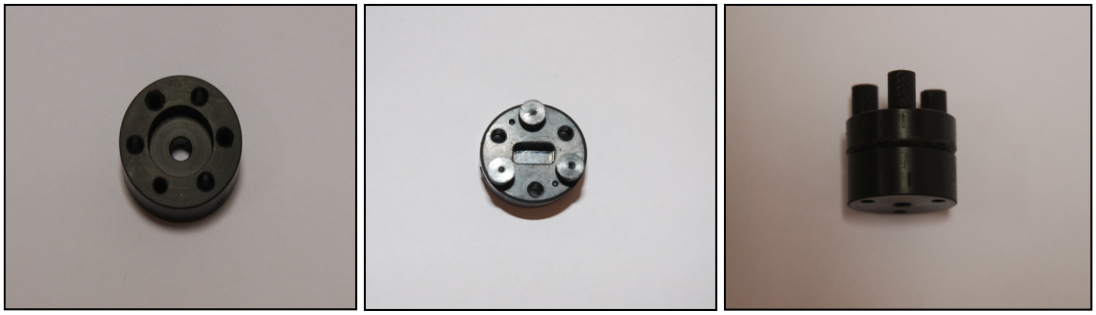

Figure 3.6: (a) Bottom face, (b) top face and (c) side view of the etching rig machined on a lathe in black nylon. The recess in the centre of the bottom was been machined to create a push-fit for a 1 inch diameter cylindrical quartz flats.

3.3.4 Assessment of the surface quality of the etched flat

The effectiveness of the etched cell design hinged on three factors- creating an accurate channel, retaining the surface finish of both the etched and non-etched parts of the flat and finally being able to form an accurate cell from the quartz components.

We employed a variety of techniques to assay the quality of the etched cuvette.

Channel sides (non-etched part of the flat): A Lapmaster monochromatic light source (using a yellow helium light source) was in conjunction with a Zerodur® $1/20^{th}$ of a waveband optical flat used to check the surface finish of the channel sides (figure 3.7). This was confirmed to be $1/20^{th}$ of a waveband or an approximate surface roughness of 30 nm over the region of the flat covered by the interference pattern.

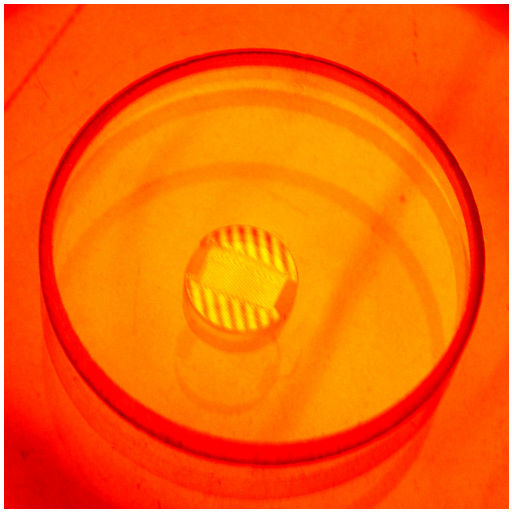

Figure 3.7: Interference pattern of an etched flat. Note the band pattern on both sides of the channel, where optical flatness has been retained.

Channel base (etched part of the flat): A WYKO NT-2000 non contact optical profiler, was used to generate images that show the etched surface of the channel.

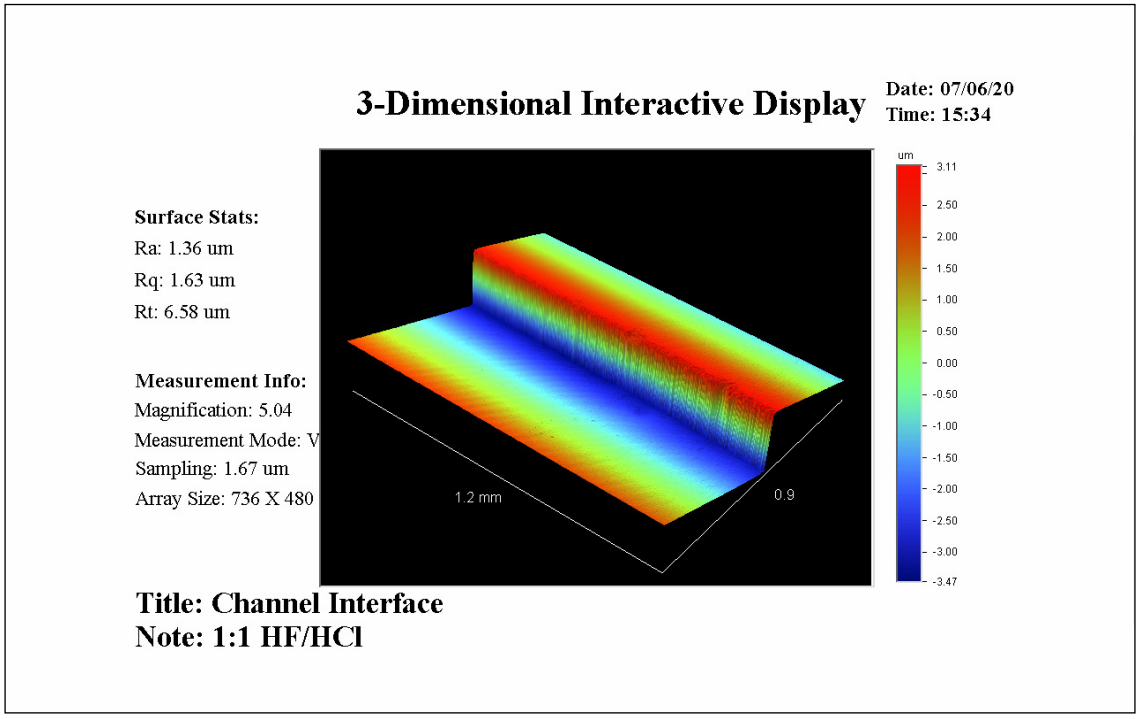

Figure 3.8: WYKO image of a 6.5 µm etched flat channel / plain surface. The surface finish of both the etched and non-etched components is of exceptional quality, in terms of surface roughness and sharpness of interface. There is very little evidence of undercutting or smoothing at the interface, proving the efficacy of the acid mask.

The data shown in figure 3.8 are of excellent quality when compared to equivalent surfaces such as silicon or even polished quartz. The degree of surface quality on the initial substrate has been maintained throughout the etching process, creating an accurate sample channel. Of particular note is the interface between the channel and the non-etched face of the quartz flat, where there is very little evidence of undercutting at the etched/non etched interface. Typically undercutting occurs at the sides of the etched area, where as well as etching downwards, HF also attacks the sides of the channel as it is formed, leading to damage of the unetched quartz face and undermining the interface.

We also confirmed the data quality generated qualitatively by obtaining an interference spectrum of the etched flat (figure 3.9).

Figure 3.9: Assembled etched cuvette inside the sample cell holder. The interference pattern of the two flats can be clearly seen, identifying the surfaces of the two pieces of quartz as being optically flat.

As can be seen in figure 3.9, the interference pattern showed that the quartz cuvette created was indeed flat on both faces, hence the straight band interference pattern observed.
The WYKO data shown in figure 3.8 (one of the most accurate means of path length determination available) put the depth of the channel at 6.58 µm (± 0.10 µm), as given by the Rt value that represents the difference between the highest point on the surface and the lowest point on the surface. As the other flat is placed on top of the etched flat, this effectively caps the channel so that the

depth of the channel is the effective path length of the cell. The depth of channel recorded by the WYKO was consistent with a measurement carried out using a Taylor Hobson Form Talysurf (data not shown), which gave a depth measurement of 6.63 µm (± 0.10 µm).

The interference fringe method[7] gave 14 full fringes (figure 3.10) between 599 nm and 366 nm. From equation 3.1 it follows that the path-length is 6.586 µm (± 0.015 µm). Reassembling and repeating the measurements leads to ~1.5% variation (compared to 10–20% for a standard demountable cell) so the path-length of this etched cell is 6.6 µm (± 0.10 µm).

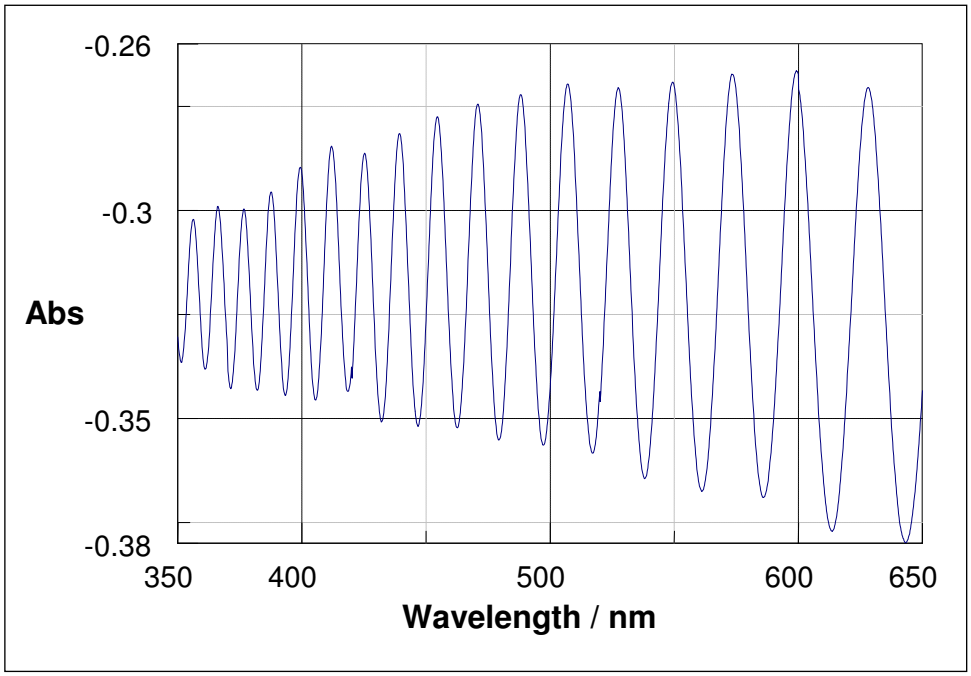

Figure 3.10: UV / Visible spectrum absorbance spectrum of the etched cell. The spectrum was acquired under the following conditions: Bandwidth 1 nm, data pitch 0.2 nm, scan speed 100 nm/min.

We also determined the path-length of the etched cell using a 0.2 M solution of potassium chromate (stabilised with a pellet of KOH). The absorbance of the solution was tested using a V-660 Jasco UV / Vis spectrophotometer.

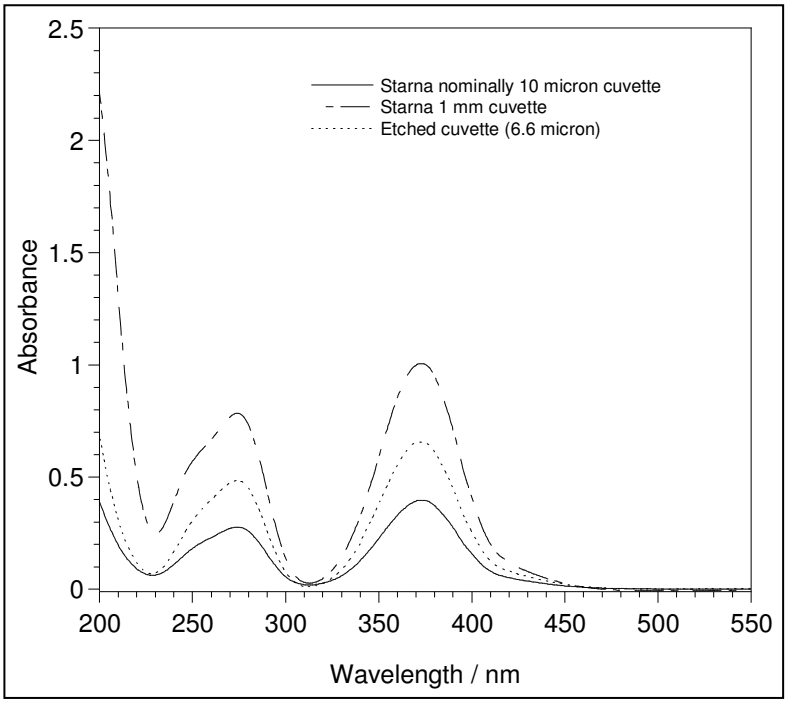

Figure 3.11: UV/Vis K_2CrO_4 path-length determination. A 0.2 M solution was used to test the micron path-length cuvettes, whilst a 0.002 M solution was used for the 1 mm path-length cuvette. Parameters for the UV/Vis analysis were: bandwidth 1 nm, data pitch 0.5 nm, speed 100 nm/min.

Using the Beer-Lambert law with the absorbance reading at 372 nm from figure 3.11, and the absorption co-efficient of potassium chromate at that wavelength of 4830 $mol^{-1}dm^3cm^{-1}$ it is possible to calculate the path-length of each cuvette. These are as follows:

1 mm cuvette = 1.041 mm (approximately 4% path-length error)

6.6 micron etched cuvette = 6.77 micron (approximately 3% path-length error)

10 micron Starna demountable cuvette = 4.104 micron (approximately 59% path-length error)

From this figure it can be shown that the error in the expected path-length for the etched cuvette is of a similar order to that of the 1 mm cuvette, whilst the 10 micron Starna demountable cuvette is very inaccurate.

3.3.5 Sample loading

The uniformity of the etched cell made loading the sample reproducibly even more challenging that with existing rectangular or cylindrical demountable cells available from e.g. Starna and Hellma. We solved this problem by grinding

(using an Elliot 618 surface grinder) a 30º recess into the side of the optical flat as illustrated in Figure 3.7. This ground area of the flat facilitates sample loading and removal using a gel-loading tip piggy-backed onto a P20 Gilson pipette tip.

3.3.6 Sample holder

The design of cuvette holder was vital to the proper functioning of the etched cuvette. The holder had to ensure equal pressure between the two quartz flats, as well as allowing the maximum amount of light possible through the cuvette. The design of the holder is detailed in figure 3.12.

The cuvette holder needed to be held in turn within the confines of the light beam. To that end, a base-plate was designed so that the cuvette holder could be placed reproducibly within the light beam (figures 3.13 and 3.14.

Figure 3.15 shows a picture of the cross section from the etched cell base-plate. This prototype was specifically designed for a Jasco CD spectropolarimeter small sample compartment (made from anodised aluminium), but the design could be equally well adapted for any spectropolarimeter. An optical mount made of black nylon was set into the base plate to support the etched demountable cuvette (illustrated in Figure 3.15). An optical iris light limiter (from Edmund Optics) was used to effectively control the shape of the incident light beam as well as the amount of light that was entering the demountable cuvette. The long tube was made of nylon to ensure parallelism of the components in the light beam.

A small hole was drilled through the female part of the etched cuvette holder allows sample injection and removal from the cuvette when aligned with the etched channel of the flat. The female component has a screw thread that helps compress the flats together to ensure an effective and reproducible seal. In the assembled unit, the flats were cushioned with rubber O rings to allow even distribution of pressure. (Pressure differences across the quartz flats would distort the crystal creating variable birefringence due to the photoelastic effect).

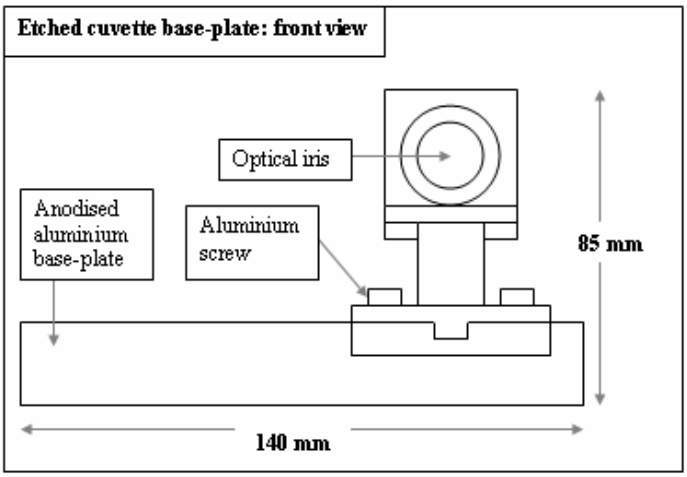

Figure 3.12: Etched cuvette holder assembly side view schematic. An aperture has been machined through the centre to allow light into the cuvette. The diameter of the aperture running through the middle of the holder is 12 mm.

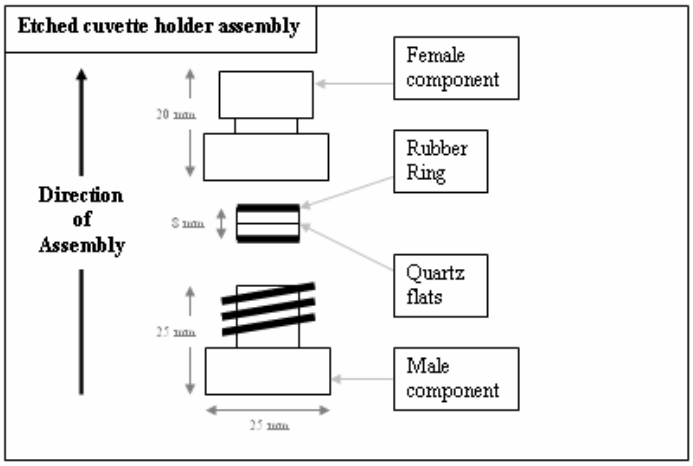

Figure 3.13: Etched cuvette base-plate side view schematic. Light source in this instance would move from left to right.

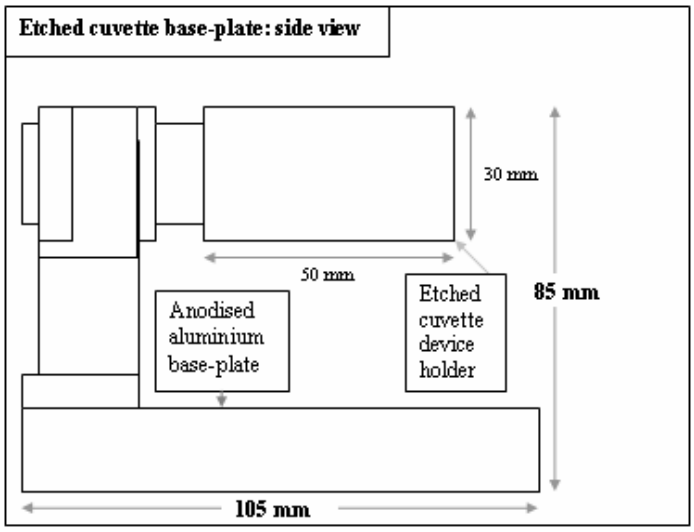

Figure 3.14: Etched cuvette front view schematic. Light source in this instance would move through plane of the optical iris.

In assembling the cell and cell holder the interference pattern between the two quartz faces should become apparent. It is important that the cell be assembled tightly but not twisted with the full force of the user. Typically two full 360 º twists are sufficient to secure the cell. As the components are optical flats if they are twisted on one another under pressure, a phenomenon known as wringing, or optical contacting, can occur, permanently fusing the silica crystals together[10].

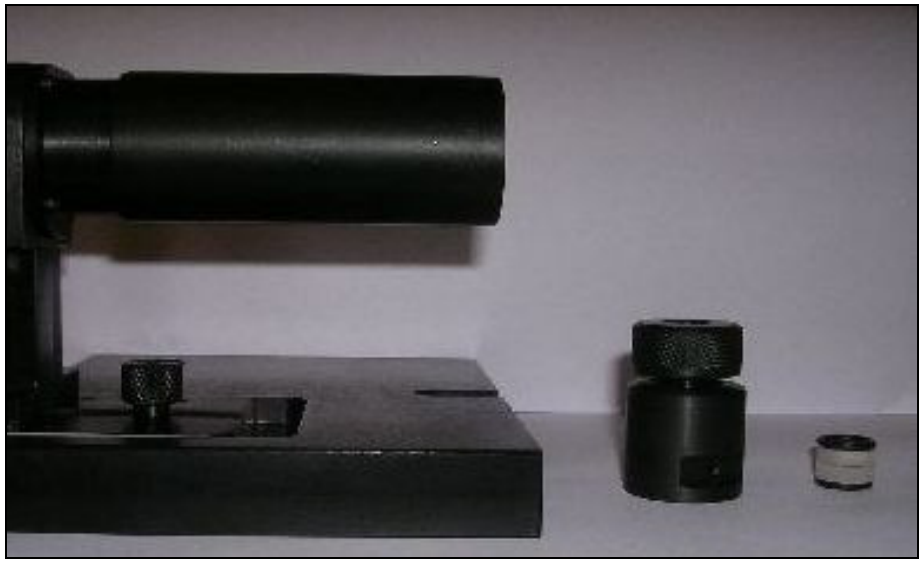

Figure 3.15: Sample holder unit. Right: quartz optical flats assembled and capped with a black rubber 'O' ring. Middle: Optical flat unit fitted inside the cell holder. Left: assembled unit indicating screw that facilitates positioning of the unit in the light path.

3.3.7 CD spectroscopic data for etched and standard cuvettes

Having confirmed the accuracy of the etched cuvette, it was important that we also confirmed its spectral performance as a CD cuvette. We tested several compounds in both an etched and a standard cuvette. The results are shown in figures 3.16-3.18.

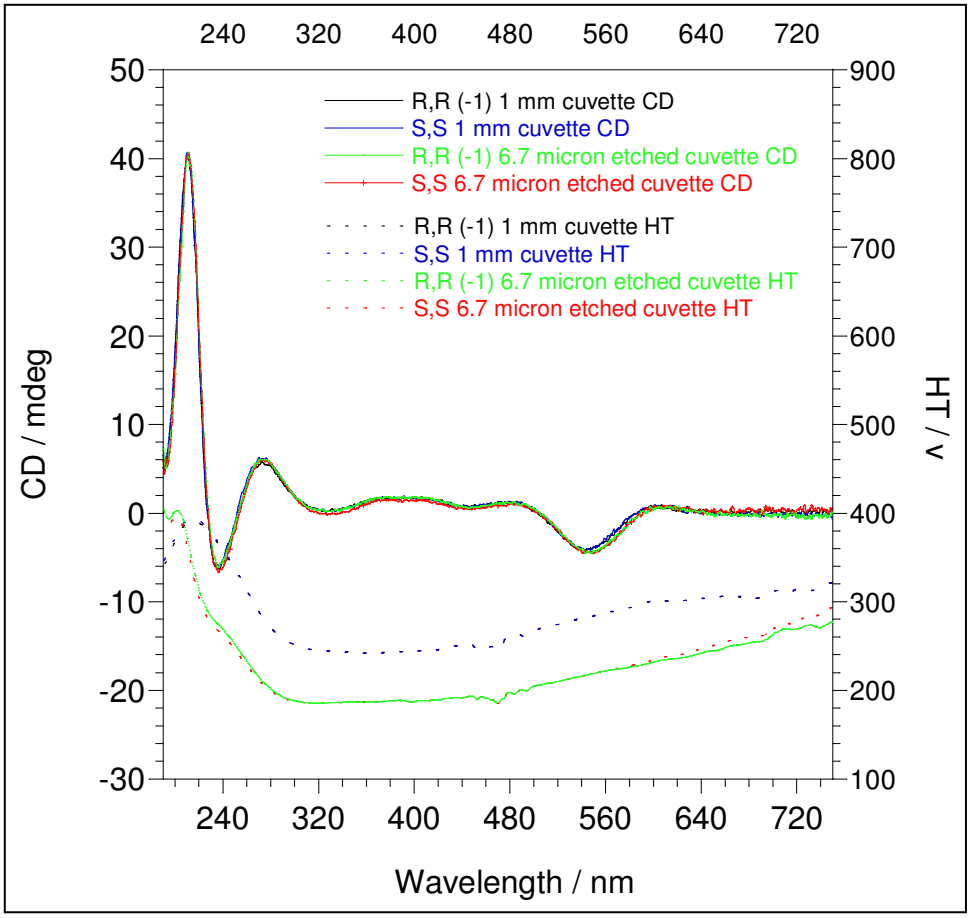

Figure 3.16: Na [Co (Edds)].H_2O spectra for 6.6 micron etched cuvette (55 mM) and 1 mm cuvette (0.55 mM). Etched cuvette spectra have been adjusted for concentration and path-length. Parameters used were 100 nm / min scan speed; bandwidth 1 nm, step size 0.2 nm for the etched cell and 100 nm / min scan speed, bandwidth 1 nm, step size 0.5 nm for the 1 mm cuvette.

Figure 3.16 shows the CD spectrum of R,R and S,S CoEDDs, a compound designed for the calibration of CD instruments. As can be seen in the figure, the CD signal of both the R,R and S,S forms are equal in magnitude across the wavelength range studied. This has important implications for the etched cell. Most importantly, this demonstrates very effectively that there is no bi-refringence produced by the etched cell quartz flats – it works very effectively. Secondly, after adjusting for path-length the magnitude of the etched cuvette spectra was the same as that of the standard 1 mm cuvette. This provides confirmation that the etched cuvette path-length was indeed 6.6 micron and perhaps more importantly, that it could replicate this path-length after each assembly.

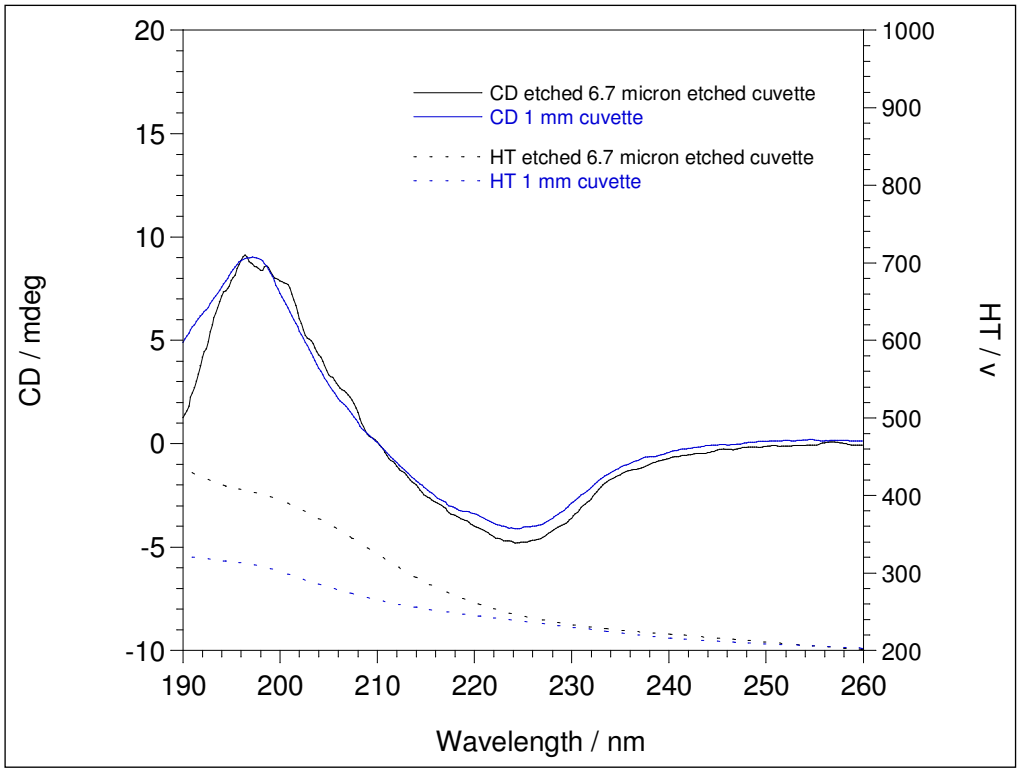

Figure 3.17: Concanavalin A spectra for 6.6 micron etched cuvette (10 mg / ml) and 1 mm cuvette (0.1 mg / ml). Etched cuvette spectra have been adjusted for path-length. Parameters used were 100 nm / min scan speed, bandwidth 1 nm, step size 0.2 nm.

Figure 3.17 illustrates the performance of the etched cell with an actual protein sample, in this instance Concanavalin A. Across the wavelength region, the spectra tally very well, with the only slight aberration occurring between 220 and 230 nm. However, this difference is sufficiently small to not affect the validity of comparison between the etched cuvette and the 1 mm cuvette.

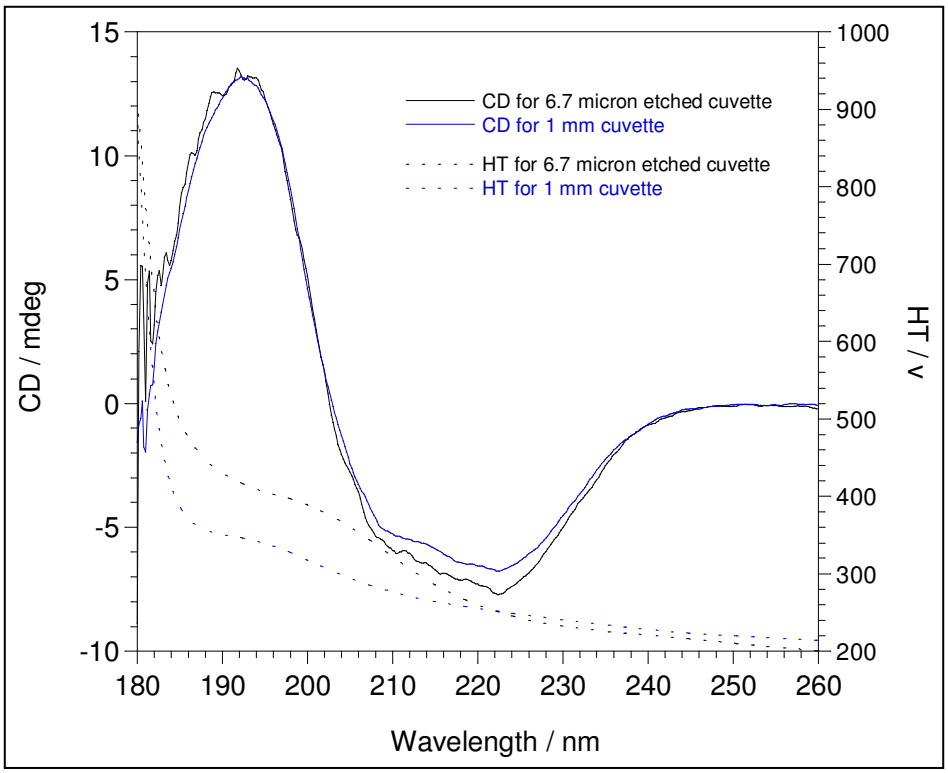

Figure 3.18: Ovalbumin spectra for 6.6 micron etched cuvette (10 mg / ml) and 1 mm cuvette (0.1 mg / ml). Etched cuvette spectra have been adjusted for path-length.

For figure 3.18 the magnitude of the signal was very similar for both the etched cell and the standard cuvette. Spectral shape was entirely consistent with the standard spectrum of ovalbumin (see the PCDDB[11]). The only slight aberration in the CD spectra recorded was between 210 and 225 nm, where there is a slight difference in magnitude. This difference could arise from several factors, including errors in both the 1 mm cuvette path-length and that of the etched cell. However, as the 195 nm peak and 260-240 nm baselines are consistent, I believe that the spectra can still be usefully compared to one another.

Overall the CD data confirms that the etched cell is both accurate and reproduces the path-length of the cuvette each and every time, for no loss of spectral quality.

3.4 Conclusions

We have successfully developed a new form of high accuracy, low path length quartz CD cuvette that can be manufactured at a variety of different path-lengths. The path-length of each cell is highly defined and each cuvette can be easily reassembled to form the same path length again and again. This design of CD can also be integrated into a flow device, where unlike CaF_2 cells there is no solubility in water, thus retaining the surface finish of the cells.
The current design of cuvette suffers principally from its inability to produce reproducible path lengths. Different users, using the same sample and the same cuvette on the same instrument will generate radically different CD spectra due to errors in cuvette assembly, design and manufacture. By using pieces of quartz in cuvette manufacture that are both too flat and of a shape that becomes impossible to kinematically mount, the standard design of CD cuvette at low path length compares very unfavourably with that of the etched cell. It should be noted that with a highly experienced user, path-length error in the Starna demountable cell can be reduced to approximately 20%. The etched cell meanwhile locates to the same path-length each time with a bare minimum of training in assembly.

Future work for this research would look further into the effect of pressure on the path length of the cuvette and integrating this device into a flow system, allowing for the creation of a brand new form of highly accurate, rapid CD data acquisition.

3.5 References

1: World Health Organisation, Expert Committee on Biological Standardization, Geneva, 19 – 23 October 2009, Recommendations to assure the quality, safety and efficacy of pneumococcal conjugate vaccines

2: World Health Organisation, Guidelines for assuring the quality of pharmaceutical and biological products prepared by recombinant DNA technology, 1991, WHO Technical Report series, No. 814

3: K. O. Webber, US Food and Drug Administration Advisory Committee for Pharmaceutical Science, Process Analytical Technology and Biotechnology Products (Presentation April 13th, 2004)

4: S.A. Baloghne, Application of difference circular dichroism (CD) spectroscopy for the determination of pharmaceutical compounds. Analysis of stereoisomers by the HPLC-CD/UV method, 2003, 73 (3), p 185 – 195, Acta pharmaceutica Hungarica

5: S.J. Shire, Z. Shahrokh, J. Liu, Challenges in the development of high protein concentration formulations, 2004, Vol 93, no. 6, p 1390 – 1402, Journal of Pharmaceutical Sciences

6: E. Hecht, Optics (4th Edition), 2002, published by Addison Wesley, ISBN 0-321-18878-0

7: A.J. Miles, F. Wien, J.G. Lees, B.A. Wallace, Calibration and standardisation of synchrotron radiation and conventional circular dichroism spectrometers. Part 2: Factors affecting magnitude and wavelength, 2005, Vol 19 p 43 - 51 Spectroscopy

8: V.K. Leko, L.A. Komarova, Kinetics of the Etching of Quartz Glass in Hydrofluoric Acid, 1973, 11, p 15 – 16 Steklo I Keramika.

9: J.A. Bornmann, C.J. Wolf, Reaction of Nitric Acid with a Solid Epoxy Resin, 1984, Vol. 22, p 851-856, Journal of Polymer Science, Polymer Chemistry Edition

10: Lord Rayleigh, A Study of Glass Surfaces in Optical Contact, 1936, Vol 156, no. 888, p 326 – 349, Proceedings of the Royal Society of London

11: L. Whitmore, B.Woollett, A.J. Miles, D.P. Klose, R.W. Janes, B.A. Wallace, PCDDB: the protein circular dichroism data bank, a repository for circular dichroism spectral and metadata, 2011, Vol 39 (suppl 1): D480-D486, Nucleic Acids Research

CHAPTER FOUR

Development of Automated multi-sample Circular Dichroism Spectroscopy (AMS-CD)

Geranium sylvaticum in both visible colour and UV.

CHAPTER FOUR: Development of Automated Multi-Sample Circular Dichroism Spectroscopy

Summary

In this chapter we report the development of an automated multi-sample instrument for circular dichroism. The design centred on the interfacing of a quartz capillary with an HPLC auto-sampler and pumping mechanism. In the work two methods of sample loading are compared against one another, with one method being found suitable for only qualitative spectra, whilst the other can be used to generate high quality data sets. The instrument is fully compatible with 96-well plates, greatly expanding the number of data sets that can be acquired for CD spectroscopy. This technique opens up several interesting applications to the life scientist, including CD investigation of refolding conditions for proteins. The successful development of the prototype instrument should allow for greatly reduced acquisition time for CD users, as well as opening up screening applications.

4.1 Introduction

4.1.1 The un-harnessed potential of circular dichroism

Whilst automation has become standard for UV / Vis absorption, NMR and MS instruments, CD continues to be limited by its inability to analyse more than a single sample at a time. This fails to take advantage of one of the greatest advantages CD holds over other techniques i.e. the rapid acquisition time for each spectrum[1]. The reasons for this difficulty are two-fold.

1.) When compared to other methods[2] CD requires a large volume of sample for each reading. This is an awkward requirement for regular CD analysis, but when applied to multiple samples the sample demands can swiftly become insurmountable.

2.) The specific demands of DUV optical transmission for any component holding sample within the light beam rules out the use of many approaches for automation that have been applied to other bio-physical techniques[3].

These issues have made the development of a large multiple sample (i.e. more than five samples) CD instrument simply impractical – any automated instrument would require so much sample volume as to be rendered non-economical, despite any savings in operator time. However, with the advances made in cuvette production and optical alignment it is now feasible to look at the development of the world's first automated multiple sample CD instrument. The potential for such an instrument is substantial. With it, CD could be used for screening pharmaceutical preparations or optimising conditions for protein refolding[4]. At a minimum it would allow for collection of more data overnight and better optimisation of valuable instrument time.

4.1.2 Capillary flow circular dichroism

The advance that has allowed the development of automated multi-sample circular dichroism (AMS-CD) is the novel use of quartz capillaries as CD cuvettes[5]. The significantly reduced sample requirement for these capillaries has made the prospect of multiple sample CD analysis feasible. In addition to the lower sample requirements, capillaries have another advantage over

traditional cuvettes which makes them ideally suited for use in an AMS-CD instrument. A quartz capillary is simply a hollow quartz cylinder with an aperture at the top and the bottom of the cylinder. Whilst for traditional CD this makes securing the sample within the light beam difficult, for an AMS-CD application it is actually an advantage. Once the light beam has been modified with DCX focusing lenses (as described in more detail in chapter two of this thesis) a quartz capillary can become an effective means of light transmission in the DUV. In addition it can be very simply made into part of a flow system, allowing different samples to pass through the capillary without the need for manual sample loading.

With this concept in mind we attempted to design an automated multi-sample CD instrument using a capillary as the central optical component/sample holder.

4.1.3 Alternative sample loading methodologies- single sample injection and queued flow

The work done previously on the optics of quartz capillaries had addressed some of the main problems with an AMS-CD device using capillaries but one major obstacle that still remained was the problem of sample loading. Any method that we chose to deliver the samples to the optical components would have a significant impact on the functionality of the instrument.
There were many factors to consider but of these, five stood out in particular.

- How to avoid air bubbles within the capillary
- Volume of each sample required for analysis
- Sample diffusion / contamination
- Cleaning of the AMS-CD system
- System stability (to what degree does the system need a constant environment)

Each of these factors had their own technical challenges to overcome. After investigating several means of placing the sample within the confines of the capillary we decided upon the use of two alternative pumping systems, each with their own advantages and disadvantages. These were queued sample

injection (QS) and single sample injection (SSI) (described in more detail in section 4.3).

Queued flow AMS-CD

Queued sample injection (QS) AMS-CD works on the principle of injecting a line with the various CD samples that are to be analysed. Once a sample is within the confines of the injecting line the sample is pumped until it enters the light beam of the target spectrophotometer. The flow then stops, allowing data to be collected. Once data collection is complete the next sample is pumped into the line, the old sample now being pumped to waste. Queued flow has the advantage of being both relatively gas-free (with few air bubbles being introduced to the system) and being a relatively simple system with the flow mechanism being based upon HPLC technology.

Single sample injection AMS-CD

Single sample injection (SSI) AMS-CD works on the principle of moving a single sample around an auto-sampler, using an injection pump to manoeuvre the sample through the sample line. By contrast, queued flow AMS-CD places several samples within the sample line at once. The SSI system does not allow for queuing of multiple samples, but it does ensure sample fidelity when in the line (as no other sample is present, diffusion and mixing of different samples is very unlikely). Once a sample has been analysed, the auto-sampler instrument pumps the old sample out, before injecting the next sample in sequence. Whilst there have been some teething problems with the technique, SSI has the potential to be an effective method of sample delivery for AMS-CD.

The following chapter details the development of the AMS-CD instrument, as well as comparing the two separate methods of sample loading and their effect on the acquired CD spectrum.

4.2 Materials and methods

4.2.1 Queued sample injection instrumentation and materials

A Jasco PU-1580 high-performance liquid chromatography (HPLC) pump was interfaced with a Jasco AS-2055 Intelligent auto-sampler with 100 µl sample loop, all of which are available from Jasco UK. This HPLC equipment was in

turn interfaced with a custom quartz capillary optic holder (see section 4.3.1), manufactured by the engineers attached to the Biology Department of Birmingham University. The device was constructed from brass, with the quartz capillaries being composed of extruded quartz (available from Enterprise-Q). The assembled components were then modified to make them suitable as an AMS-CD system (see section 4.3.2).

For focusing the light within the queued flow set-up, PCX and DCX quartz lenses were employed. These were purchased uncoated from Edmund Optics, at path lengths ranging from 60 to 100 mm, depending on the spectrophotometer used as a light source. The J-715 CD spectrophotometer housed in the laboratory of the Dafforn group, Biology Department, Birmingham University was used to generate all QF spectra presented here.

4.2.2 Single sample injection instrumentation

For SSI AMS-CD, a Jasco ASU-605 Auto-sampler (without racks or tubes) was used as a means of pumping samples into the custom quartz optic holder manufactured in-house at Birmingham University. Data for the SSI AMS-CD instrument was collected at the synchrotron light source ASTRID at ISA, University of Aarhus.

4.2.3 Cleaning methods

For both sample loading methods, the sample lines were cleaned using 1% Hellmanex® solution that was left in the sample line for 15 minutes to remove any contaminants from the system. After this, distilled water was flushed down the sample line continuously for 15 minutes at 1 ml/min to ensure all traces of the detergent had been removed.

For the quartz capillary, cleaning was achieved by removing the capillary component from the holding device. The quartz capillary was then placed in 6 M Nitric acid for 30 minutes, with great care being taken to ensure that all surfaces, both external and internal, of the capillary were in contact with the acid. A pair of plastic tongs was used to manipulate the quartz capillary whilst in the acid bath. After removal from the acid bath the capillary was washed in

copious amounts of distilled water before being cleaned with a 1:1 ethanol/water mix and dried with compressed air.

4.2.4 Consumables

Ovalbumin, lysozyme, concanavalin A and horse radish peroxidase were all purchased from Sigma-Aldrich and were used without further purification.

4.3 Results and Discussion

4.3.1 Development of AMS-CD flow optic

Building on previous work using capillaries as CD sample cuvettes (in the caCD cell[5]) we developed a new type of flow optic device that could be incorporated into a CD spectrophotometer. Our approach was to create a device that could be placed directly in front of the detector (figure 4.1) in a CD spectrophotometer.

Figure 4.1: Jasco J-715 spectrophotometer. Note the long tubular detector on the right.

A detector-centred approach to sample holder design has several advantages over a base-plate approach. By placing the sample holder directly in front of the detector any optical divergence of the light beam is minimised, allowing more light to reach the detector. In addition, in the case of a collimated light beam a centrally located sample holder is able to take full advantage of its properties, as all optical components will be linearly aligned between the light source and detector. However, a device of this type had not been invented before and so it had to be designed from scratch.

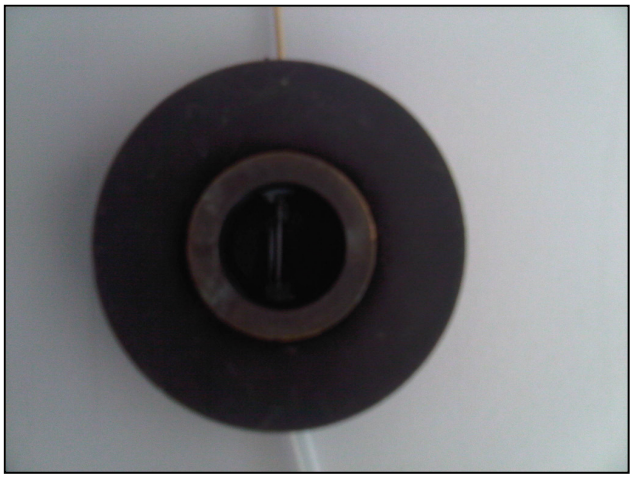

Figure 4.2: AMS-CD flow optic holder.

The shape of the flow optic holder (figure 4.2) by necessity had to be circular in order to integrate properly with the detector (through a hole in the spectrometer, with sufficient depth to be secure in its placement inside the spectrophotometer). In addition the diameter of the device has to be such that the optic could be taken out and put back in easily, whilst ensuring optical fidelity. Another method of 'fixing' the holder in place was considered i.e. extending the screws of the detector itself to allow the device to be truly in line with the detector, but it was thought that for a non-dedicated instrument this would provide too many barriers for the average user to change modes very easily. As such a 'push fit' approach was decided upon *i.e.* the holder can be slid into place in a specially made slot in front of the detector.

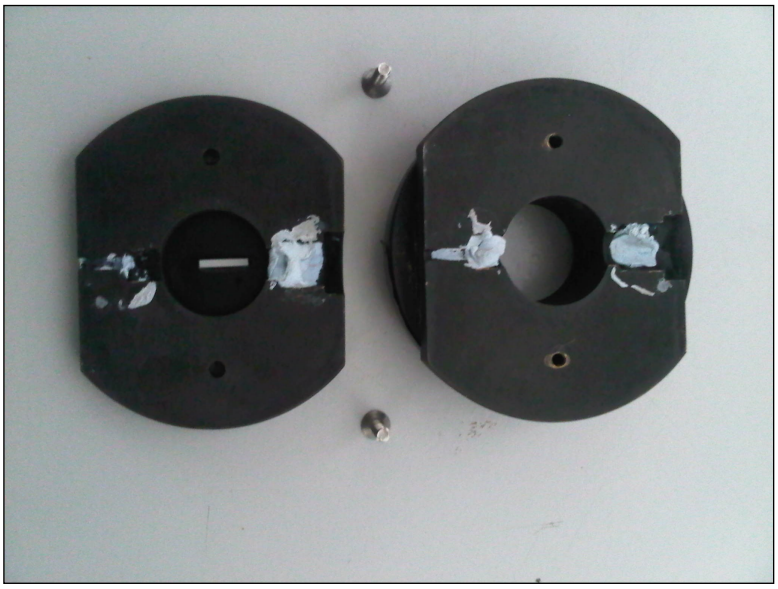

Figure 4.3: Brass plates that hold the capillary optic in place. Blu Tack® was used to secure the PEET tubing that connects the capillary optic to the HPLC auto-sampler.

Figure 4.3 shows the holder itself, which has been machined from brass and consists of two plates which 'sandwich' the quartz flow optic in place. Holes in the top and bottom of the device allow for the sample line to be connected to the quartz flow optic, allowing the passage of sample into the capillary and waste to flow out of the capillary. A quartz capillary with an external diameter of 3 mm was chosen as the flow optic as its properties at this point were well understood[5]. In addition the lower sample volume afforded by this size of capillary (compared to one of greater internal and external diameter) made it significantly easier to align the sample within the sample line (a point that will be expanded upon below in section 4.3.2).

The capillary optic was masked prior to light entering the capillary to ensure that the light pushed through the sample would be collimated and to stop any stray scattered light that may enter the detector. Although the AMS-CD system was set up so a lens would not necessarily be needed, if more light was required for a particular spectrum then a DCX or if possible, PCX focusing lens could be used to focus the light beam onto the capillary. With the positioning of the capillary so close to the detector the system had the potential to be more effective than the caCD instrument[5] at maximising the detection of transmitted light, although ensuring correct focusing of the light beam could prove more difficult if the optical elements such as the lenses were separated.
Both QS and SSI methods have been interfaced with this particular flow optic but the means of sample loading are radically different for each technique.

4.3.2 Queued sample injection AMS-CD development

Sample loading was a key consideration when designing the AMS-CD instrument. It was of vital importance that the sample flowed effectively through the system and that the system was highly resistant to biological agents. HPLC technology has been widely adopted across the world as a standard means of sample separation and purification. The technology has undergone several redesigns and now comes in a host of standardised fittings that provide an excellent starting point for any flow system. As such HPLC offered a

flexibility and availability that made it an ideal method for sample loading in the AMS-CD instrument.

In order to position effectively the sample in the light path it was important to fulfil three goals (i) integrate a suitable pump with the flow optic device, (ii) calculate the 'dead volume' in the sample line (that had to be cleared before the sample could be delivered) and (iii) program the pump to deliver the sample. All three goals would have to be fulfilled in order for the AMS-CD instrument to work effectively.

Integration of AS 2055 intelligent auto-sampler

For this application we looked at using an HPLC auto-sampler as the pump for our instrument. This readily available piece of technology was relatively cheap, programmable and allowed us a great degree of control over the sample loading. The sample lines that connected the pump to the capillary were made of standard HPLC tubing, of a small internal diameter so as to make the sample easy to 'catch'. Once the auto-sampler was fully interfaced with the optical component it was necessary to check how reproducible data were on this instrument. In order to ascertain whether or not the optical elements of the system were stable we decided to run water blanks on the AMS-CD to ensure that spectral fidelity was maintained. The results are shown in figure 4.4.

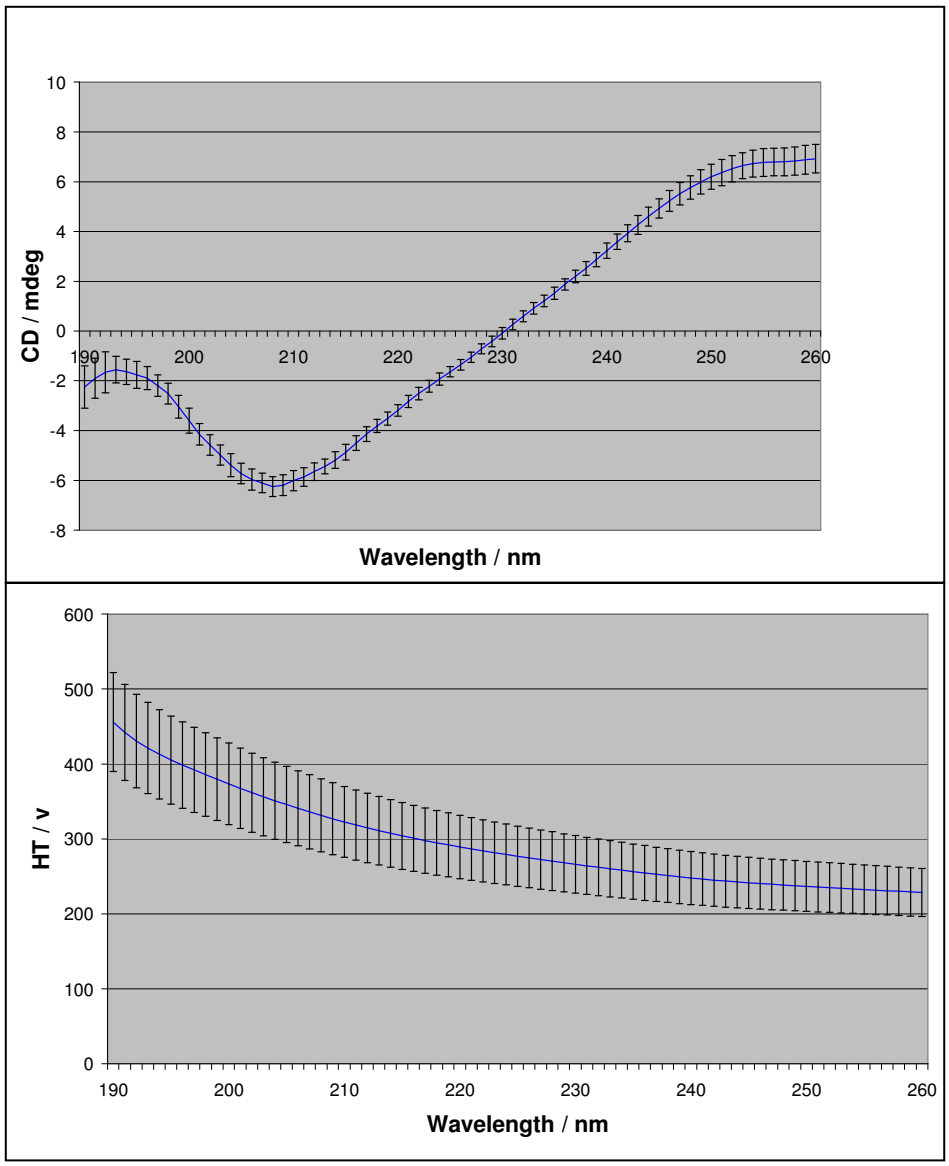

Figure 4.4: Averaged CD spectrum and HT of 48 water samples, in order to verify spectral fidelity of the AMS-CD set-up. CD parameters were as follows: Bandwidth 2 nm, response 1 second, data pitch 0.2 nm, 2 accumulations. Error bars are given to one standard deviation.

As shown in figure 4.4, the CD signal of water across the wavelength range is in broad agreement across the 48 spectra. Whilst not ideal for quantitative assessment, the qualitative shape of the water signal is conserved across all the spectra. This is confirmed by the CD standard deviation shown across the entire wavelength range. In figure 4(iv) it can be seen that the HT can vary across the wavelength range and between spectra, but not to the extent that the HT value exceeds that of producing reliable data (i.e. above a value of 700 V on the HT). As would be expected, the standard deviation of the HT increases with decreasing wavelength (as the slit size of the Jasco instrument increases).

The variation here is well within acceptable parameters for qualitative assessment of CD spectra as the spectral shape generated by the AMS-CD is conserved across the data. This result, whilst important, was relatively easy to achieve. Rather than injecting a sample into the capillary optic chamber we filled the entire sample line with water to ensure the optic was filled. This rough and ready approach worked in this instance, but in order for the instrument to be truly effective as a means of sample delivery we had to properly position an aliquot of sample into the capillary chamber. This was the next challenge to overcome to create a working AMS-CD instrument.

Programming the AS 2055 intelligent auto-sampler and PU-1580 HPLC pump

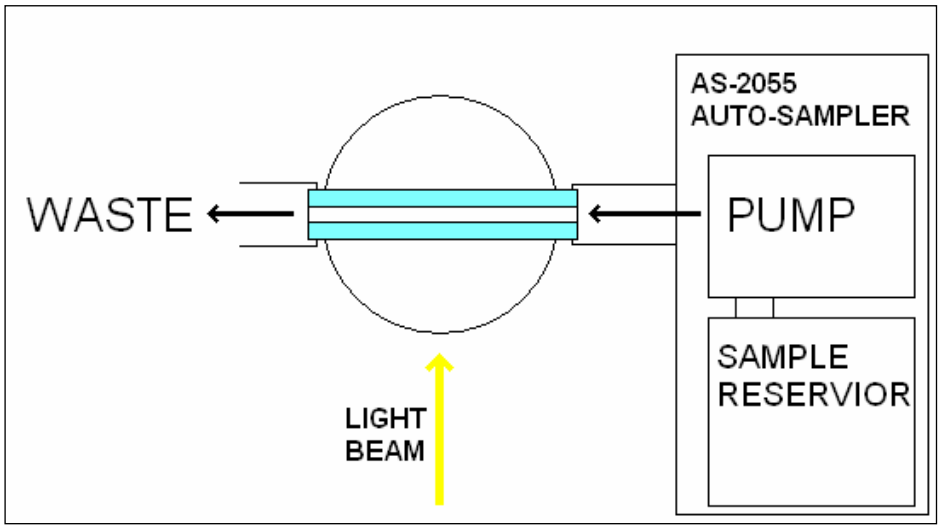

Figure 4.5: Functional schematic for the AMS-CD flow device.

Catching the sample within the confines of the capillary (see the blue area in figure 4.5) using the HPLC auto-sampler was the biggest technical challenge posed during the development of the QS method. The maximum volume the auto-sampler could deliver for injection was 100 µl, due to the choice of sample loading coil within the auto-sampler itself (figure 4.6). The specific issue to overcome in this instance was to shift the dead volume within the sample line (i.e. the non analysed fluid in the sample line) whilst delivering the sample to the light beam. The size of the installed sample loop for the HPLC system allowed injection volumes between 0.1 µl and 100 µl. With the difficulties

inherent with sample alignment we decided it was best to inject the maximum volume per aliquot *i.e.* 100 µl.

Figure 4.6: The Jasco AS-2055 HPLC auto-sampler with integrated PU-1580 HPLC pump, modified for use with a CD spectrophotometer.

The shorter the sample line the less dead volume is present within a system. The dead volume is the amount of fluid present in the sample line that is required to pass before the sample is delivered into the chamber – if not recovered this volume is wasted. With a short sample line dead volume is reduced and sample loading times are reduced – however, a certain length of sample line is required to give the user flexibility in instrument positioning. The difficulties of programming the pump stemmed from the ramping pumping gradient of the PU-1580 HPLC pump. Both the auto-sampler and the pump had to be synchronised with one another to allow effective sample delivery. The PU-1580 pump has a maximum pump rate of 2 ml / min and a minimum pump rate of 0.1 ml / min. Different speeds can be selected only in 0.1 ml/min increments. Additionally the pumping speed is controlled in 6 second bursts, so any program that the system runs can only be in those time increments. Finally, when moving for example from 0.2 ml/min to 0.1 ml/min this change happens over the course of the 6 second time period- with the starting flow rate being 0.2 ml/min and the finishing flow rate being 0.1 ml/min the average flow rate over the time period is 0.15 ml/min. Whilst seemingly obvious, this means that when one changes the flow rate the command will take effect over the next 6 seconds,

not immediately. All these factors together make programming the auto-sampler to deliver samples effectively rather difficult.

Aligning the sample within the confines of the capillary is not the only difficulty in designing an effective pump program – of almost equal importance is to minimise the load time for each injection. At a pump speed of 0.1 ml/min it is relatively simple to align the sample – but the time taken to align the sample would be great indeed due to the slow pump rate. For the AMS-CD system, our use of a 96-well plate (and therefore having 96 samples) meant that the alignment speed was critical.

At a scan speed of 100 nm / min, with two accumulations for each spectrum over 190 – 260 nm, spectra for the entire 96 well plate would take a minimum of 2 hours and 15 minutes to acquire, before any sample loading was factored in to the equation. A delay of even one minute for each sample rapidly increases the total run time – if each sample took 5 minutes to load, a run would take 10 hours and 15 minutes, limiting a user to one AMS-CD run per day. We therefore programmed the AS-2055 and PU-1580 to deliver the sample aliquot both as accurately as possible and as quickly as possible.

Queued sample injection testing

In order to see exactly where the sample was in the sample line we decided to view the sample in the sample line by both visual and spectroscopic methods. By using blue dye as the sample we changed the pump parameters until the aliquot of blue dye was delivered to the confines of the light beam once pumping stopped. Initially the tubing used in the application was PTFE. This was chosen due to its chemical inertness as well as its flexibility (an important factor when trying to interface the tubing with the capillary). Upon testing, PFTE proved to be too flexible for this application, with leaks occurring where the tubing and capillary met. As a result of this, we changed the tubing we used for the system to PEEK tubing. PEEK, like PTFE tubing is highly resistant to chemical attack, but its rigidity and density allows the tubing to be machined. We therefore machined the end of the PEEK tubing to form a push-fit interface with the capillary, rendering the entire system water-tight. This system worked well but is not the most user friendly tubing to use as a result of its rigidity. Once the loading of the dye was visually confirmed, we then attempted to test the sample alignment via spectroscopy. The spectroscopic test was to acquire

48 spectra of 0.1 mg / ml ovalbumin in both the QS AMS-CD instrument as well as in a standard cuvette CD (of 1 mm path length). The results are shown in figure 4.7.

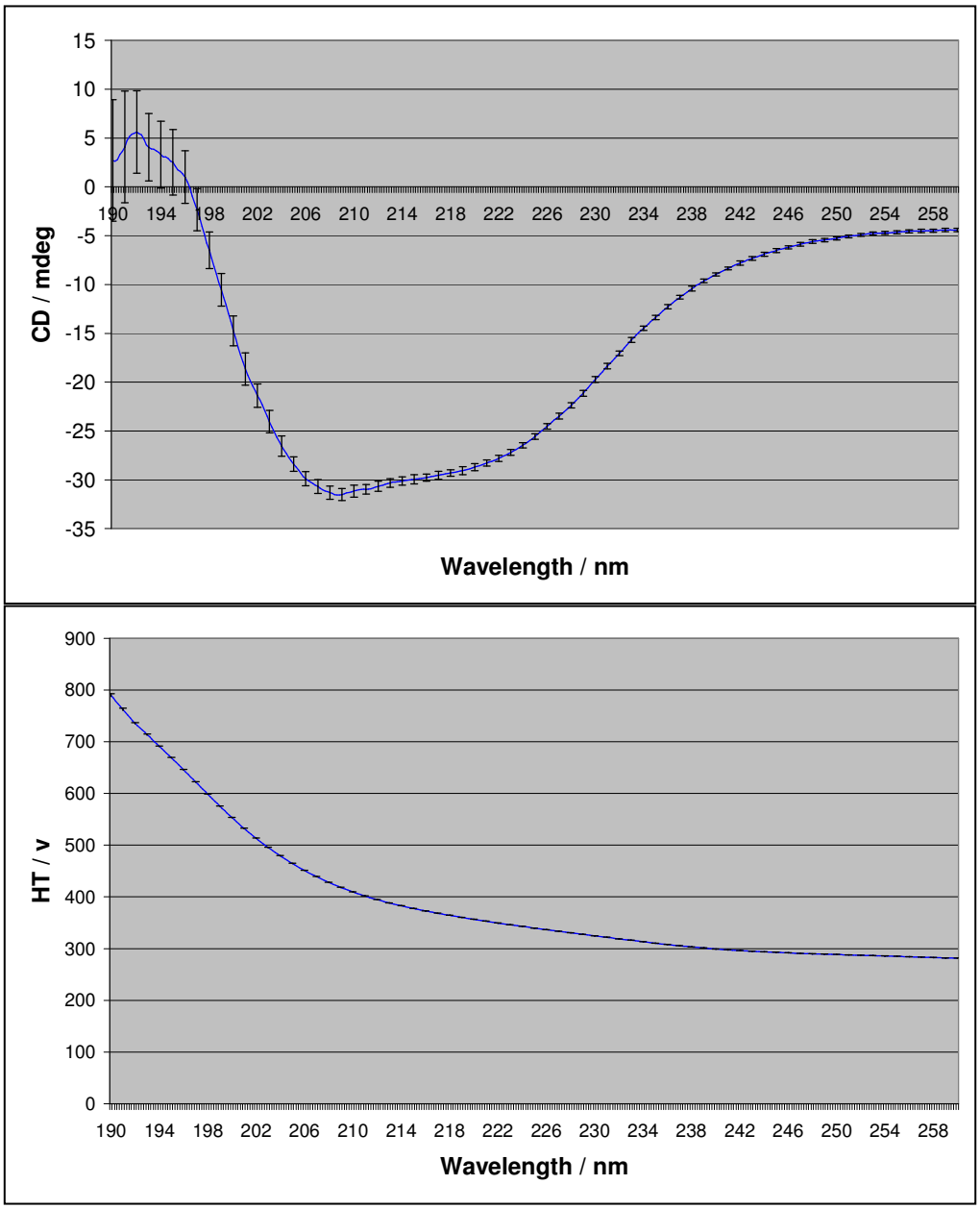

Figure 4.7: Mean CD spectrum of ovalbumin (0.1 mg/ml) Capillary spectra (not baseline subtracted). Data were acquired on a J-715 spectrophotometer using the QS AMS-CD (1.12 mm ID capillary) system. CD parameters were as follows: Bandwidth 2 nm, response 1 second, data pitch 0.2 nm, 2 accumulations. All error bars display +/- one standard deviation of the mean.

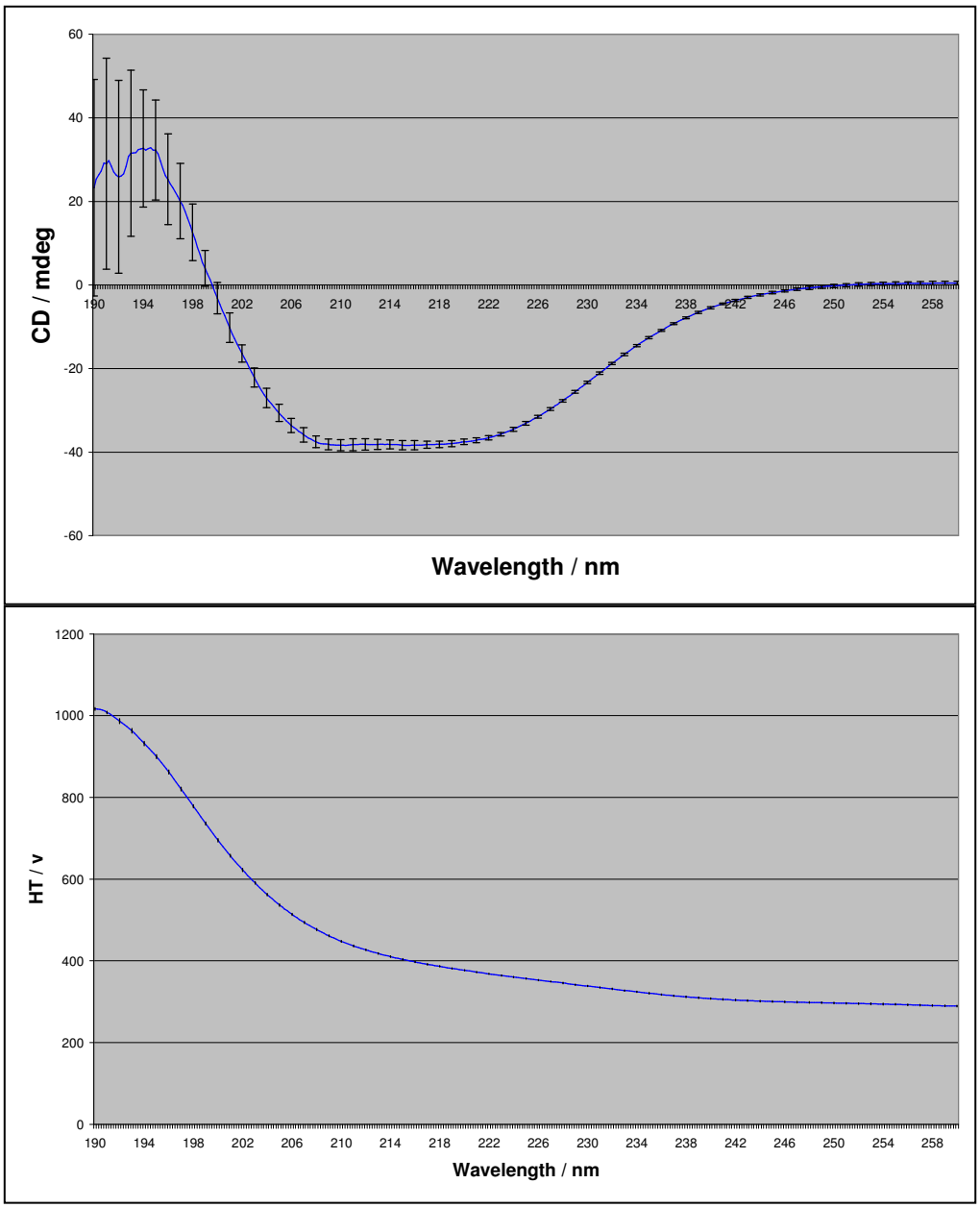

Figure 4.8: Overlay of forty eight Ovalbumin (0.1 mg/ml) Cuvette spectra (not baseline subtracted). Data was acquired on a J-715 spectrophotometer using a Starna 1 mm cuvette. CD parameters were as follows: Bandwidth 2 nm, response 1 second, data pitch 0.2 nm, 2 accumulations.

The spectra generated by the AMS-CD instrument, whilst slightly noisier than the single sample data, shown in figure 4.8 (especially at low wavelength), still correlate well with one another. The variation observed is only slightly higher (+/- 1 additional millidegree compared to the capillary data) across the wavelength range 260-200 nm than that observed for the cuvette data sets, which in turn have a higher standard deviation at the lower wavelengths (<200

nm). The variation observed below 200 nm in figure 4.8 is consistent with an instrument that has surpassed the HT threshold – these data are no longer reliable, as shown by the increase in the standard deviation of the CD signal at these wavelengths. There is also evidence of more variation in the HT of the cuvette data sets. In conclusion, the capillary data is comparable in terms of reproducibly to that of a cuvette acquired spectrum. However, reproduction of the CD data was not perfect so it was decided to look at the reliability of repeated loading of protein within the capillary system.

Figure 4.9 is a time course measurement of alternating lysozyme and water injections measured at 225 nm. It was intended to be a test of the effectiveness and reliability of sample loading to the capillary. The HT graph below shows that the lysozyme sample is entering the capillary and is being retained within the confines of the capillary for the allotted time. There is a slight baseline shift in the capillary data – this is due to adhesion of the protein to the walls of the capillary (this adhesion can also be seen in the HT trace). Whilst not an ideal situation to be in, baseline subtraction can lead to more reliable data.

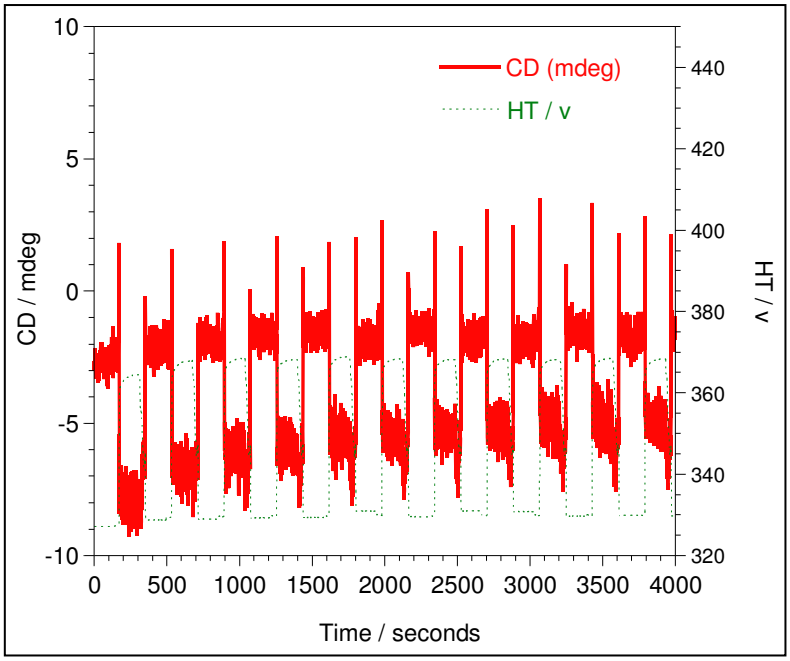

Figure 4.9: Time course measurement of 11 sample injections of 0.1 mg/ml lysozyme preceded by water injections, under repeated injection at 225 nm using QS AMS-CD. The path-length of the capillary in this instance was 1.1 mm. (determined through use of potassium chromate). The CD signal accumulation of water corresponds to the upper bunches of readings; lysozyme corresponds to the lower bunches.

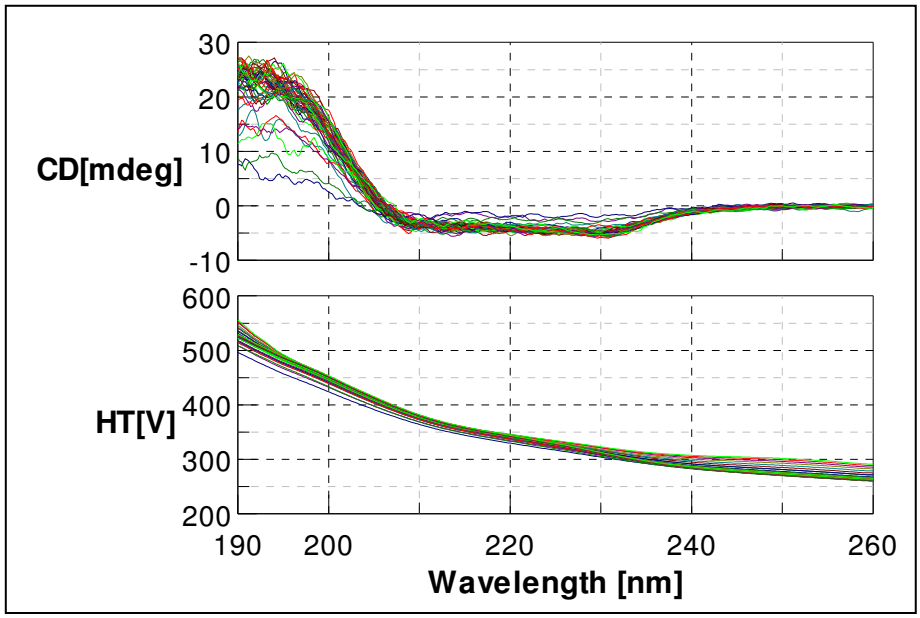

Figure 4.10: QS AMS-CD spectra of lysozyme (0.5 mg/ml baseline subtracted). The image above shows 48 lysozyme spectra, with a water baseline recorded after each lysozyme sample. CD parameters were as follows: Bandwidth 2 nm, response 1 second, data pitch 0.2 nm, 2 accumulations.

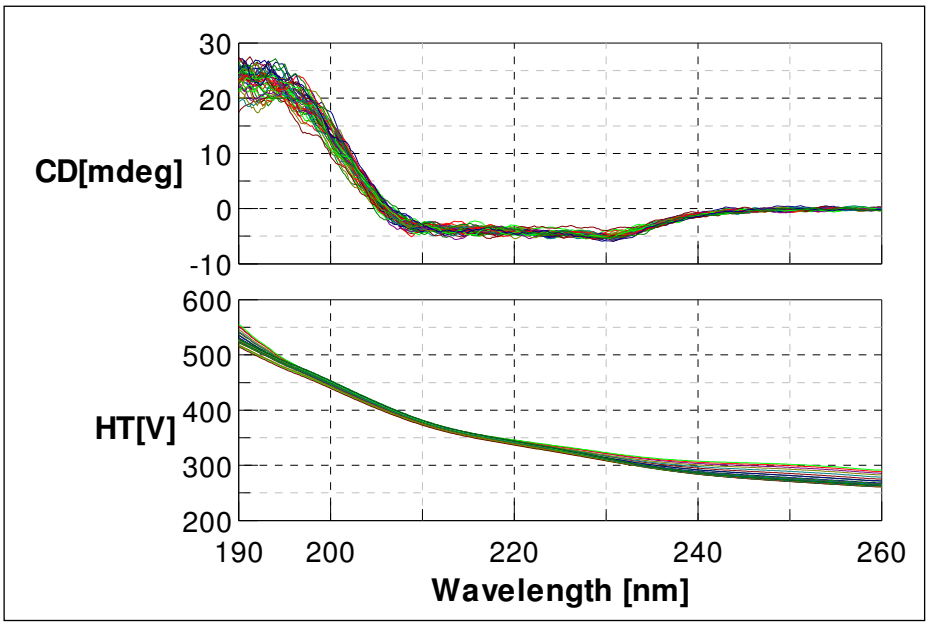

Figure 4.11: QS AMS-CD lysozyme spectra (0.5 mg/ml, baseline subtracted). Spectra that were more than 25% away from the mean ellipticity at 195 nm were omitted. CD parameters were as follows: Bandwidth 2 nm, response 1 second, data pitch 0.2 nm, 2 accumulations.

Figures 4.10 and 4.11 show the baseline subtracted CD spectra generated by the QS AMS-CD instrument for alternating lysozyme/water samples. Figure 4.10 shows all the baseline subtracted data sets – from this graph it can be seen that in all the spectra the shape of the lysozyme can be clearly seen. However there

are seven anomalous spectra within the forty eight recorded. These spectra are characterised by a loss of recorded ellipticity across the wavelength range with this effect being particularly noticeable at 195 nm. These spectra all lie in the latter half of the data sets recorded, with three of the spectra being those in the last five acquired. Due to the nature of the QS-system, all errors through the run are cumulative, making spectra acquired later in the run more susceptible to error. In order to clean up the accumulated data sets in figure 4.11 we have eliminated those spectra with a 195 nm CD value that is more than 25% away from the mean. As can be seen from the spectra above the cleaned up data set is far better defined and agree better with one another.

We hypothesise that the anomalous spectra were caused by air bubbles being formed from the solutions inside the sample line. These air bubbles damage spectral quality by changing both the refraction of light through the capillary but also through their lower capacity of UV absorbance (i.e. taking the CD of air rather than of the protein). Degassing any samples used for QS-AMS CD is a reasonably effective means of minimising these effects, but it is very difficult to eliminate them entirely. This is in part due to imperfect seals within the sample line, although this is a very small effect. A more likely factor is the alternation between the pumped water and sample via injection. The injection process to place the sample in the line was very sensitive to movement of the instrument – if movement was present (i.e. a heavy object banging upon the surface that the instrument was set-up upon, vibrating the instrument) then small air bubbles would be introduced to the system through the injection system, generating anomalous spectra.

When assessed under the five criteria for an effective loading system as set out in section 4.1.3, queued flow AMS-CD generates the following answers:

- How to avoid air bubbles within the capillary

QF samples need to be degassed to avoid the formation of air bubbles, but once in the sample line further contamination with air is avoided.

- Volume of each sample required for analysis

Due to the requirements of the internal pumping loop of the auto-sampler used herein, each sample must be at least 100 µl in volume.

- Sample diffusion/ contamination

Sample diffusion can occur within the flow system, but as the system is built upon HPLC technology sample separation is generally very good. Whilst diffusion occurs on a molecular level instantaneously, in practice a sample could sit in the cell housing for at least one hour without any loss of signal strength.

- Cleaning of the AMS-CD system

Cleaning of the instrument can be difficult, especially for any optical components. The effects of build-up can be mitigated by collection of spectral baselines but this remains an important issue

- System stability (to what degree does the system need a constant environment)

The QF system is vulnerable to shocks (i.e. external vibration) as well as modification, with small changes in the system set-up ruining the alignment of the sample. When carrying out an experiment it is important that the instrument or its environment is not interfered with in any way.

Queued sample AMS-CD applications

One of the most important applications of this device is its use in screening refolding solutions for recombinant proteins. As protein secondary structure is a vital part of successful refolding, AMS-CD analysis could be an effective approach in selecting for refolding solutions.

As with any structurally investigative technique, AMS-CD would not be sufficient on its own to isolate an effective refolding mixture as it can only be relied upon to yield secondary structural information, but when used in tandem with other methods the technique has the potential to yield excellent results. As a result, we combined QS AMS-CD analysis with ELISAs (Enzyme-linked immunosorbent assay) to assess the effectiveness of a chemical refolding screen (full data sets not shown). The ELISA agent chosen in this instance was ABTS with hydrogen peroxide.

We attempted to refold denatured Horse Radish Peroxidase (HRP) with a selection of chemicals. HRP was chosen as a target protein for the wide variety of structures within the protein, including co-ordinated calcium ions and disulphide bridges. All ELISA assays were carried out by Lisa Tuckley (an MRes toxicology student I was responsible for at Birmingham University), using a Bio-Teck Instruments KC4 v2.6, Plate Reader. After carrying out an

initial AMS-CD screen of each sample (figure 4.12), we acquired the following averaged spectra for every possible combination of two refolding agents (see figures 4.13, 4.14 and 4.15).

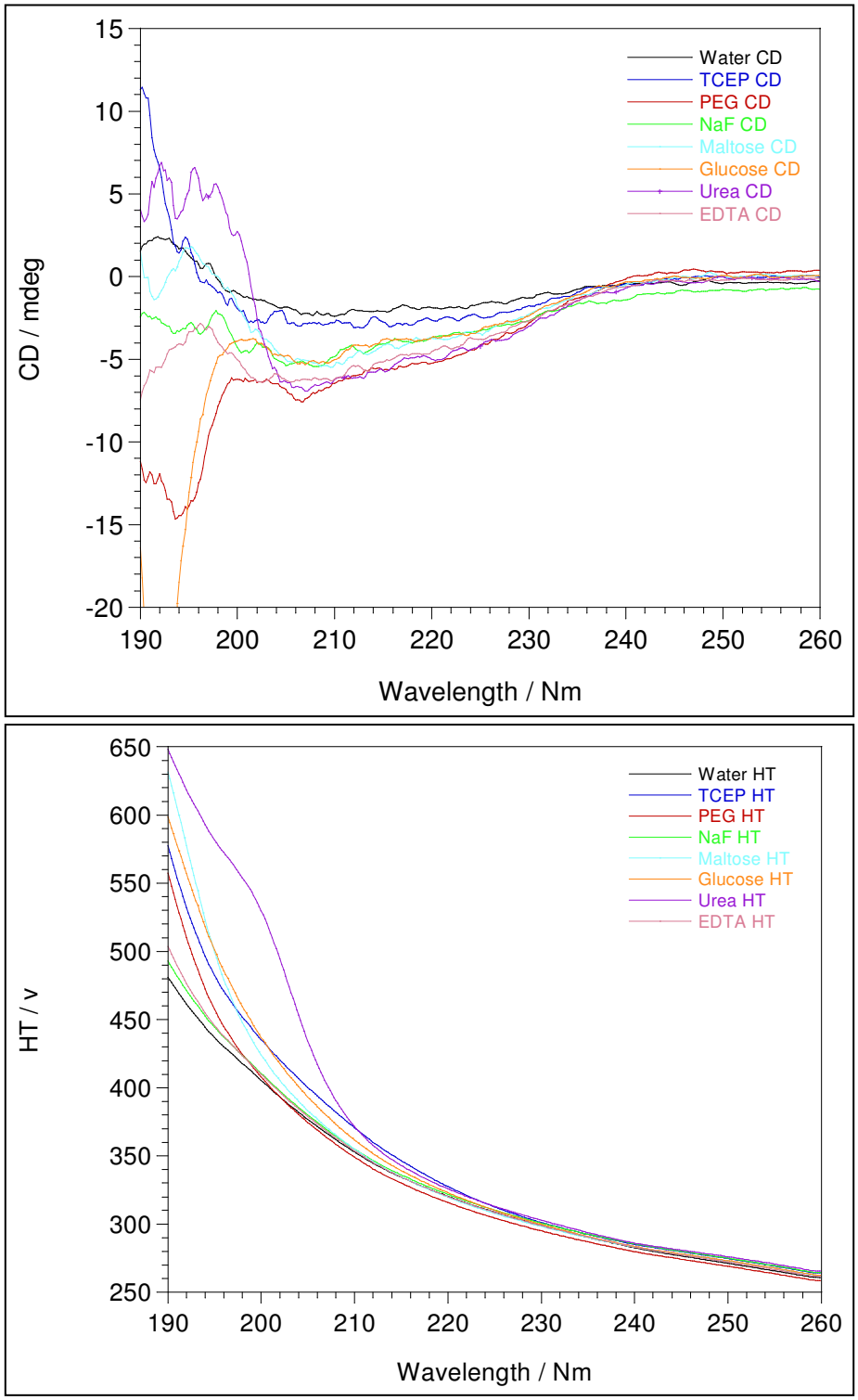

Figure 4.12: QS-AMS CD data of initial refolding agent screen. HRP concentration for all samples was at 0.5 mg / mL of denatured HRP protein. CD parameters were as follows: Bandwidth 2 nm, response 1 second, data pitch 0.2 nm, 2 accumulations.

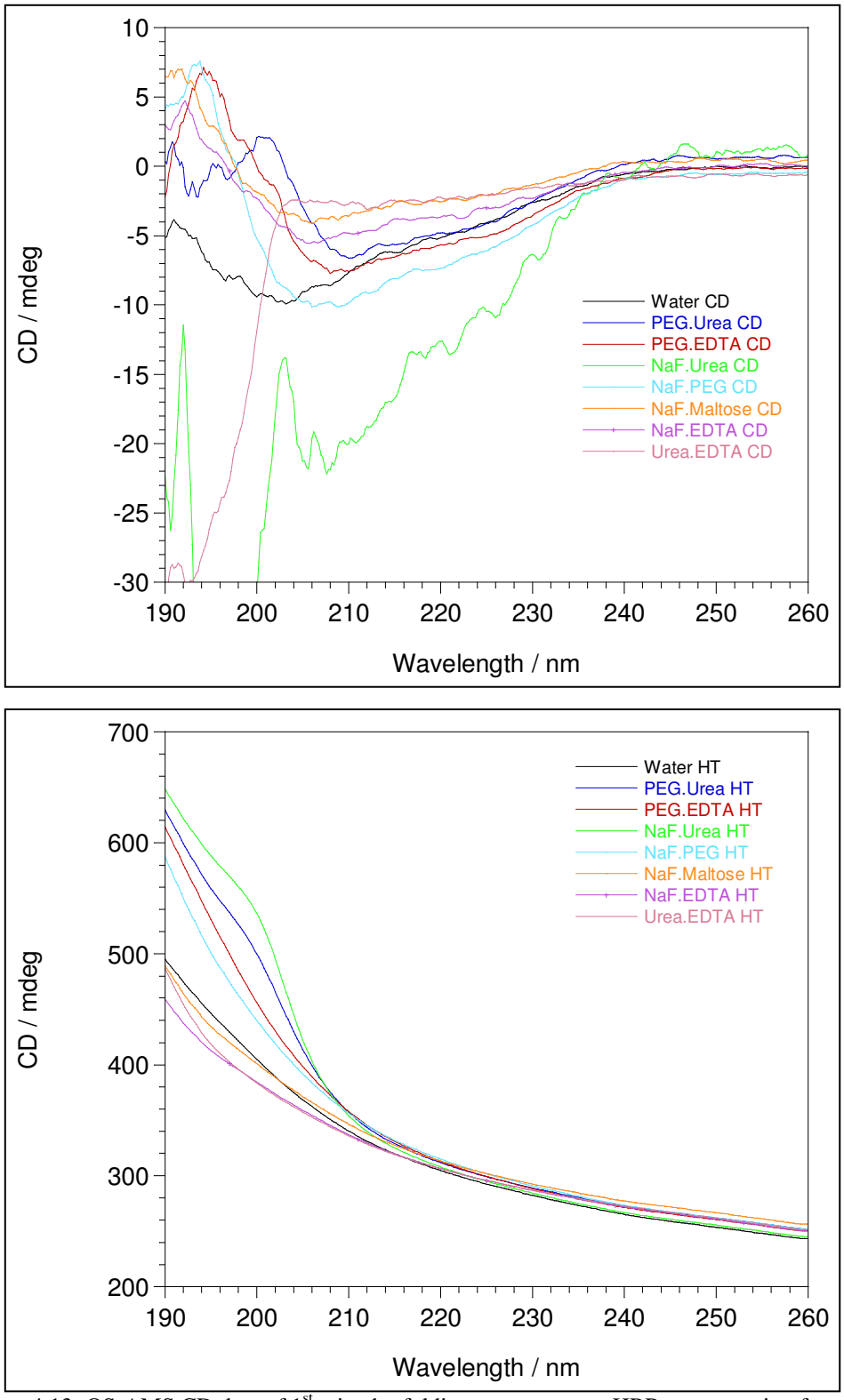

Figure 4.13: QS-AMS CD data of 1st mixed refolding agent screen. HRP concentration for all samples was at 0.5 mg / mL of denatured HRP protein. CD parameters were as follows: Bandwidth 2 nm, response 1 second, data pitch 0.2 nm, 2 accumulations.

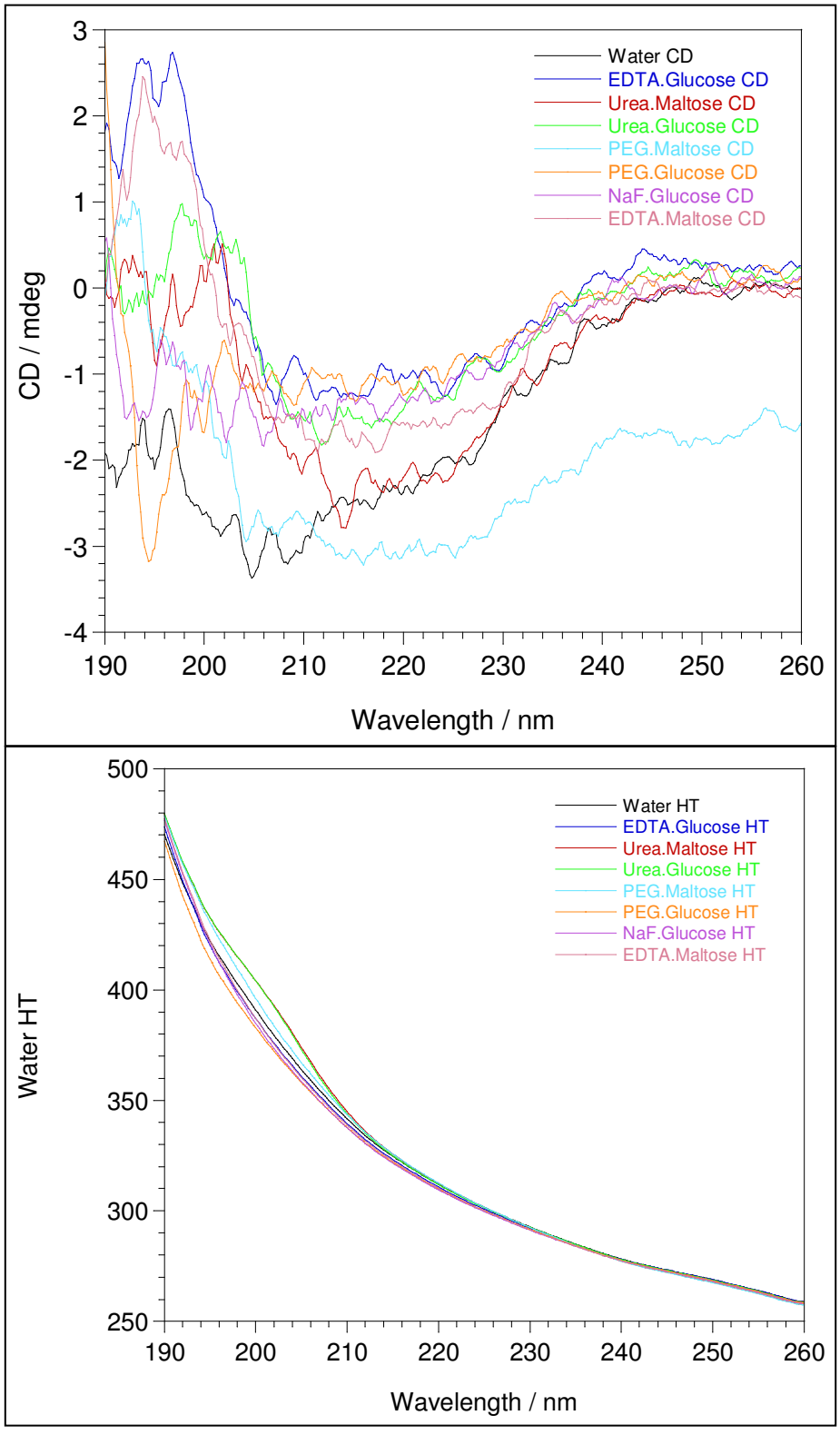

Figure 4.14: QS-AMS CD data of 2nd mixed refolding agent screen. HRP concentration for all samples was at 0.5 mg / mL of denatured HRP protein. CD parameters were as follows: Bandwidth 2 nm, response 1 second, data pitch 0.2 nm, 2 accumulations.

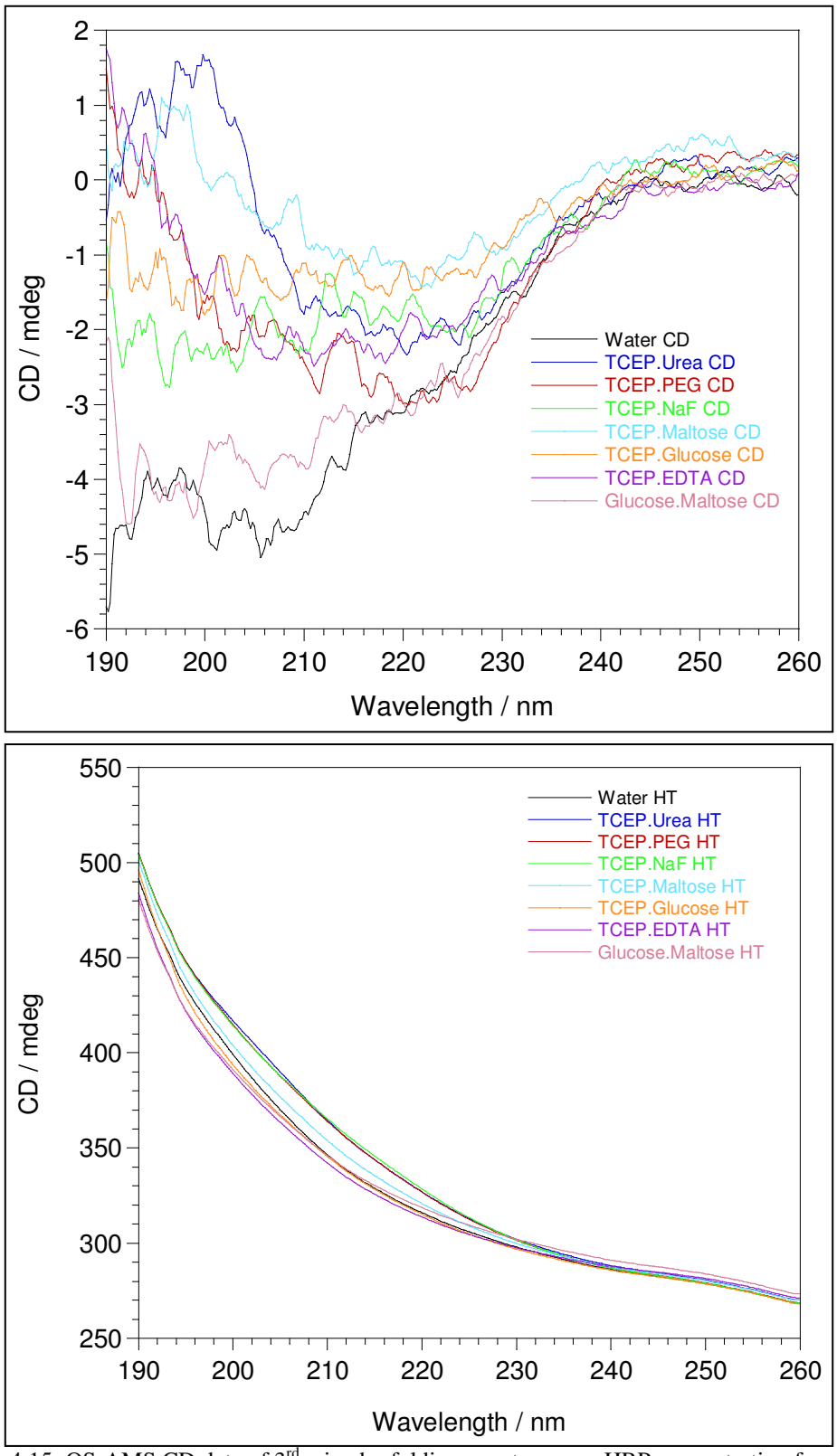

Figure 4.15: QS-AMS CD data of 3rd mixed refolding agent screen. HRP concentration for all samples was at 0.5 mg / mL of denatured HRP protein. CD parameters were as follows: Bandwidth 2 nm, response 1 second, data pitch 0.2 nm, 2 accumulations.

However, the AMS-CD data could not be relied upon to generate quantitative results- whilst general spectral shape can be made out from the data, the relative magnitude of protein signal for each refolding mixture could not. As a result, interpreting relative amounts of secondary structural differences between partial secondary structures is very difficult.

To illustrate this, figure 4.16 shows the averaged CD spectra of the four best and three worst combinations of refolding agents as defined by activity.

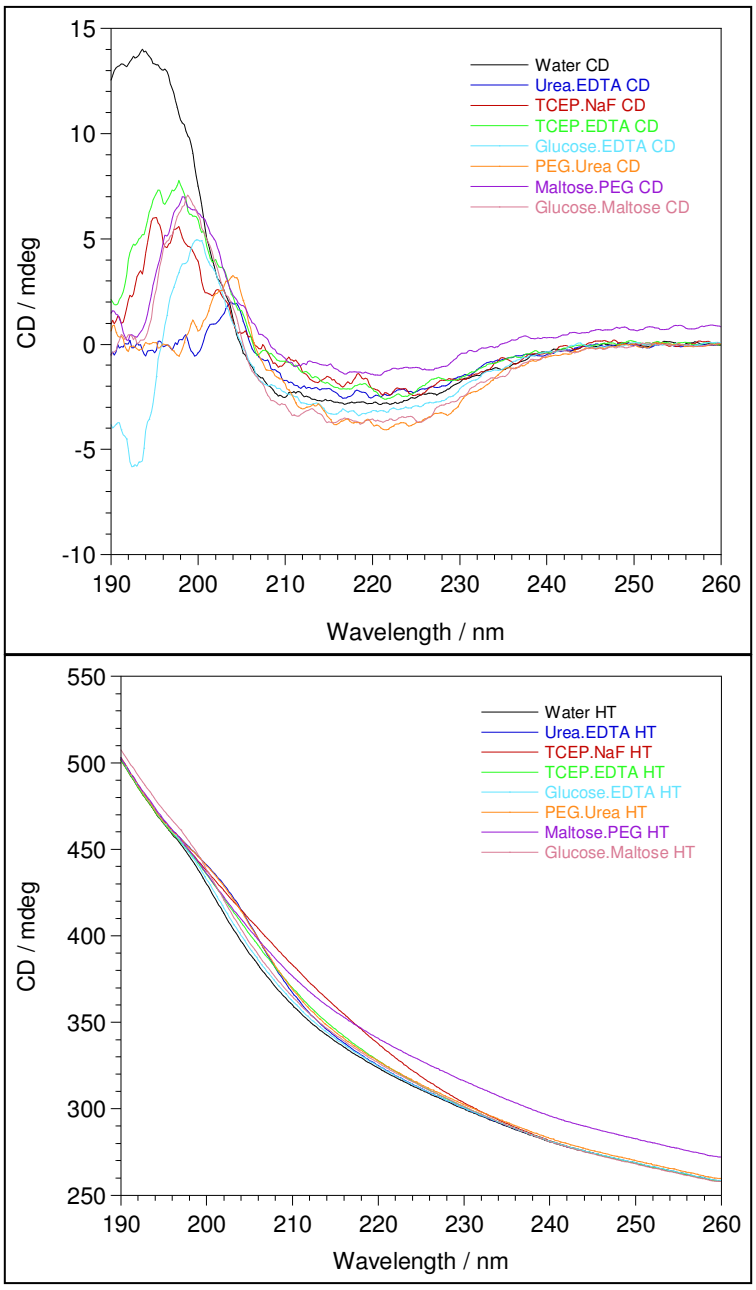

Figure 4.16: CD spectrum comparison between four best performing refolding agents against the three worst (by activity), all data acquired by QS-AMS CD. All HRP concentrations are at 0.5 mg / mL. For the purposes of comparison, the water CD spectrum is using un-denatured HRP.

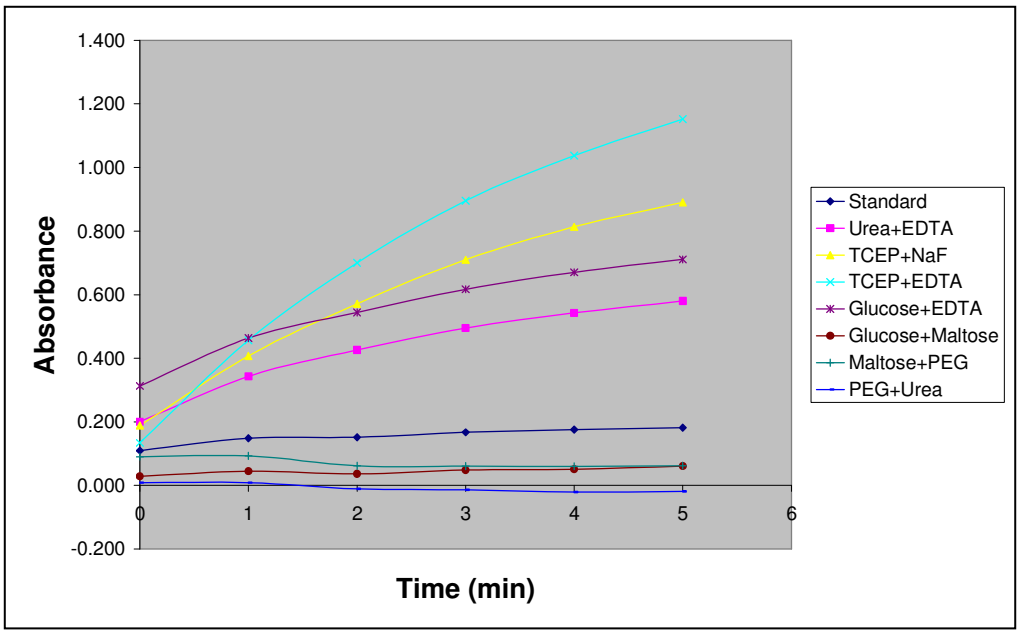

Figure 4.17: ELISA activity assay data for the best vs. worst performing refolding agents. Water baseline is marked as 'standard' (data acquired by Lisa Tuckley, Birmingham University).

ELISA assays were taken of every combination of refolding agent (figure 4.17). These assays gave an insight into the activity of each HRP in different refolding agents. By comparing the CD of these refolding agents solutions against their activity assay, we hoped to show a link between the secondary structure and the activity of the protein. The answer to the question proved more complicated. All of the refolding agents aided the formation of alpha helical structure within HRP, but the most active form (i.e. TCEP/EDTA) did not exhibit the strongest alpha helical secondary structure. Also, the worst performing refolding agents also showed the correct secondary structure. From these results, I believe that secondary structural analysis alone cannot be a sufficient measure of activity. Protein secondary structure is ultimately a necessary, but not sufficient criterion for successful protein refolding – future work on CD refolding screens must be supplemented with another technique, the combination of techniques allowing the experimentalist to draw conclusions that would otherwise not have been supported by the data.

Whilst effective at distinguishing between those refolding mixtures that definitely do not work with those that have the potential to be applicable, the QS design of AMS-CD instrument simply could not deliver suitable spectral quality to distinguish between varying levels of secondary structure. This is due in part to poor consistency in baseline acquisition for the QS system, which comes as a

result of cleaning difficulty. Another reason is accumulated error in the system. Earlier tests carried out on ovalbumin were highly reproducible and the data generated of good quality, but these were all suspended in the same solvent (in the initial tests shown in figure 4.7, water) and with the same protein in the same chemical state. Contrast this with the AMS-CD refolding screen, where different chemical compounds and HRP in different structural states are all passing through the capillary. The potential for adhesion both of organic and inorganic material to the capillary in this instance poses a serious challenge. Additionally, with the QS system, all errors with the system are cumulative. As all samples travel a fixed volume within the system, any air bubbles, issues with sample alignment or sample contamination will build up, leading to greater error in later runs. Whilst data collected at the start of the QS run may be of high quality, the quality rapidly degrades as these problems accumulate. We therefore looked towards the SSI system to improve the quality of spectra gathered and realise the potential of the technique.

4.3.3 Single-sample injection AMS-CD development

The pumping system used for SSI AMS-CD was of a different design to that used for QS AMS-CD. An experimental auto-sampler device developed by Jasco, the ASU-605 auto-sampler (figure 4.18) moved the sample via means of the NCS-609 syringe pump (figure 4.19). The device is highly programmable, but does require a significant degree of set-up to use effectively.

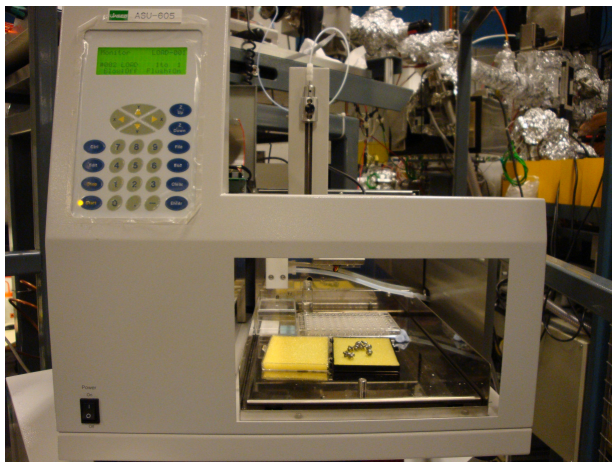

Figure 4.18: Jasco ASU 605 auto sampler. A robot arm can move in the X,Y and Z directions, with an external pump being used to actually inject samples into the capillary optic.

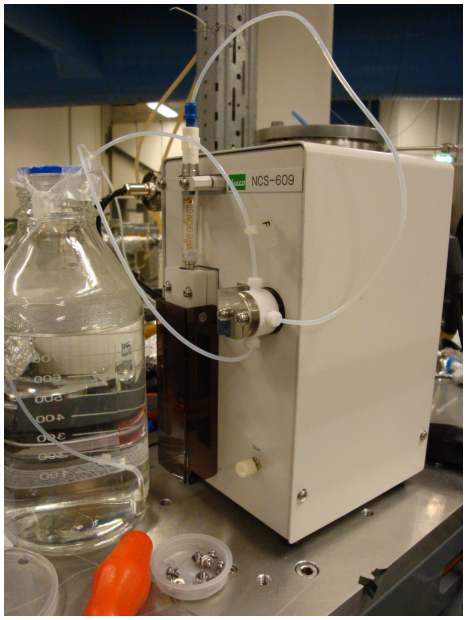

Figure 4.19: NCS-609 Syringe pump.

There are several advantages to the syringe pump method over a more traditional 'push' pump or peristaltic pump. The most readily apparent advantage is the ability to move a sample both ways in the sample line, i.e. the ability to push and pull the sample through the sample line. This two-way pumping motion allows for the sample to be recollected after analysis – an advantage to this method that is further enhanced by CD being a non-destructive technique. In addition each sample that is pumped using the syringe method is completely separate from every other sample – there is no risk of sample contamination in the sample line or risk of sample diffusion into one another.

The syringe pump method used in the Jasco auto-sampler is effective, but there are some difficulties associated with this pump method. As it pumps each sample individually (with air either side of the aliquot of sample) the pumping method has no associated hydraulic qualities *i.e.* it can be very easily compressed. With the QS system, as the sample line is completely filled with liquid then compression effects are not observed. With the SSI method, the air gap between samples can be compressed. The possibility of compression is not usually a problem, but great care must be taken to leave any sample draining areas completely clear, as any standing volume of liquid will stop the flow within the system. Additionally as the sample is bordered only by air whilst in

flow the hydrophobicity of the sample is very important in keeping the aliquot together as it is pushed around the sample line. This discovery was made after the introduction of hellmanex® into the sample line to clean the optical element. Several subsequent samples would not form a coherent aliquot of sample through the sample line, as the detergent disrupted the interaction between the liquid and the PEEK tubing. The addition of air bubbles in the sample line is nothing short of a disaster for any CD spectra taken on the sample, as artefacts and light scattering will be introduced into the sample. Care must therefore be taken in selecting the right type of conditions to test with this apparatus, in addition to any cleaning agents that are used. Below we have detailed a cleaning method that was successful for α-helical protein samples (β-sheet samples require more rigorous cleaning methods such as 6 M nitric acid).

ASTRID light source

ASTRID, or the **A**arhus **st**orage **r**ing in **D**emark is a particle storage ring based at the Department of Physics and Astronomy at Aarhus University, Denmark. Operated by ISA (Institute for storage ring facilities in Aarhus) it has been an operational synchrontron light source since 1991.

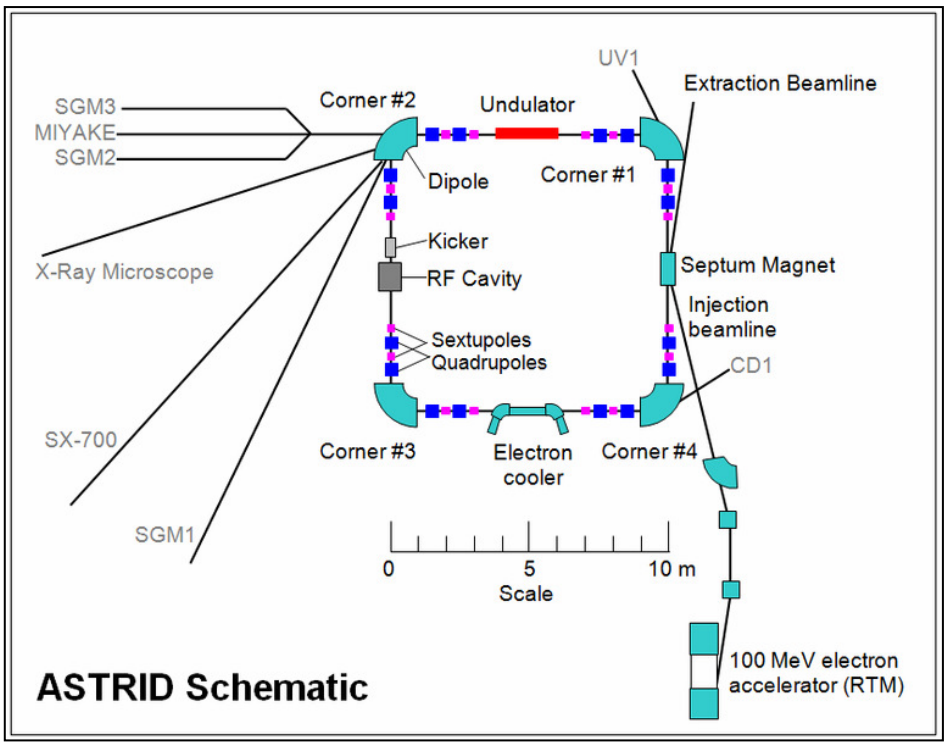

Figure 4.20: Schematic of the ASTRID light source. Image available at http://commons.wikimedia.org/wiki/Main_Page.

At ASTRID we used the CD 1 beamline (figure 4.20), which uses corner magnet four as a means of extracting light from electrons held within the storage ring. Offering a wavelength range of 125 – 700 nm, and with a photon flux of over 1000^{10} photons per second, this light source is ideal to gather CD data of excellent quality.

Single-sample injection capillary holder

The capillary holder (figure 4.21) used in the SSI had a design that was slightly adapted from that detailed in section 4.3.1. Changes in the design were to account for the differences in optical set-up at ASTRID, where the system was tested as it was felt that the SSI set-up could take better advantage of the facilities there.

A longer length of capillary (8 cm compared to 4 cm) was used to facilitate better access for tubing to each end of the capillary in addition to a reworking of the light mask employed. The aperture in the light mask created was thinner and longer than the original light mask had been, to take better advantage of the light beam at the CD 1 beam-line. As each form of light source has its own shape and intensities, it is important to adapt the masking methods employed.

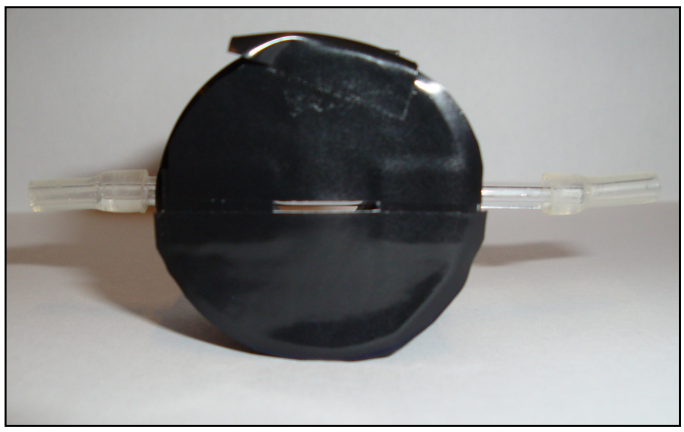

Figure 4.21: Masked capillary holder for the SSI AMS-CD apparatus that was tested at the ASTRID beam-line, Aarhus.

The CD1 beam-line at Aarhus features a sample chamber (figure 4.22) that has several access points in and around its housing, enabling the capillary holder to be connected up to the sample chamber relatively easily.

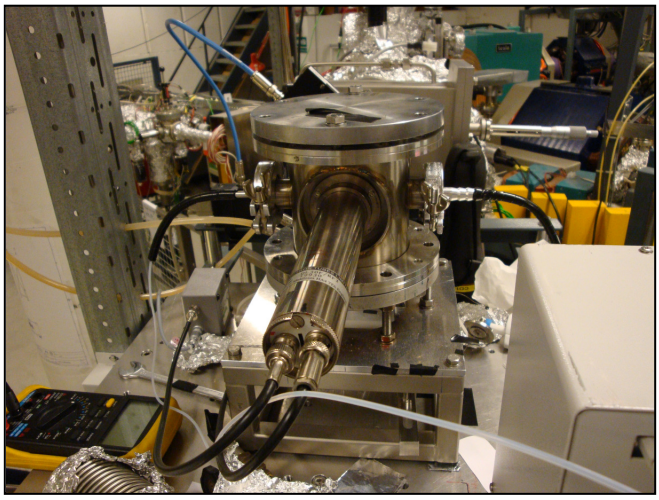

Figure 4.22: ASTRID CD1 beam line sample chamber. The storage ring is behind the sample chamber in this shot, with the detector for the beam-line in the foreground. To the left and the right of the sample chamber can be seen the black piping used to connect the capillary holder with the AMS-CD device.

For the SSI AMS-CD application we used the two side holes to pass the sample line through, with the capillary being placed inside the sample chamber (figure 4.23).

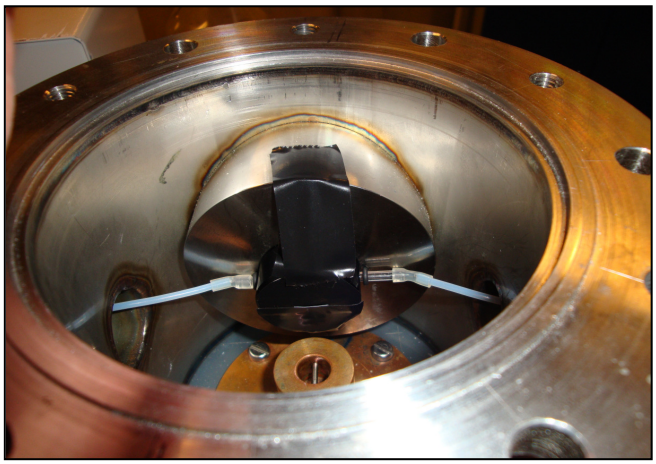

Figure 4.23: The capillary holder flow optic interface with the ASTRID CD1 beam line. Samples that were injected into the capillary would flow from left to right. The capillary flow optic was slotted into place in front of the detector, before being secured into place using electrical tape.

Care must be taken with fixing the sample line in place inside the sample chamber – we initially encountered significant issues with light scattering and other artefacts entering the spectrum, despite the sample chamber being completely sealed. This effect was being caused by light using the sample line as a kind of 'light guide', creating spectral abnormalities. To counter this, we

fed the sample line through two lengths of black plastic piping bent to form a 90º bend (figure 4.24). The resulting masked sample line successfully eliminated all stray light entering the sample chamber.

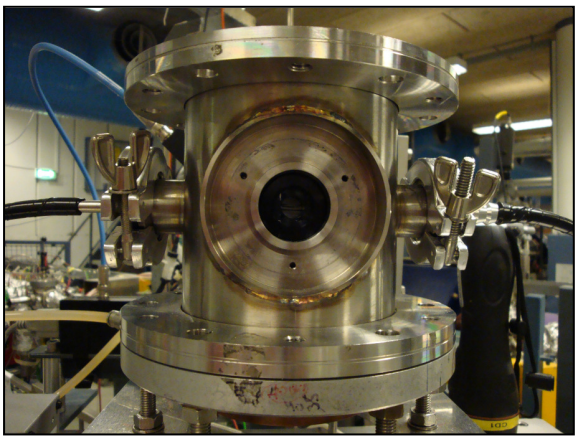

Figure 4.24: Capillary holder and sample lines after integration into the ASTRID CD1-beamline. The detector has been removed to show the location of the capillary optic inside the sample chamber.

Upon successfully integrating the capillary flow optic with the CD1beam line the SSI AMS CD device was fully complete (figure 4.25) and ready for testing.

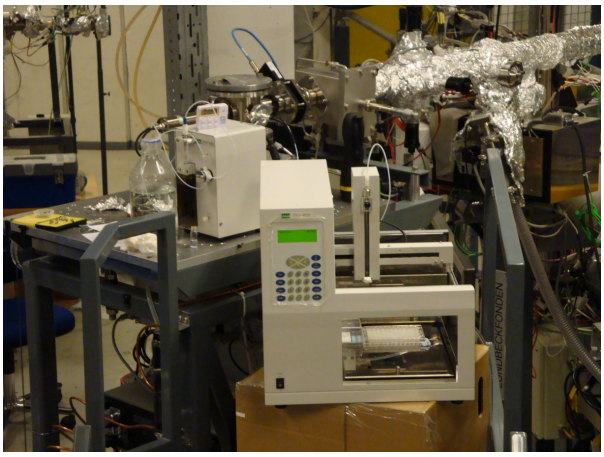

Figure 4.25: Fully integrated and assembled SSI AMS CD device at the CD1 beam-line at ASTRID, Aarhus University. The cylinder wrapped in aluminium foil (top right) is the beam line link to the storage ring.

Single- sample injection testing

When testing the SSI AMS-CD set-up, we were fortunate enough to have access to the ASTRID synchrotron at Aarhus University. The reduced sample dead-time and ability to acquire data throughout a 24 hour time period without a user

being present would help optimise the efficiency of any beam-line time, always a very precious resource. It was decided to try to first of all confirm the accuracy of the instrument by loading various protein samples into the capillary and contrasting these with CD spectra generated using a cuvette. The results of this are displayed in figures 4.26-4.29.

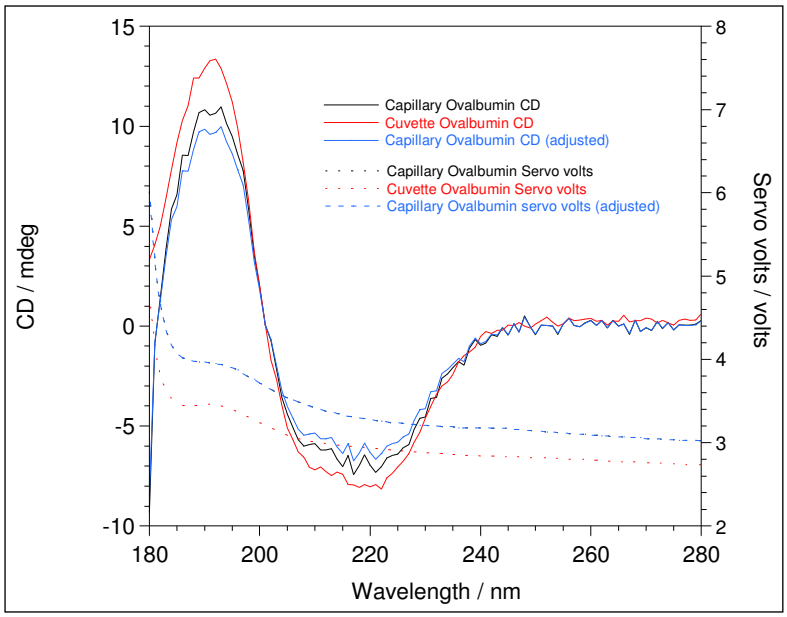

Figure 4.26: CD spectra of 0.1 mg / ml Ovalbumin, (capillary path-length 1.1 mm). All CD spectra were acquired at the ASTRID synchrotron light source at ISA, Aarhus University.

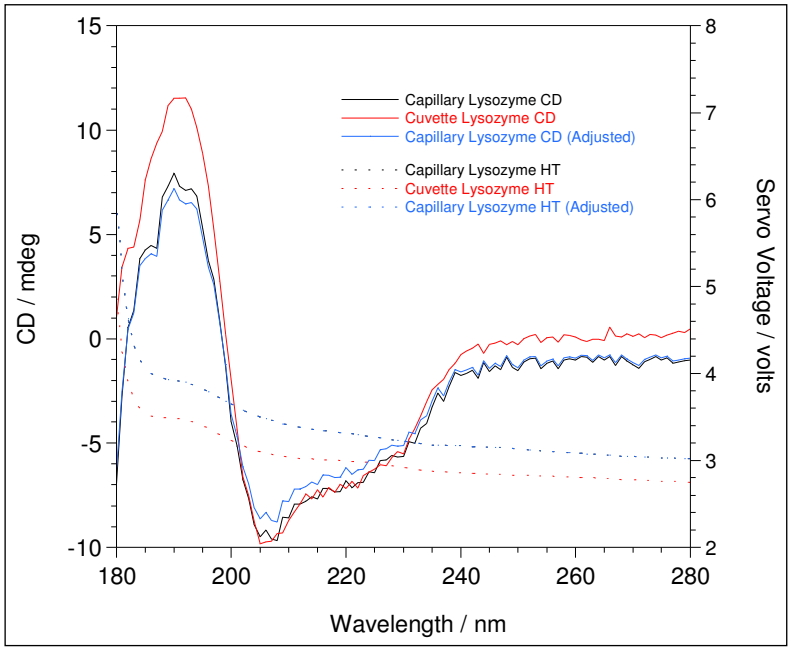

Figure 4.27: CD spectra of 0.1 mg / ml lysozyme (capillary path-length 1.1 mm). All CD spectra were acquired at the ASTRID synchrotron light source at ISA, Aarhus University.

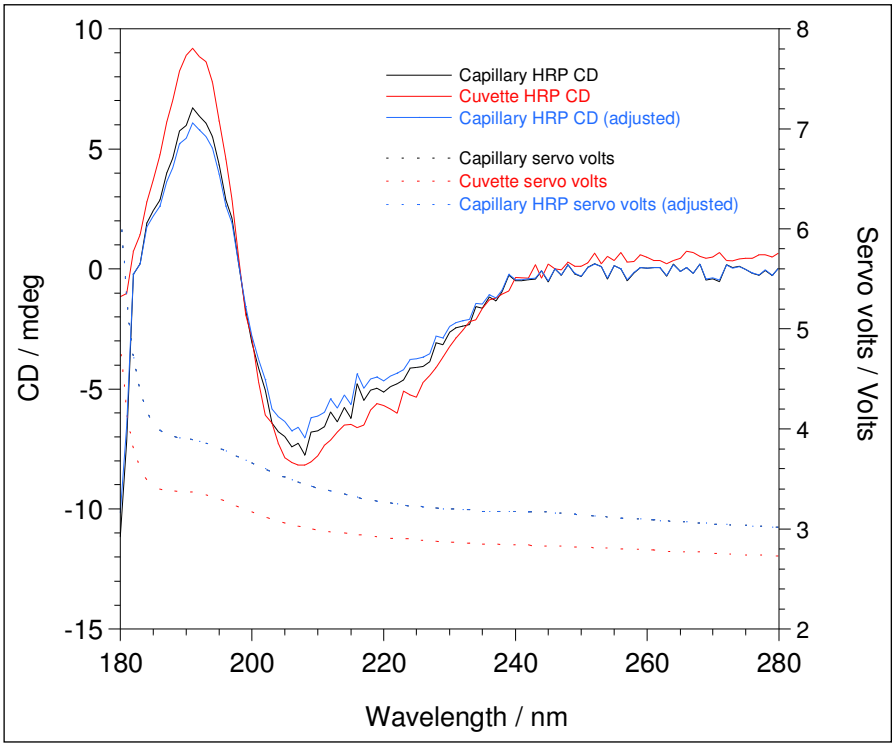

Figure 4.28: CD spectra of 0.2 mg / ml Horse Radish Peroxidase (capillary path-length 1.1 mm). All CD spectra were acquired at the ASTRID synchrotron light source at ISA, Aarhus University.

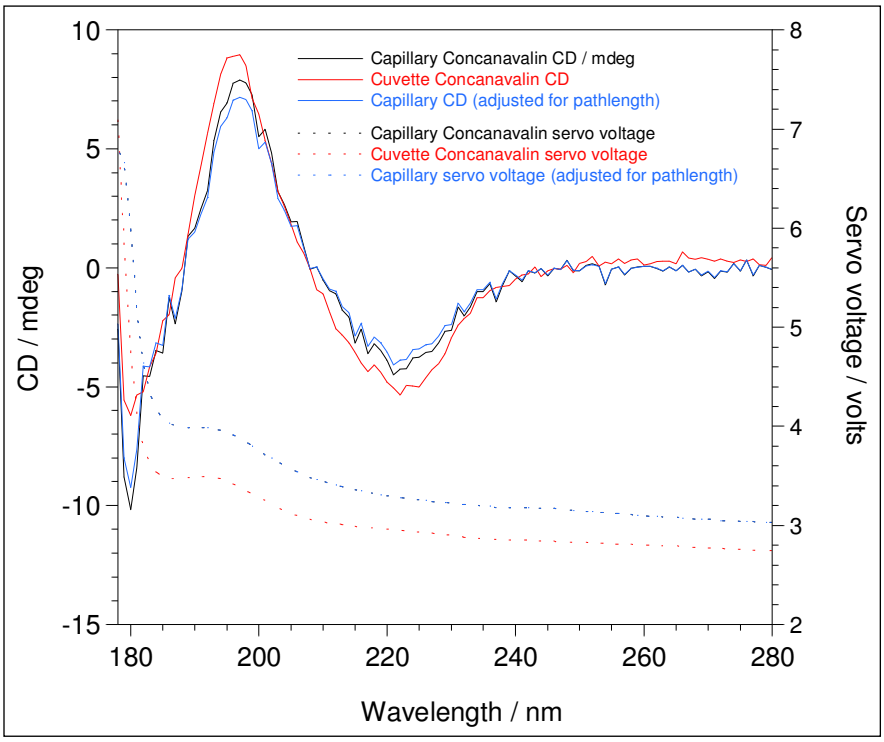

Figure 4.29: CD spectra of 0.1 mg / ml Concanavalin A (capillary path-length 1.1 mm). All CD spectra were acquired at the ASTRID synchrotron light source at ISA, Aarhus University.

As can be seen from figures 4.26-4.29, there is a strong correlation between the cuvette data sets and the capillary data. This data was obtained without the use of a focusing lens due to the excellent optics within the CD1 beam-line, which maximised photon flux, but did not counteract the optics of the capillary, leading to the differences observed between the two types of spectra. The loss of signal intensity at spectral regions of high absorbance is consistent with a capillary CD cell without a focusing lens (see chapter 2 for more information). However, the relative peak/trough ratio and shape of spectrum is consistent between the capillary and cuvette spectrum. We were therefore confident that for the purposes of proving the SSI system the optical set-up was sufficiently accurate for CD work on the synchrotron light source. This said, the loss of signal intensity does in this iteration of the design rule out absolute quantitative assessment using capillaries in a synchrotron. A focussing lens of some description must be used to modify the optical characteristics of the capillary before quantitative data can be gathered.

In order to assess the effect of the capillary cell upon the secondary structure, Dichroweb [7,8,9] analysis was done on all data sets using the CDSSTR [10,11,12] method, reference set number 3 (185-240 nm). All data sets had a normalised root mean square value of less than 0.01; the secondary structure results of the analysis are displayed below.

Protein	Helix Segments	Ave Helix Length	Strand Segments	Ave Strand Length
Lysozyme Cuvette	5.967	12.758	2.705	4.198
Lysozyme Capillary	7.165	11.341	1.506	3.278
Ovalbumin Cuvette	5.720	10.806	5.478	3.198
Ovalbumin Capillary	4.664	12.323	3.195	4.732
Concanavalin Cuvette	2.542	18.794	6.291	3.756
Concanavalin Capillary	1.564	26.766	6.289	4.877
HRP Cuvette	6.533	11.795	3.103	2.936
HRP Capillary	6.251	10.021	3.664	2.917

Table 4.1: Dichroweb[7] analysis of SSI AMS-CD data compared against cuvette data, collected at the ASTRID beam-line. CD data sets used for analysis are the same as those presented in figures 4.26 – 4.29.

Protein	Helix1	Helix2	Strand1	Strand2	Turns	Unordered	Total
Lysozyme Cuvette	0.52	0.24	0.06	0.05	0.03	0.09	0.99
Lysozyme Capillary	0.53	0.29	0.02	0.03	0.04	0.10	1.01
Ovalbumin Cuvette	0.39	0.23	0.07	0.11	0.09	0.12	1.01
Ovalbumin Capillary	0.39	0.19	0.09	0.06	0.07	0.20	1
Concanavalin Cuvette	0.38	0.10	0.11	0.13	0.15	0.14	1.01
Concanavalin Capillary	0.36	0.06	0.18	0.13	0.07	0.21	1.01
HRP Cuvette	0.51	0.26	0.03	0.06	0.04	0.10	1
HRP Capillary	0.38	0.25	0.03	0.07	0.11	0.16	1

Table 4.2: Dichroweb[7] secondary structure analysis of SSI AMS-CD data compared against cuvette data, collected at the ASTRID beam-line. CD data sets used for analysis are the same as those presented in figures 4.26 – 4.29.

The data shows that the calculated secondary structure content of each cuvette/capillary data set for each protein shows strong agreement. In absolute terms the greatest difference is observed in the HRP data set, where the alpha helical content of the HRP has been estimated as lower than that of the cuvette sample. However, for the rest of the secondary structure content of the proteins, there are great similarities between the data sets for each protein. For the helix segment size, average, helix length, strand segments and average strand length, all values across a protein are of a similar order in both cuvette and capillary data sets, but these values tend to be far more sensitive to changes in the data set used. In table 4.3 Ovalbumin (cuvette) was compared using CDSSTR reference data set 1 and 3. The results are shown below:

Protein	Helix Segments	Ave Helix Length	Strand Segments	Ave Strand Length
Ovalbumin Cuvette Data set 1	4.956	12.697	5.233	2.662
Ovalbumin Cuvette Data set 3	5.720	10.806	5.478	3.198

Protein	Helix1	Helix2	Strand1	Strand2	Turns	Unordered	Total
Ovalbumin Cuvette Data set 1	0.43	0.20	0.03	0.10	0.11	0.14	1.01
Ovalbumin Cuvette Data set 3	0.39	0.23	0.07	0.11	0.09	0.12	1.01

Table 4.3: Full Dichroweb results for the same Ovalbumin cuvette data set analysed using the CDSSTR program. A different reference set was used for each analysis. Data set the same as that presented in figure 4.26.

Whilst the paper[7] talks about minimising the NRMSD to generate the most effective data, the difference between the data sets is minimal, with set 1 having a value of 0.003 and set 3 having a NRMSD value of 0.002. In fact, the secondary structure information between capillary and cuvette is in better agreement than the same sample information analysed with two different reference sets. Whilst not an exact reproduction of cuvette SRCD spectra, SSI AMS-CD spectra can be relied upon to generate data of sufficient quality to generate secondary structural information. The data are in broad agreement between the capillary and the cuvette data sets according to Dichroweb secondary structure analysis.

After the sample chamber was tested, we then moved onto the instrument's ability to deliver multiple samples, with an aim to prove the reproducibility of sample alignment in the set-up. The performance of the instrument was tested using an injection of lysozyme followed by water, using alternating samples of both protein and water every 90 seconds over 20 minutes. The data generated from that experiment are shown in figure 4.30.
The data clearly show good sample separation with each injection, showing that the SSI system of sample loading was very effective. A delay time of 90 seconds between each sample injection was necessary in order to dispose of each sample and prime the instrument to inject the next sample in sequence. A sharp increase in CD signal before each sample entered and left the capillary was observed in each instance – this leads to the characteristic 'loading peak' before and after each sample. The uniformity and consistency of the recorded instrument baselines showed the effectiveness of SSI loading system, with a

consistent signal and loading peak in the observed spectrum illustrating the operation of the system.

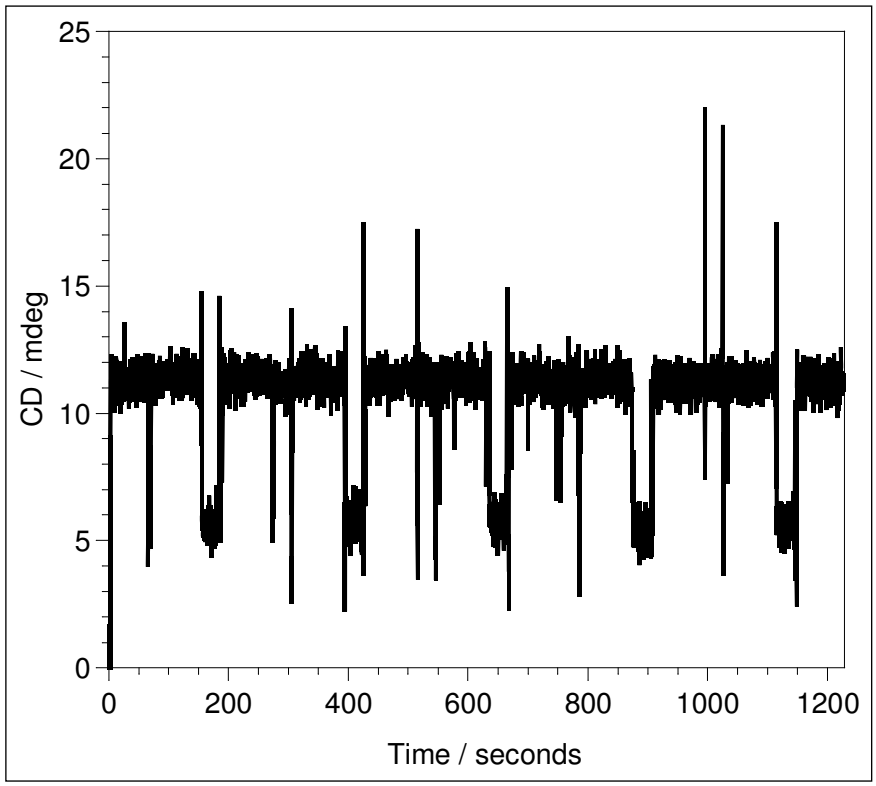

Figure 4.30: CD time course measurement of five alternating water/ 0.1 mg/ml lysozyme samples at 225 nm. Each sample was in the sample chamber for 30 seconds, with a 90 second gap between samples for disposal and loading of each new sample. This CD spectrum was acquired at the ASTRID synchrotron light source at ISA, Aarhus University. The spikes in the recorded CD signal are when an aliquot of sample reaches the capillary.

Figure 4.30 was final confirmation of the effectiveness of the SSI AMS-CD method. This method delivers excellent quality data, being able to take full advantage of the high quality light source at ASTRID over multiple sample injections.

When compared against the criteria put forward in section 4.1.3, SSI AMS-CD performs in the following way:

- How to avoid air bubbles within the capillary

Air bubbles can be an issue with this method as the sample is held within an air-filled sample line. Careful control of the flow speed can reduce this effect.

- Volume of each sample required for analysis

The sample volume for this technique can be very small, to around 15-20 µl in volume per analysis sample.

- Sample diffusion/ contamination

Sample diffusion and contamination within SSI is very unlikely, due to the isolated nature of each sample.

- Cleaning of the AMS-CD system

Cleaning of the sample line is trivial under this set-up as it is very easy to flow cleaning agents such as Hellmanex®, but the cleaning of optical components within the AMS-CD system remains more difficult.

- System stability (to what degree does the system need a constant environment)

The system is relatively robust with good system stability and reproducibility a boon in its favour. However, the sample itself passes through the sample line through air pressure, with the sample aliquot remaining in place in part through the hydrophobic effect. Should any residue remain inside the sample line that disrupts the formation of a meniscus (e.g. a detergent) then the aliquot of sample can disband in transit, ruining the CD spectrum.

4.4 Conclusions

We have developed two separate methods for automated multi-sample circular dichroism which can perform to a high degree of accuracy. This has been brought about by advances in our understanding of capillary circular dichroism and the development of a novel sample holder for CD spectrophotometers.

Queued sample AMS-CD is a reliable method, based upon proven HPLC technology. Using a simple pump system, samples are delivered into the quartz sample capillary with a high degree of regularity and accuracy. Whilst excellent for qualitative assessment of samples, it is difficult using QS AMS-CD to deliver consistently high quality CD spectra of a high enough standard for quantitative analysis.

Single sample injection AMS-CD is the next generation of AMS-CD instrument we have worked on. The syringe drive pumping system is a more flexible, isolated and controllable system that also allows for the reclamation of samples. Most importantly, the data quality that this sample delivery method affords the user would make it the preferred method for AMS CD development in the future.

In conclusion, QS AMS-CD is a fully operating system that is effective at generating CD data for qualitative applications. SSI AMS-CD is a very promising development that can be currently used to generate good quality CD spectra and that has the potential in the future to be used to quantitatively assess the structure of different solutions.

4.5 References

1: N.J. Greenfield, Using circular dichroism spectra to estimate protein secondary structure, 2006, Volume 1 no. 6, 2876 – 2890, Nature Protocols

2: H.C. Jarrell**,** Reducing the NMR sample volume using a single organic liquid: Increased sensitivity for mass-limited samples with standard NMR probes, 2009, 198, 204-208, Journal of Magnetic Resonance

3: B.R. Johnson, What's Different about Ultraviolet and Infrared Optics? SPIE Critical Review Vol. CR43, p.61-75., Optomechanical Design

4: B.A. Wallace, R.W. Janes, Synchrotron radiation circular dichroism spectroscopy of proteins: secondary structure, fold recognition and structural genomics, 2001, vol. 5, p 567 – 571, Current Opinion in Chemical Biology

5: D.E. Waldron, R. Marrington, M.C. Grant, M.R. Hicks, A. Rodger, Capillary Circular Dichroism, 2010, 22 Suppl 1:E136-41, Chirality

6: S.M. Kelly, T.J. Jess, N.C. Price, How to study proteins by Circular dichroism, 2005, 1751, p 119 – 139, Biochimica et Biophysica Acta

7: L. Whitmore, B.A. Wallace, Protein Secondary Structure Analyses from Circular Dichroism Spectroscopy: Methods and Reference, 2008, vol. 89, p 392-400, Biopolymers

8: L. Whitmore, B.A. Wallace, DICHROWEB: an online server for protein secondary structure analyses from circular dichroism spectroscopic data, 2004, vol. 32, p 668 – 673, Nucleic Acids Research

9: A. Lobley, L. Whitmore, B.A. Wallace, DICHROWEB: an interactive website for the analysis of protein secondary structure from circular dichroism spectra, 2002, vol. 18, p 211-212, Bioinformatics

10: L.A. Compton, W.C, Johnson Jr., (1986) Analysis of protein circular dichroism spectra for secondary structure using a simple matrix multiplication, 1986, vol. 155, p 155-167, Anal. Biochem

11: P. Manavalan, W.C. Johnson Jr., W.C., Variable selection method improves the prediction of protein secondary structure from circular dichroism spectra, 1987, vol 167, p 76 – 85, Anal. Biochem

12 N. Sreerama, R.W. Woody, R.W., Estimation of protein secondary structure from CD spectra: Comparison of CONTIN, SELCON and CDSSTR methods with an expanded reference set, 2000, vol. 287(2) p. 252 – 260, Anal. Biochem

CHAPTER FIVE

Linear Dichroism of Biological Systems

Lapsana communis in both visible colour and UV.

CHAPTER FIVE: Linear Dichroism of Biological Systems

Summary

In this chapter we report the first confirmed UV LD spectrum of a bacterium, *Bacillus Subtilis* under both Couette flow LD and linear flow LD. We also report the first LD spectrum of flagella, with supporting E.M. images showing the isolation of this class of biological macromolecule. This study shows that the LD signal generated by B. Subtilis does not come from any orientation of its attached flagella, but rather from the main body of the bacterium itself. Additionally, there is preliminary evidence of lateral association between flagella under Couette flow that quite closely follows behaviour observed in tubulin. This area merits further research.

5.1 Introduction

5.1.1 Linear dichroism as a means of analysing biological systems

UV linear dichroism (LD) spectroscopy is now an established means of investigating the structural properties of macromolecules, especially biological macromolecules[1]. Currently UV LD is used to look at sample molecules in isolation, or within a predominantly uniform environment, e.g. a membrane protein embedded within a liposome. However, the potential exists to analyse bigger and more complex samples than this. Provided that the sample has UV active chromophores and can be orientated in flow, then it should be possible to generate an LD spectrum for it. With this in mind, UV LD has been successfully applied to many different classes of molecule, including DNA[2], fibrous proteins[3], membrane proteins[4] (within a liposome to replicate the protein's native conformation) and even carbon nano-Tubes[5]. In this chapter we consider its applications to bacteria and flagella.

5.1.2 Bacteria

Bacteria are microorganisms that are typically several microns in length. They can be found in an array of different shapes and sizes and have the capacity to evolve rapidly. There are approximately $4 – 6 \times 10^{30}$ individual bacteria worldwide[6]. Bacteria form a vital part of any ecosystem, with bacteria living both independently and in symbiosis with a whole host of organisms, including humans. Bacteria can also be keys instigators of disease, rapidly infecting a host and transmitting infectious agents to other areas[7].

The most common way currently used to distinguish between types of bacteria is the Gram test. Developed in 1884 by Hans Christian Gram, he discovered that different strains of bacteria stained differently when placed into contact with crystal violet. In his initial paper on the subject[8], Gram managed to effectively distinguish between *Klebsiella pneumoniae* and pneumococcal bacteria. The pneumococcal bacteria were heavily stained with the dye producing a purple colour, being referred to as Gram positive, whilst the *Klebsiella pneumoniae* stained very lightly and are now referred to as Gram negative. This distinction between the two types of bacteria arises from the different structures of the outer membrane of each type of bacteria. Gram negative bacteria typically have two cell membranes separated by a periplasm, whilst

Gram positive bacteria have a thicker peptidoglycan layer outside the membrane. The structure of a bacterium's outer membrane is vital, as it not only helps determine the structure and shape of the bacterium as a whole but can also have a significant impact on the effectiveness of antibiotics.

Gram-positive cell walls are made of predominately peptidoglycan. The thick peptidoglycan layer of the cell wall is anchored to the cytoplasmic membrane through teichoic acids. The entire ensemble carries a negative charge. In many different bacteria, attachments to the surface are often found, most notably protrusions such as pilli or flagella that allow each individual bacterium to move within its surroundings[9]. The cell wall aids a bacterium in maintaining cellular homeostasis, as well as maintaining the structure of the bacterium.

In this study, we used the gram positive bacterium *Bacillus Subtilis* extensively. *Bacillus Subtilis* was a good bacterium to work with on this project for a number of reasons. First and foremost, the bacterium in its stable phase displays a rod-like structure that we anticipated would be significantly easier to orientate than other bacteria, such as *Escherichia coli*. This factor, when combined with the versatility, ease and rapidity of growth and non-pathogenicity makes them ideal species to study using LD methods. Once orientated, material inside the bacteria such as chromosomes[10], plamids[11] (which code for some proteins within the cellular environment) and proteins could potentially generate the required electronic transitions to produce an LD signal.

5.1.3 Whole organism linear dichroism

The first attempt at collecting an LD spectrum of bacteria was by Dr. Adair Richards, a researcher working within the research group of Prof. Alison Rodger. There had already been a successful LD spectrum of other biological organisms such as bacteriophages, where the protein coat of the bacteriophage allowed a high degree of alignment which translated into a high signal LD spectrum[12].

Obtaining an LD spectrum for a whole organism, especially a bacterium would be a big advance both in LD spectroscopy but also in the study of bacteria as a whole. By being able to quantitatively analyse a whole organism, many useful applications could be opened up, including monitoring the life cycle of bacteria, examining changes in

structure induced by environment and perhaps mostly importantly, real time monitoring of anti-bacterial agents working on a bacterial sample.
The data produced by Adair Richards are given in figure 5.1.

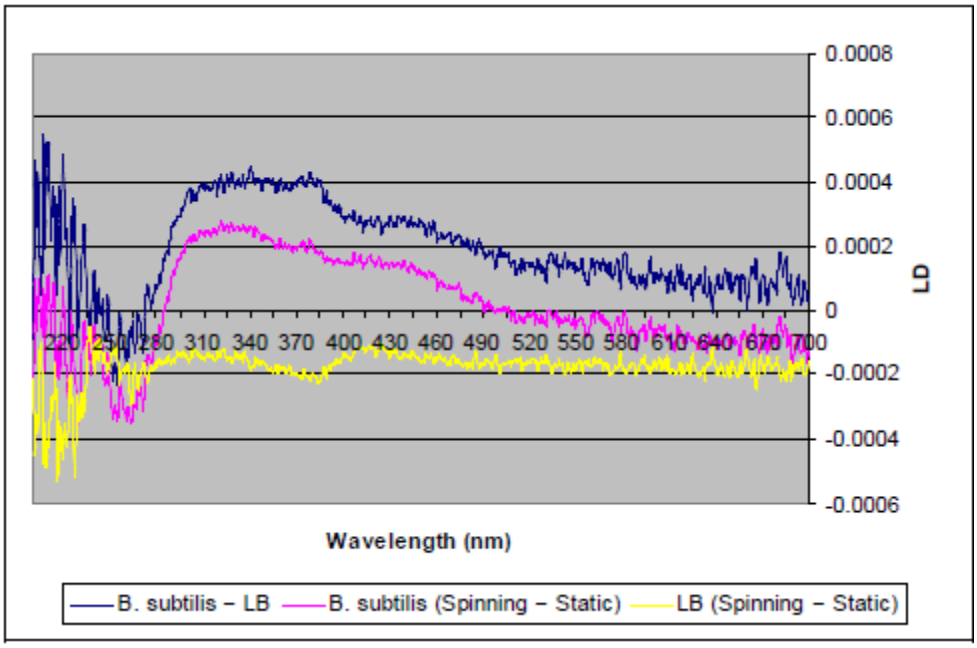

Figure 5.1: LD spectra of Bacillus Subtilis in Luria Broth. Final LD signal is shown in blue. Figure taken from the thesis of Dr. Adair Richards 'Taking the fight to the Superbugs: Interactions of Synthetic DNA-binding Metallomolecules with Biological Systems'. Figure used with permission.

The magnitude of the LD signal is very small, but there does appear to be a signal where one would expect a peak in the DNA region of the spectrum (at approximately 260 nm). The signal is however two orders of magnitude smaller than that expected from DNA. This weakness of signal could be attributed to a number of factors, including a lack of alignment or a small concentration of LD active groups within the sample. At these magnitudes, this signal could simply be background noise, or caused by another source.
In order to prove the viability of whole organism LD as an area of study, it was necessary to acquire a definite spectrum of a bacterium. The work done by Adair Richards represented an excellent starting point but was not itself clearly a true bacterial signal.

Looking at the experiments pursued by Dr. Richards, it became apparent that his method was not ideal through its use of LB as the 'solvent'. LB is a rich chemical soup filled with many biological molecules that is fully capable of supporting life

(hence its main use to grow bacteria). Whilst the bacteria would survive well in this media, its opaque nature makes it unsuitable for spectroscopy. As a result, we decided to use 0.1 M phosphate buffer at pH 7 as a buffer for the *B. Subtilis*. The bacteria can survive for two to three hours in phosphate at this concentration as the osmotic pressure the cell is under allows it maintain homeostasis and avoid going hypertonic. Additionally, due to the lack of halide counter-ions present in phosphate buffer the solution is also relatively easy to study in the UV, making this an ideal solution for our purposes.

5.1.4 LD from other sources in the cell

The signal of the *B. Subtilis* from Adair Richards work was very small – was it possible that the signal was generated by something other than the bacteria itself? The easiest forms of molecule to detect using UV LD tend to be very long, thin molecules. *B. Subtilis*, as most bacteria uses long, thin filaments known as flagella, or their structural (though not functional) equivalents pili[13].

Flagella are tail-like protrusions that are anchored into the cell membrane of the cell; typically they are involved in cellular locomotion. They can be found amongst prokaryotes, eukaryotes and Archaea, with distinct differences in the structure of any flagella found.

Bacterial flagella are comprised of the protein flagellin, which forms a hollow tube that is just 20 nm thick. Most flagella observed in bacteria tend to be comprised of 11 protofilaments, which are bundled together to form the main flagella filament. Each protofilament is in turn comprised of tandem protein chains. Each individual flagellum is anchored inside the outer membrane of the cell by a hook-like protrusion. This protrusion also helps with the flagellum's locomotive function, as the hook allows the flagella to be orientated directly away from the cell. Locomotion itself is achieved via a screw-like rotation of each flagellum, which can turn at anything between 200 – 1000 rpm. Interestingly, when assembling a flagellum, bacteria build them not from the base, but from the tip. Flagellin and other compounds used in the construction of the flagellum pass through its internal bore to form the filament[14].

B. Subtilis itself is heavily flagellated [15], allowing each individual bacterium to propel itself swiftly through its environment. However, it was possible that the (small) signal previously observed from the bacteria was created by plasmids or

chromosomal DNA within the bacteria. Additionally, the presence of the flagella could be in some way affecting the alignment of the bacteria.
Of equal interest, there was the prospect that *B. Subtilis* could generate a signal produced by orientated flagella rather than the bacterium itself. We therefore set-out to confirm whether it is possible to acquire an LD spectrum of a whole bacterium, whether or not the signal observed was being affected by attached flagella and finally, whether flagella themselves could generate an LD spectrum.

The work outlined in this chapter describes the measurement of the first confirmed LD spectrum of bacteria and of flagella. Details are given about how the bacteria were expressed and purified. Additionally, experimental methods of orientating LD samples are detailed, opening up new and exciting avenues of study.

5.2 Materials and methods

5.2.1 Materials

Bacillus Subtilis 168 was used for all bacterial experiments, with all cultures grown in Luria Broth (LB). Initial cell plates were made of an agar/LB, with all incubations taking place at 37 ºC. Phosphate salts were purchased from Sigma-Aldrich.

5.2.2 Methods

B. Subtilis cell culture preparation

A cell culture of *Bacillus Subtilis* 168 was prepared by streaking a glycerol stock of the bacteria onto a prepared LB agar plate that was subsequently left in an incubator at 37ºC overnight. From this plate a single colony was selected for inoculation into 10 ml of autoclaved LB. This suspension was in turn placed into an incubator under constant motion at 15 strokes per minute, and a temperature of 37ºC overnight.
10 ml of the inoculated suspension was then mixed with 500 ml of fresh autoclaved LB. This solution was in turn left overnight in the incubator, under constant motion at 37ºC overnight.
When preparing the bacterial culture for UV spectroscopy the cell culture was spun down in a Beckman J2-21 centrifuge at 3000 rpm for twelve minutes to form a cell pellet. The supernatant was poured off, with the pellet being washed three times with 0.1 M phosphate buffer at pH 7.0. The cell culture was then re-suspended in the

phosphate buffer before undergoing an A280 measurement to ascertain the concentration of bacteria within the suspension. The suspension was then diluted to 1.5 OD (at an A280 measurement) before undergoing CD and LD analysis.

Flagella Preparation

The same protocol as outlined above was used to create a *B. Subtilis* cell culture. However, once spun down, the cells were washed and re-suspended in double distilled water. The A280 of the suspension was taken and the cells diluted to a 20 OD solution. This suspension was then homogenised using a Polytron kinematic GmbH CH-6010 homogeniser at 20,000 rpm for three minutes. The extreme shear force applied to the cells causes the 'hook' part of the flagella to break, releasing the individual flagellum into the suspension. One of the side effects of this is the partial destruction of some of the bacterial cells, releasing their contents into the suspension as well.

Once homogenised, the cell suspension was then spun down at 3,000 rpm for 12 minutes using Eppendorf 5810 R centrifuge. The supernatant from the spinning down was removed from the pellet to undergo ultra-centrifugation.

In order to get a flagella sample of good purity the supernatant from the previous step was taken and loaded into the specialised sample boats for the Beckman TL-100 ultra-centrifuge. At this stage it is vital to get the weight of the filled sample boats as close to one another as possible. In order to separate the flagella from other cell debris, the flagella sample was spun at 50,000 rpm (100,000 G) for one hour. The pellet from the ultra-centrifuge was then taken and resuspended in double distilled water, ready for further analysis.

Electron Microscopy sample preparation

Electron Microscopy (E.M.) copper grids prepared as described below were used to collect E.M. micrographs:

1) Dip a clean microscope slide in a solution of 0.25% by volume Formvar® (polyvinyl formal) dissolved in chloroform. Once the slide is removed from the solution, as the chloroform evaporates a thin film of Formvar is left on the surface of the slide (altering the concentration of the Formvar will change the thickness of the film created).

2) Remove the Formvar film from the slide using a pair of tweezers and place the film into a bowl of water, so that the film floats on top of the meniscus. Once the film is floating, place copper grids onto the film.
3) Place a piece of parafilm onto the floating Formvar film, ensuring that it is the same size as the Formvar film. This should create a parafilm / Formvar 'sandwich', with the copper grids nestled in between.
4) Cut out each individual copper grid from the surrounding films - the grids are now ready for use.

The biological sample that is to be analysed by E.M. is placed upon the grid and then stained using the following method:
1) Take a drop of the analysis sample (in solution) and place a single drop of it onto a clean hydrophobic surface e.g. a piece of parafilm, Petri dish. The hydrophobic effect will cause the droplet to bead rather than spread out, making the rest of the process easier.
2) Place the prepared grid onto the sample droplet (Formvar side down) and leave it in place for five minutes. During this time hydrophobic parts of the analysis sample will diffuse into the Formvar film.
3) Place three droplets of distilled water onto the hydrophobic surface, each approximately 1 cm apart. Use these droplets to wash the grid by placing the grid directly into each individual droplet, for five minutes per water droplet. This step minimises crystal growth (which can damage the E.M. image) by placing as many salts from the analysis sample into the polar solution of the water droplets.
4) Place the copper grid into a droplet of 1% ammonium molybdate solution with 70 µg / ml Bacitracin to act as a surfactant. This negative stain darkens the background of the E.M. image, with any biological material showing up as pale on the dark background rich in heavy metal ions. Ammonium molybdate does not crystallise under these conditions, making it an ideal stain for E.M.
5) Remove any excess stain from the grid using the edge of a piece of filter paper or another absorbing material so that only a thin layer of stain is deposited on the copper grid – any more than that and it is possible to swamp any biological material present on the grid with stain, rendering the entire slide useless.

Instrumentation

UV LD spectra were acquired using a Jasco-715 CD spectropolarimeter in conjunction with a Couette flow LD cell, available from Dioptica Scientific Ltd. CD spectra were acquired using a Jasco 815 spectropolarimeter and a 1 mm quartz cuvette, available from Starna.

E.M. images were recorded using a Philips CM120 BioTWIN Transmission Electron Microscope.

UV/Vis data was acquired using a Kontron Uvikon 923 spectrophotometer.

5.3 Results

5.3.1 Bacillus Subtilis

The first confirmed LD spectrum of B Subtilis was collected at Birmingham University using phosphate buffer as the solvent, producing the spectrum shown in figure 5.2.

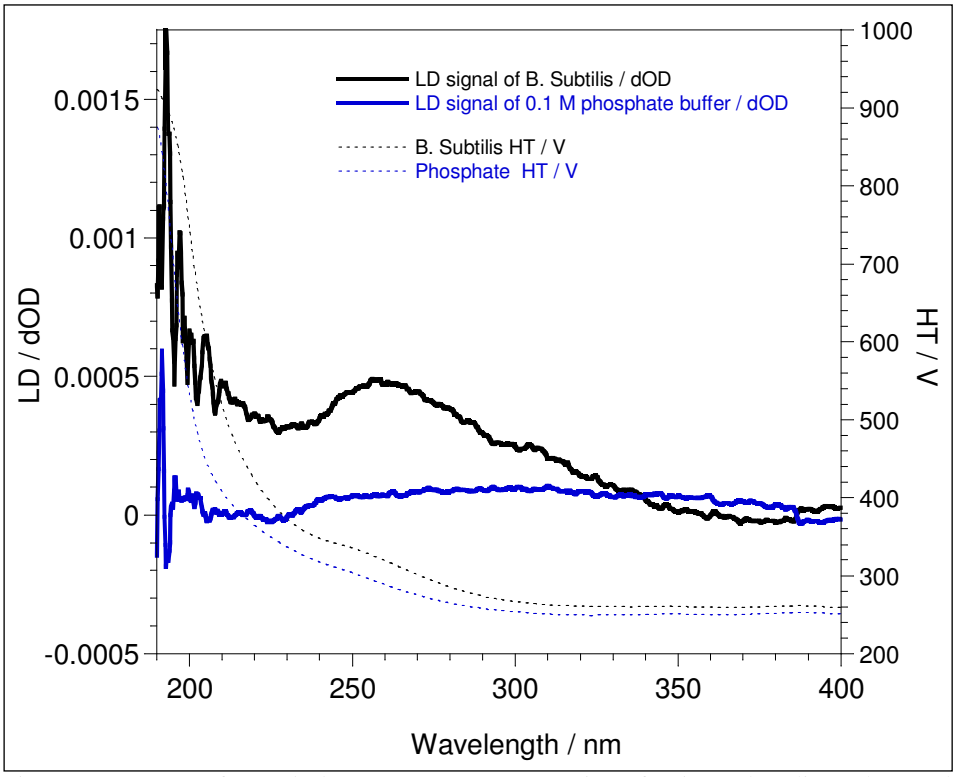

Figure 5.2: LD spectrum of *B. Subtilis* at an A280 concentration of 1.5 OD (baseline subtracted). The phosphate buffer baseline is included here to facilitate comparison. The bacteria were buffered in pH 7, 0.1 M phosphate solution. Orientation of the sample was achieved using a Couette LD cell under standard conditions.

The signal for the *B. Subtilis* is small, but there is definitely some change from the phosphate baseline. There is a positive peak at 260 nm, an area of the spectrum

where DNA should give a signal, but its magnitude is very small. A lot of the most interesting information with regards protein signal is lost due to HT cut-off at 600 V, but this remains a possibility for some of the signal generated. The size of signal is consistent with a solution of relative large bodies, which to their size and shape are difficult to align. The difference between the parallel and perpendicular absorbencies would be small in the instance of a difficult to align sample, which results in a small recorded LD signal.

The spectrum shape itself is hard to analyse. The helical band at 210 nm has been lost due to HT cut-off, but there is signal being generated in the DNA region. One possibility is that the many proteins that are present both on the surface and within the bacteria themselves are more randomly orientated due to the nature of the sample (i.e. as they would be in a living system), generating perpendicular signal at 230 nm from the $n \rightarrow \pi^*$ transitions that are perpendicular to the orientation axis, in addition to any 210 nm transitions that are influencing the spectrum (whilst obscured at 210 nm, the transition is relatively broad and if a powerful effect, could influence the spectrum at slightly higher wavelength). Additionally, the 220 nm peak of the DNA could also be averaged with the potentially strong protein signal from the rest of the bacteria.

With the *B. Subtilis* posing several interesting challenges, we decided to investigate the bacteria for evidence of a potential source of a 210 nm absorbance band. An excellent source of this would be flagella, of which *B. Subtilis* is sometimes known to exhibit. These long fibres would be relatively easy to align in flow and would generate a strong protein signal at 210 nm. We therefore decided to investigate the bacteria culture we were using for evidence of flagellated *B. Subtilis*.

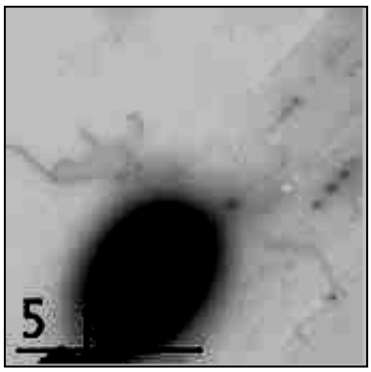

Figure 5.3: E.M. image of *B.Subtilis*. The sample was taken from a solution of LB media, rather than agar to properly reflect the number of flagella present per bacterium as measured by other methods. The large black object towards the bottom left of the image is a *B.Subtilis* bacterium, whilst its flagella can be most clearly seen centre left and centre right, protruding from the rear of the bacterium

Having confirmed the presence of flagella within our sample of *B. Subtilis* (shown in figure 5.3), we attempted to acquire a LD spectrum of isolated flagella, in order to quantify their LD signal. Flagella are very long, thin structures that are comprised entirely of flagellin, a protein with equal amount alpha helix and beta sheet content[16]. As flagella are comprised of an α-helical protein, the signal they produce should be weighted towards the lower end of the UV range at 210 nm, the wavelength at which helices parallel to the direction of orientation have their $\pi \rightarrow \pi^*$ transition. No signal should be produced at 260 nm. In order to obtain the LD spectrum, it was necessary to purify a sample of the flagella for LD analysis.

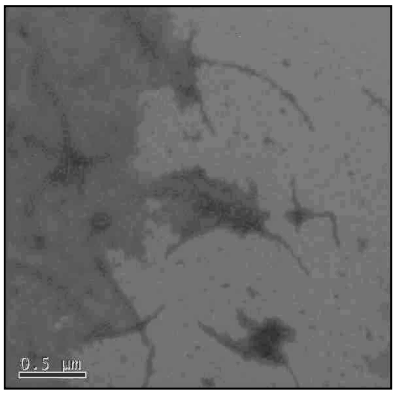

Figure 5.4: E.M. image of cell extract post homogenisation. The sample was taken from the suspension of the homogenised solution after centrifugation. This fraction contains cell debris, as well as individual flagella (the long thin objects within the image, the best example being in the top right hand corner of the E.M. image).

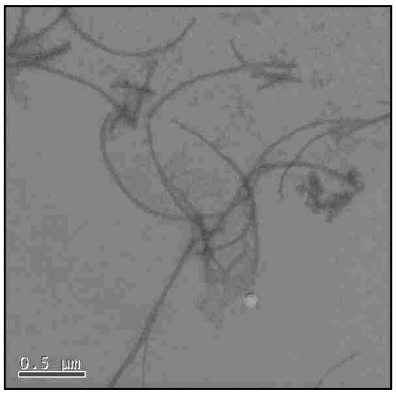

Figure 5.5: E.M. image of purified flagella, taken from a re-suspension of the pellet produced via ultra-centrifugation.

Following the method set out in section 5.2.2, we prepared a flagella solution for LD analysis, confirming each step of the purification process using electron microscopy. The results of this are shown in figures 5.4 and 5.5. It is at this point important to note that during the homogenization process, individual flagellum can be broken into

pieces, reducing the width/ length ratio of the molecule. The LD spectrum generated from the flagella solution is given in figure 5.6.

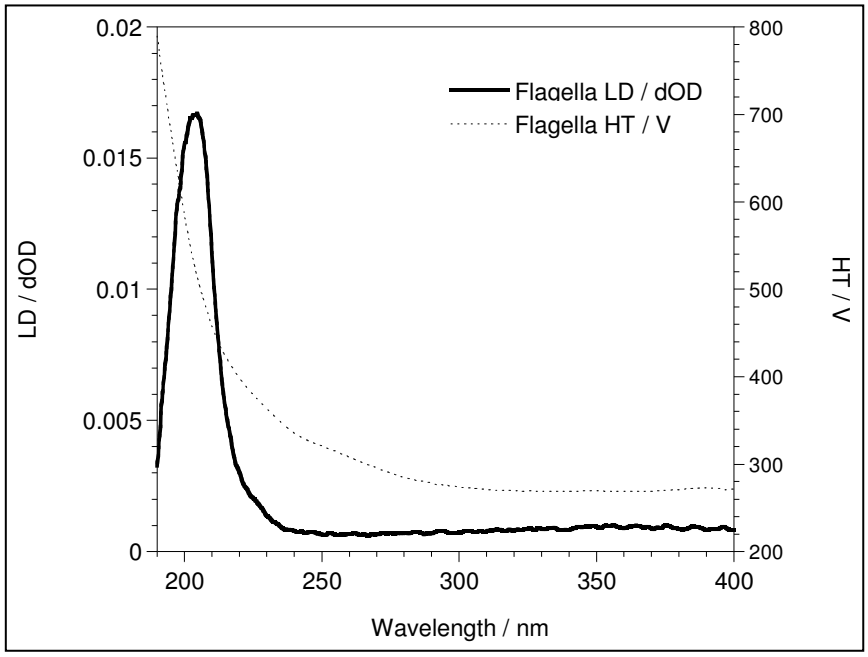

Figure 5.6: LD spectrum of 0.25 OD Flagella.

Figure 5.6 has a peak at 210 nm, which is consistent with that of a protein signal, with no other absorbance bands being present across the entirety of the UV/Visible region. The position of the signal is consistent with that of a helical structure orientated parallel to the orientation direction[17]. The signal strength is relatively large, but this is in part due to effect of concentration, especially when compared to that generated from *B. Subtilis* whole organism data set. This difference between the *B. Subtilis* spectrum and that of the flagella could be due to the elevated concentration of flagella in this solution, as the 1.5 OD solution of *B. Subtilis* would necessarily have far fewer flagella than this sample as they have not been concentrated and purified.
Additionally, the solution of flagella had a lower HT cut-off than the *B. Subtilis* solution, allowing acquisition of the peak at 210 nm that was not possible for the bacteria

The protein region in the *B. Subtilis* will undoubtedly exhibit some of its signal from the 210 nm transition of the B. Subtilis, but this will be modified by the presence of other proteins within the bacteria, whose overall orientation will only be affected to a very small degree by the alignment of each individual bacterium.
An additional effect to the random orientation of proteins through a bacterium is to-do with the alignment method itself. Linear dichroism in a Couette system assumes

that as each molecule is relatively small compared to size of the LD cell then the analyte molecule experiences an aligning force in only a single direction. However, in the case of the whole organism work, the size of the analyte molecule is relatively large and thus may experience slight angular momentum as it is forced to flow around the circular couette system. Models of Couette flow assume the molecule flows in a straight line, but in reality the molecule is under a constant turning force. Whilst it may be argued that this does not apply on a molecular level, the same logic does not necessarily apply at the micron level i.e. to objects the size of bacteria. A micron represents a statistically significant amount of the total circumference of a Couette cell , with objects at this size experiencing some turning forces. This turning force may have an especially potent effect on bacterial flagella, which are often tethered to the cell wall at an angle (rather than moving in a longitudinal fashion as eukaryotic cells, bacterial flagella move in a way more akin to a blade on a propeller[18]). Key to this is the question of whether, under the same flow conditions do micron sized cellular objects behave in the same manner as biomolecules such as DNA. Whilst not covered in the scope of this work, an investigation into this relationship is of great importance to the expansion of whole organism LD.

We hypothesised that the angular momentum experienced by the flagella was such that, when tethered in a non-optimal position to the orientation axis of the bacteria would serve to hinder the alignment of the flagella under Couette flow conditions. However, if the bacteria were aligned using another means of flow then this effect could be potentially avoided. Perhaps more importantly, the use of another means of sample orientation could allow higher flow speeds, aiding the alignment of the bacteria (for LD spectroscopy, bacteria are very large objects to orientate). This would allow us to increase the flagella signal relative to the other LD active constituents of the *B. Subtilis.*

When choosing an alternate method of sample alignment the most important feature of the method had to be the conservation of laminar flow conditions. If the flow within the system is not laminar (when fluids flow in parallel layers, without disruption between layers) then LD analysis cannot be achieved as a steady orientation axis cannot be maintained. We therefore investigated linear flow as a new means of sample orientation.

Linear flow has several disadvantages over Couette flow, with the biggest and most difficult to overcome being the large sample requirements for linear flow LD.

Couette systems have the great advantage of being able to recirculate the sample throughout the analysis system, allowing data collection for as long as the user needs and minimising the amount of sample required for each LD analysis. By contrast, linear flow is highly constrained by sample volume, requiring a large amount of sample for the most basic of LD analysis. Fortunately, *B. Subtilis* allows for production of large amounts of sample – bacteria culture is easy to make up in bulk and phosphate buffer is an inexpensive salt to purchase. A stock 1.5 OD *B. Subtilis* solution was made and orientated by continuously pumping the solution through a clean capillary system as described in chapter four of this thesis. The apparatus used was the same system as the QS-AMS CD instrument, with the J-715 spectrophotometer used in LD scanning mode rather for CD. Different pump speeds were used to orientate the B. Subtilis to see what effect increasing the flow rate would have upon any LD signal generated. The results of this can be seen in figure 5.7.

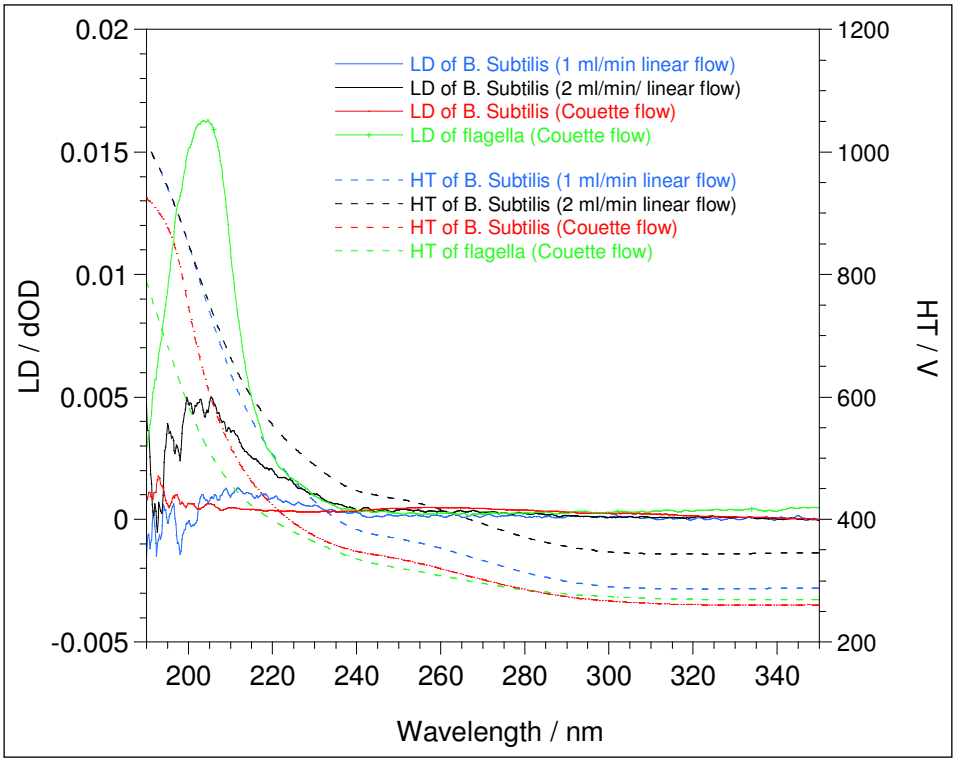

Figure 5.7: LD spectrum of *B. Subtilis* under different flow conditions. All B. Subtilis spectra were acquired at an Å280 concentration of 1.5 OD The LD spectra of A 0.25 OD couette aligned purified flagella and the original Couette LD B. Subtilis have been added to the figure for comparison.

As can be seen from figure 5.7, the *B. Subtilis* spectra acquired through linear flow exhibits a peak starting in the same region as the flagella spectrum. Additionally, the signal strength is higher for the 2 ml / min alignment sample than for the 1 ml / min.

Even when using an HT cut-off of 700 V, you can still clearly see a rise in the recorded absorbance for each linear flow sample. This can be contrasted with the protein region of the original *B. Subtilis* spectrum, where there were no readily defined spectral peaks within the protein region. Finally, the DNA peak observed in the Couette flow *B. Subtilis* cell is virtually indistinguishable from the background as soon as the flagella signal was achieved – the height of this peak is substantially larger. The *B. Subtilis* solution was purified via centrifugation and ultra centrifugation to isolate any flagella that could be knocked off – this solution was analysed using E.M. where no flagella could be found. Linear flow LD proved to be a more effective means of generating bacterial LD spectra for this specialist application than the standard Couette method of LD alignment and should be the preferred technique if such spectra are required in the future.

5.3.2 Flagella association

When analysing the flagella solution using Couette flow linear dichroism, a strange effect was observed – the LD signal of the flagella solution increased as the system underwent alignment via Couette flow (see figure 5.8).

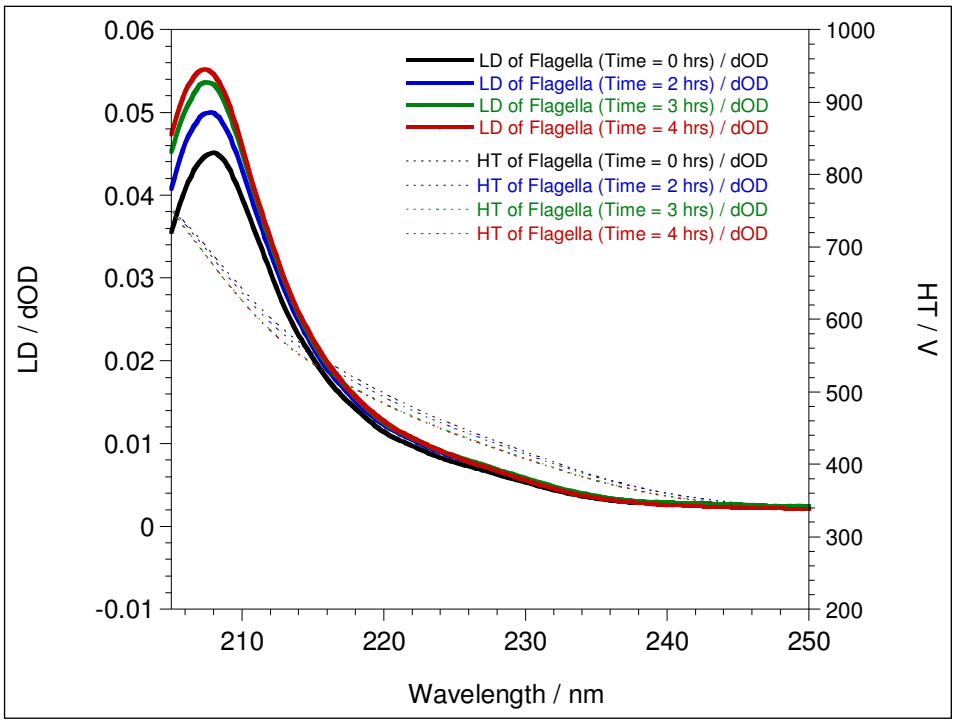

Figure 5.8: LD as a function of time for 0.5OD flagella (as calculated by A280). Under constant laminar flow, the LD signal increases over time. The LD spectra were acquired in a standard 3 mm O.D. extruded quartz capillary with a 1.1 mm quartz rod.

This result, whilst unusual was not entirely unexpected. Flagella are on a macro-structure level quite similar to FtsZ, a bacterial tubulin homologue that exhibits lateral association. Both FtsZ and flagellin form linear polymers in a head to tail bonding assembly and both with self-assemble. If lateral bundling was occurring between flagella during flow orientation in *B. Subtilis* it could account for a great many of the properties exhibited in both the *B. Subtilis* spectra and the flagella spectra.
In our case, flagella bundling and its induced cellular association could result in a loss of the *B. Subtilis* couette LD signal in the protein region through lateral association of flagella. The angular momentum effect, when coupled with lateral association and back eddies from the flow all conspire to nullify the protein signal. Additionally, flagella bundling could lead to a multi-cellular lump of cells, giving rise to the weak DNA signal observed in the initial couette flow LD spectrum.

5.4 Conclusions

We have managed to obtain a definite LD spectrum of *Bacillus Subtilis* and have successfully boosted the recorded signal using a different form of sample orientation – that of linear flow LD.
The possibility that the bacterial signal is being induced solely by attached flagella has been disproven and has led to the separate collection of the first flagella UV LD spectrum. This isolation of flagella has been confirmed using E.M. imaging, with the acquisition of the first flagella LD spectrum opening up the potential for further structural studies on this important type of biological molecule. We have also managed to boost the LD signal of *B.Subtilis* sufficiently using linear flow orientation for it to have possible experimental applications, such as real time analysis of antibacterial agents. Finally, there is evidence suggesting the formation of flagella 'bundles', suggesting a degree of inter-molecular self-assembly between flagella.

5.5 References

1: Bengt Nordén, Alison Rodger and Timothy Dafforn, Linear Dichroism and Circular Dichroism. A Textbook on Polarized-Light Spectroscopy. ISBN: 978-1-84755-902-9. The Royal Society of Chemistry – London 2010.

2: Hannon, M.J., Moreno, V., Prieto, M.J., Molderheim, E., Sletten, E., Meistermann, I., Isaac, C.J., Sanders, K.J., Rodger, A. "Intramolecular DNA coiling mediated by a metallo supramolecular cylinder", 2001, 40, 879–884, Angewandte Chemie

3: Elaine Small, Rachel Marrington, Alison Rodger, David J. Scott, Katherine Sloan, David Roper, Timothy R. Dafforn and Stephen G. Addinall 'FtsZ Polymer-bundling by the Escherichia coli ZapA Orthologue, YgfE, Involves a Conformational Change in Bound GTP' 2007, 369: 210-221, Journal of Molecular Biology

4: Hicks, M.R., Damianoglou, A., Rodger, A., Dafforn, T.R., "Folding and membrane insertion of the pore-forming peptide gramicidin occurs as a concerted process", 2008, 383, 358-366, Journal of Molecular Biology

5: Rodger, A., Marrington,R., Geeves, M. A., Hicks, M., de Alwis, L., Halsall D.J., Dafforn, T.R, 'Looking at long molecules in solution: what happens when they are subjected to Couette flow?' 2006, 8: 3161-3171, Physical Chemistry Chemical Physics

6: W. B. Whitman, D. C. Coleman & W. J. Wiebe, 1995. Prokaryotes: The

unseen majority., **95**, 6578-6583, PNAS

7: G. Fracastoro 'De contagionibus et contagiosis morbis et eorum curatione libri tres' (Three books on Infection and Infectious Diseases and Their Treatment). First published in 1546.

8: H. C. Gram, 1884. Uber die isolierte Farbung der Schizomyceten in Schnittund Trockenpraparaten, 2, 185-189, Fortschritte der Medizin

9: J. Mann & M. J. C. Crabbe, Bacteria and Antibacterial Agents, Spektrum Academic Publishers, Oxford, UK, 1996.

10: M. Thanbichler, S. C. Wang & L. Shapiro, 2005. The Bacterial Nucleoid: A Highly Organized and Dynamic Structure, 96, 506-521 Journal of cellular biochemistry

11: D. Dubnau, 1999. DNA uptake in bacteria,, 53, 217-244, Annual review of Microbiology

12: B.A. Clack, D.M. Gray, 1992. Flow linear dichroism spectra of four filamentous bacteriophages: DNA and coat protein contributions, 32, 795 – 810, Biopolymers.

13: Bardy, S.L., Ng S.Y., Jarrell K.F. "Prokaryotic motility structures", 2003, 149 (Pt 2): 295–304, Microbiology

14: Minamino, T., Imada, K., Namba, K., (2008). Mechanisms of type III protein export for bacterial flagellar assembly. 2008, Mol. Biosyst. 4, 11: 1105–15

15: DePamphilis , M.L., J. Adler, Purification of Intact Flagella from Escherichia coli *and* Bacillus Subtilis*,* 1971, 105(1): 376–383. Journal of Bacteriology

16*: F.Vonderviszt, H. Uedaira, S. Kidokoro, K. Namba,* Structural organization of flagellin, 1990, 214 (1):97-104, Journal of Molecular Biology

17: B.M. Bulheller, Circular and Linear Dichroism Spectroscopy of Proteins, Nottingham University. http://etheses.nottingham.ac.uk/866/1/BenBulheller-Thesis.pdf

18: R. N. Doetsch, Some speculations accounting for the movement of bacterial flagella, 1966, volume 11, issue 3, 411-417, Journal of Theoretical Biology

CHAPTER SIX

Conclusions & Future Work

Oenothera biennis in both visible colour and UV.

CHAPTER SIX: Conclusions and Future Work

Summary

The work presented in this thesis focuses for the most part on instrument design in polarised spectroscopy, to improve the effectiveness, scope and performance of chiro-optical methods that are in use in laboratories across the world. Primarily the focus of the work has been on circular dichroism (CD), with improvements to the technique including reducing the sample requirements necessary for analysis by two orders of magnitude and opening up the possibility of automated, multiple sample CD instrumentation. This increase of utility for the technique will hopefully allow its use to spread to other areas, including novel applications within the life sciences that have previously been either inefficient or impossible to pursue. A novel micron path-length cuvette has also been developed to facilitate collection of high concentration CD data that is both accurate and reproducible. Finally, the first confirmed LD spectrum of living bacteria and flagella have been acquired, opening up an interesting new avenue for LD research as well as the possibility of an integrated LD and CD automated sample loading device.

Using the work presented in this thesis, it should be possible to design a new form of chiro-optical sample device for both CD and LD analysis, allowing for 384 samples to be analysed within a single run and requiring very small sample volumes.

Conclusions

This project developed several aspects of sample handling in chiro-optical spectroscopy; including sample cuvettes and loading, with the intention on developing a new form of CD sample loading instrument (see future work). To this end, the project was spilt into several avenues of research. The first objective to be looked at was a means of reducing sample requirements for CD without losing any spectral quality. Sample size is often a limiting factor in CD applications, especially for protein CD. Many proteins that are of interest to researchers are produced via recombinant methods. Recombinant methods, whilst an excellent way of producing protein can often be extremely time consuming and/or expensive, rendering large sample requirement a hindrance to CD analysis. By lowering the sample requirements for CD we could widen the use and application of the technique, as well as making it more sample efficient.

The reasons for the large sample requirements in CD are twofold. Firstly, due to the Beer-Lambert law the absorbance of a sample is proportional to its concentration and the path-length of solution travelled through. For dilute solutions (0.01 mg/ml or less) a path-length of 1 cm is required. As a result, this 'minimum size' of path-length provides a barrier to sample reduction, as a minimum amount of sample is needed to fill the path-length.
The issue of path length leads in turn to the second issue – the shape of the CD cuvette. By using rectangular cuvettes, a sample of at least 150 μL is required to obtain a protein spectrum – more typically sample requirements are in excess of 300 μL. By using a better shape of sample cuvette it was possible to minimise sample requirements for the technique, reducing them to a minimum of 3 μL.
The use of quartz capillaries as a means of transmitting polarised UV light had been previously tested by Rachel Marrington, where the capillaries in question were shown to be non-birefringent and possessing no optical defects. The real challenge in this instrument design piece was to correctly harness the unique optical properties of the capillaries whilst simultaneously maximising photon flux through the sample within the capillary. Previous work by Rachel Marrington had correctly identified the size and shape of the incident light beam

from the spectrophotometer to be the major issue in the effective use of capillaries in CD. However, the approach of masking the light beam, as well as the use of two lenses meant that too much light was being absorbed by the optical system and not enough was being transmitted through the system. Additionally, and perhaps of greater importance to spectral quality, the light path taken through the capillary was not all through the sample – the optics of the capillary were not properly understood and thus stray light that had not entered the sample chamber was being registered at the detector as transmitted light.

The solution to this issue was to understand and then harness the optics of the capillary to work in tandem with the focussing lens employed to control the size and shape of the initial light beam – by taking advantage of the lensing effect shown within the cross-section of capillaries the capillary itself could act as a focussing lens, turning a slightly divergent light beam into a collimated one at the detector. In addition to this, any light that was successfully transmitted through the capillary would have had to pass through the sample chamber, resulting in a truly accurate, low volume CD spectrum. The capillary CD system was evaluated using the relatively new CD standard CoEDDS. This showed excellent agreement across a wide wavelength region between the quartz cuvette and the quartz capillary. Additional data was taken in the form of the predominantly alpha helical protein lysozyme, the beta sheet protein Concanavalin A as well as the hormone progesterone. From these samples the resulting data sets were collected using a minimum of sample (3 μL) whilst still securing high quality data sets.

Improvements in capillary circular dichroism would hinge upon the fabrication of a more cylindrical quartz capillary. The typical error in the wall of a 3 mm O.D. capillary was 50 micron – this error induces additional lensing effects into the capillary's complicated optical properties. With the manufacture of better quality capillaries, greater accuracy of focusing could be achieved allowing sample volumes to be reduced even further.

The development of the etched cell was motivated by the relatively poor performance of the currently available demountable cuvettes with a path-length

in the micron region. The path-length of these cuvettes was neither reproducible nor accurate, creating a large source of error in the CD analysis of high concentration samples. This is a serious limitation of CD instrumentation, as pharmaceutical products are increasingly being formulated to these high concentrations (in excess of 10 mg/ ml). The etched cell design was made possible by the properties of HF acid etching on a quartz surface, where the surface quality of the original surface is retained. By using quartz optical flats (pieces of quartz that have been polished to a very high standard of surface flatness) as the base materials, it was possible to fabricate a cell of sufficient accuracy that would locate to form the same path-length every time. The design of a device for controlling the flow of acid during the etching process was a vital part of this work, as was the development of a cuvette holder that would create equal pressure across the face of the etched flat whilst maximising the amount of transmitted light. The finished etched cuvette device delivers a known, reproducible micron scale path-length that will allow future users to analyse concentrated samples confident of the path-length that they are using. Additionally, the etched cuvette opens up the possibility of flow applications, as the etched channel covers the entire face of the etched quartz flat. This opens up several interesting possibilities, which are discussed in the future work section below.

The etched cuvette, whilst being precision engineered in terms of its crystalline, plastic and metallic components can still be improved. Liquid HF or 'wet etching' has proved very effective in making a channel, but using HF in a vapour or 'dry etching' could allow the user greater control of the etching reaction, although at the cost of increased potential health hazard and financial cost. Additionally, the cuvette holder could be better engineered to only allow a certain degree of compression, stopping the possibility of over-tightening when assembling the cuvette. This would serve to make the instrument more user-friendly and prevent accidental damage to the instrument.

Automated multi-sample circular dichroism (AMS CD) was developed in order to take better advantage of the rapid data acquisition times afforded by chiro-optical spectroscopic methods. In this work a capillary optic was coupled to an

HPLC auto-sampler, which acted as both sample-loader and pumping mechanism. This leads to an increased number of samples that can be analysed for the user, as well as opening up a host of potential new applications for the CD user, not least the possibility of using CD as a means of screening refolding buffers for proteins. A two way syringe pump (SSI) has been compared in effectiveness to a push-only pumping system (QF). Whilst effective as qualitatively assessing the CD of samples, the push only system does not deliver a CD spectrum that can be fully relied upon quantitatively. By comparison, the two way pump system can be used to acquire quantitative CD spectra, as well as permitting sample reclamation and cleaning. Finally, the two way system can be adapted to accept multiple sizes of plate, including 384-well plates. The development of this technology allows the CD user to acquire multiple data sets after a relatively small set-up time, freeing up user time from data acquisition.

The AMS-CD instrument has great potential as a method of sample loading for chiro-optical spectroscopy, where its sample pumping can be used to both load samples for CD and align samples for LD.

In this work the potential of generating LD signals from living organisms has been explored as a new and exciting area of research for LD. The successful acquisition of the first confirmed LD signal from a bacterium allows for the possibility of real time analysis of bacteria through LD, enabling the study of interactions between the bacteria and chemical agents, including antibiotics. The first confirmed LD spectrum of flagella has also been collected, confirming that the LD signal of the bacterium in question, *Bacillus Subtilis* originates from the bacterium itself under Couette flow conditions. Additionally, linear flow has been successfully employed to align samples of the bacteria- this can be used to generate bacterial LD signal by aligning the flagella of the bacteria in flow. This opens up the possibility of a new form of LD device that uses re-circulating linear flow to align samples.

Future work

The ultimate goal of the project at the beginning was to develop a low volume, multi-sample CD and LD instrument that could take advantage of future designs of spectropolarimeter, whilst opening new applications for current CD and LD users. Each part of the thesis was originally focused on this goal, with the intention of developing each component of the final instrument individually as a stand-alone work, before bringing each separate component together to form a cohesive whole. However, due in part to funding constraints work could not go ahead as planned. This thesis should however provide an excellent template for carrying this work forward. Future work would primarily involve coupling the etched cell device to the SSI AMS-CD instrument. This combination would further reduce sample volumes in comparison to the capillary and has a greater flexibility of potential path-lengths. Using a focusing lens set on an adjustable base-plate this device could combine together both high quality CD spectra and multiple sample automation. Additionally, the low volumes required would widen the potential applications as sample size would no longer prove such a limitation.

For this application, it is very important to construct the optical elements from quartz rather than CaF_2. Whilst CaF_2 offers excellent transmission of light, it has several issues that make it unsuitable for this application. CaF_2 is slightly soluble in water at a solubility of 0.0015g / 100 ml water at 18 ºC. Whilst this is not an issue for standard CaF_2 cuvettes, this level of solubility will spoil the surface finish of an etched cuvette and thus make it both less accurate and less easy to assemble. The etched cuvette can only function effectively if the very high degree of surface flatness is maintained – any solubility of the material would introduce surface damage and a loss of the optical qualities of the cell. In this instance, the issue is not so much the sample degrading the cuvette as the required wash steps to ensure the cuvette would be clean between each sample. Additionally, CaF_2 is soluble in mineral acids and ammonium salts, both of which encountered during protein CD analysis. Quartz encounters none of these issues.

CaF_2 is also very brittle, which could lead the ground corners of the etched channel to break. These shards could cause a great deal of surface damage to the cuvette, detrimentally affecting the performance of the cuvette.
Finally, CaF_2 is not ideal for flow through spectroscopy. Cuvette design will have to sufficiently flexible to allow for these new methods. With lots of samples flowing through the cell, solubility, sensitivity to different chemical environments and robustness of material will become increasingly more important concerns in cuvette design.
The etched cuvette as an optical device offers another benefit. As the area of the etched cuvette is very small, it would be relatively easy to fit within the instrument a Peltier temperature control system. By coiling the sample line excellent contact could be made between the fluids within the system and the Peltier chip. As such, applications that require rapid heating and cooling such as PCR and kinetic measurements would be very easy to achieve. Finally the relatively small path-lengths of the etched cuvette should be excellent for aligning LD samples under linear flow conditions- relatively low flow rates should be able to effectively align samples, although care must be taken to avoid introducing LD artefacts into CD spectra when using this method.

Appendix 1- Capillary circular dichroism paper

CHIRALITY 22:E136–E141 (2010)

Capillary Circular Dichroism

DANIEL E. WALDRON,[1] RACHEL MARRINGTON,[2] MARCUS C. GRANT,[1] MATTHEW R. HICKS,[1] AND ALISON RODGER[1]*
[1]*Department of Chemistry, University of Warwick, Coventry, United Kingdom*
[2]*Department of Clinical Biochemistry and Immunology, Birmingham Heartlands Hospital, Birmingham, United Kingdom*

Contribution to the CD ISBC 2009 special issue

ABSTRACT Circular dichroism (CD) has become an increasingly important tool in the study of biological molecules as it enables structural information to be obtained non-destructively on solution-phase samples. However, sample requirements for CD are often seen as being too high with protein backbone measurements in standard cuvettes typically requiring ~100–300 μL of 0.1 mg/ml protein. To address this issue, we have designed a new form of CD sample holder, which reduces the sample requirements of the technique by two orders of magnitude, with a sample requirement of less than 3 μl. This sample saving has been achieved through the use of extruded quartz capillaries, the sample being held within the internal diameter of the quartz capillary through capillary action. The extruded quartz capillaries exhibit remarkably little birefringence, although still transmitting high energy UV circularly polarized light. The optics associated with capillaries were investigated. A configuration has been adopted with the light beam of the spectrophotometer being focused in front of the front face of the capillary using a biconvex lens and advantage being taken of the additional focusing effect of the capillary itself. The focusing is vital to the low wavelength performance of the cell, where we have acquired reliable data down to 180 nm using a Jasco J-815 spectrophotometer. The system performance was validated with Na[Co(EDDS)].H_2O (EDDS = *N,N*-ethylenediaminedisuccinic acid), concanavalin A, lysozyme, and progesterone. *Chirality 22:E136–E141, 2010.* © 2010 Wiley-Liss, Inc.

KEY WORDS: circular dichroism; capillary circular dichroism; low-sample volume; capillary; Na[Co(EDDS)].H_2O

INTRODUCTION

Circular dichroism (CD) is a form of spectroscopy that uses circularly polarized light to probe the structure of molecules. To have a CD spectrum in the solution phase, a molecule must have absorption bands in the wavelength range of interest and must be chiral. CD is not limited to molecules in a particular size-range or solvent environment. It is a technique particularly suited to the analysis of biological macromolecules, because a CD spectrum can be obtained in ~10 min, with data analyzed as quickly to give secondary structure information about proteins and nucleic acids.[1,2] This rapidity of acquisition and analysis has resulted in CD becoming adopted across the world in biological laboratories.

CD data are typically collected using flat faced, circular or rectangular quartz cuvettes as the sample holder, or in certain instances CaF_2 cuvettes. This design of cuvette has many things in its favor. First, the optical qualities of a cuvette are very simple and easy to control: the light passes through four flat interfaces. Optics of this simplicity lead to a well-defined optical path for the light beam. Second, at least in non-demountable cuvettes, sample recovery is straightforward. Finally, the standard quartz cuvette can easily be made in a wide range of path-length range, which enables a correspondingly wide range of sample concentrations to be used. For example, protein backbone CD spectra can be collected from 0.001 mg/ml protein solution (typically 10 cm path-length) up to 10 mg/ml protein solution (typically 0.001 cm).

However, there are a number of issues with currently-used cuvettes for CD, which makes them non-ideal for some applications.

The greatest consideration is that of sample size. A typical rectangular cell of path length 1 mm requires 100–300 μl of 0.1 mg/ml protein (i.e. 10–20 μg) to generate a good quality CD spectrum. In some applications this is not an issue, but in others there is simply not enough protein available to collect a spectrum.

A secondary consideration is that one needs a spectrum of the same solvent/buffer in the same cuvette and with the same parameters. To do this, the cuvette must be cleaned and dried between baseline and analyte samples.

Contract grant sponsors: The Engineering and Physical Sciences Research Council; Contract grant number: EP/D075750/1
*Correspondence to: Professor Alison Rodger, Department of Chemistry, University of Warwick, Coventry, CV4 7AL, United Kingdom.
E-mail: A.Rodger@warwick.ac.uk
Received for publication 21 December 2009; Accepted 14 April 2010
DOI: 10.1002/chir.20878
Published online 1 June 2010 in Wiley Online Library (wileyonlinelibrary.com).

This is a time consuming manual process, which reduces the number of samples that can be analyzed in a given time frame and precludes any option of high throughput data collection, because perfectly matched CD cuvettes are hard to source.

Finally, the problem of sample cross-contamination is an issue. While correct experimental procedure can reduce this possibility, many biomacromolecular samples adhere to quartz enhancing the risk of the previous sample remaining in the cuvette even after cleaning.

These issues, but predominantly the large sample requirements, pose serious limitations on the application of CD spectroscopy in the field of biological research and analysis.

To address these issues, we have therefore developed quartz capillaries as an alternative method of holding the sample in the path of the light beam. The capillaries are formed from high purity fused silica, which is heated till they are molten and poured into capillary molds. The resultant capillary has a very good uniformity (deviation of the outer diameter is a maximum of 50 μm, as determined with a micrometer) and excellent optical qualities, generally free from imperfections. The key to success of the capillaries for CD is that we have found they exhibit remarkably little intrinsic birefringence. Moreover they have the same CD spectrum recorded at different points along the length of the same capillary.

Capillary CD (caCD) offers the potential to use significantly smaller sample volumes, whilst obtaining good quality data. If one replaces a 1 mm rectangular cuvette with a 1 mm internal diameter capillary, the required sample volume can be as small as 3 μL (with care even smaller). However, to be of any use, this requires the light beam to be focused so as to pass only through the sample. The alternative of limiting the light incident on the capillary by heavily masking the beam removes a significant percentage of the photons and results in extremely poor signal to noise ratio data, especially below 200 nm on a bench top instrument.

MATERIALS AND METHODS

Materials

Lysozyme and concanavalin A were purchased from Sigma-Aldrich (Dorset, UK). Medroxyprogesterone acetate was procured from Harsen Jakarta (Indonesia). Na[Co(EDDS)].H_2O (EDDS = *N,N*-ethylenediaminedisuccinic acid) was kindly provided by Prof. Peter Scott, Department of Chemistry at Warwick University.[3] All other chemicals and solvents were of analytical grade purity or higher.

Lengths of extruded quartz capillary of internal diameter ~1.1 mm was purchased from Enterprise-Q (Manchester, UK) before being cut into appropriate lengths at Crystal Precision Optics (Rugby, UK).

Circular Dichroism Spectroscopy

All CD spectra were recorded using a Jasco J-815 spectrophotometer, with standard sized sample compartment, under a nitrogen flow rate of 10 l/min. All spectra reported in this work had high tension (HT) values on the photomultiplier tube below 600 V. We have found that for most applications, if the HT is kept below 600 V, the CD magnitudes follow the Beer Lambert law and the data are reliable. Path-lengths for each sample cell were determined from the absorption option on a Jasco J-815 with the capillary in the capillary holder using K_2CrO_4 (0.002 M, basic solution) whose extinction coefficient is 4830 mol^{-1} dm^3 cm^{-1} at 372 nm.[4]

The path-length used for all cuvette CD spectra was 1 mm. The path-length of the capillaries used to acquire the caCD data was determined to be 1.12, 1.16, and 1.19 mm. The relevant path lengths are noted in figure captions. To facilitate direct comparison between the two sample holders, all caCD spectra shown below have been scaled by dividing the magnitude of the CD signal by a factor of the appropriate path length of the capillary used in the experiment.

The wavelength range for data acquisition is indicated in the spectra. Other parameters are as follows:

Band width	1 nm
Response	1 sec
Sensitivity	Standard
Data pitch	0.2 nm
Scanning speed	100 nm/min
Accumulation	16
Temperature	Room temperature

Loading the Capillary

The capillaries used in this work for caCD are extruded quartz cylinders ~4 cm in length with an aperture at both ends of the cylinder. The external diameter of the cylinder is 3 mm, and the internal diameter is 1.12–1.19 mm. To load samples into the capillary into the correct position and without bubbles, a gel-loading tip was "piggy-backed" onto a standard Gilson P100 tip. This enables a combination of the depth penetration of a gel-loading tip with the accuracy and sample size of a standard pipette tip.

When loading the sample into the capillary using the "piggy-back" method, the tip of the pipette is placed against one of the internal walls of the capillary. As the sample is injected into position, the tip is moved around the capillary, which facilitates capillary action, holding the sample in position with aqueous samples. Practice and careful measurement of the light beam position is required for experiments with small sample volumes to ensure a minimum volume sample is correctly located so the entire beam passes through sample. When the sample has been loaded, if one aperture (or both) of the capillary is capped with Blu-Tack® or another suitable Bingham plastic/nylon bung, the sample remains *in situ* for extended periods of time. If a cap is not used, a very slow drift of the sample downward is observed. Removal of the cap after data collection enables the capillary to be cleaned by flowing solutions through it, which is significantly easier than the process required for a normal cuvette.

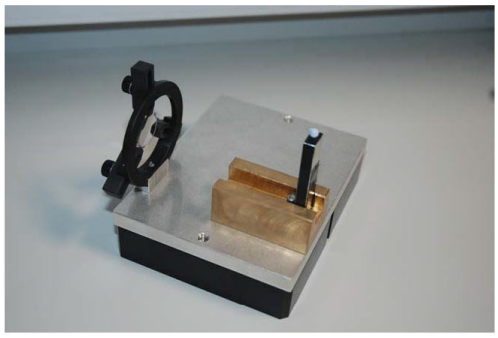

Fig. 1. Picture of the caCD cell holder showing focusing lens holder on the left with 10 cm focal length lens designed to focus green light 1.5 mm in front of the front face of the capillary. The capillary holder is on the right. The sizes of the aperture in front of the capillary and behind it are both 1.2 mm wide with a 1 mm gap between the aperture and capillary.

RESULTS AND DISCUSSION

Design of caCD Cell-holder

The caCD cell-holder was designed to minimize the number of additional optical components within the instrument, because each optical component within the light beam of the spectrophotometer causes some loss of photon flux by reflection. The capillaries, in addition, scatter light significantly more than flat-faced cuvettes. Scattering is minimized by ensuring that only the central core of the light beam is incident on the central part of the capillary. Thus caCD requires some element of masking of the light beam to remove scattering components. Unfortunately, any masking does reduce the photon flux.

Attempts to use a nonfocused light beam with the capillary proved ineffective as too much light was lost resulting in poor signal to noise ratio. As a result, it was decided to employ a double (or bi) convex focusing lens (DCX) of focal length 10 cm as a means of focusing the light effectively onto the capillary. It quickly became apparent that the capillary itself is also a key component of the optical properties of the system not merely a sample holder. The optics of a capillary are very complex, with different entry points into the capillary leading to different light paths through the sample and to the detector. As a general rule, light passing through the internal bore of a solution-containing capillary (that is to say passing through the sample area), is focused by the capillary, whereas light that travels only through the material of the capillary tends to diverge.

The key features of the design illustrated in Figure 1 are therefore the precise alignment and positioning of the focusing lens relative to the capillary holder. By placing the focal point of the lens in Figure 2, just before the light beam enters the capillary (1.5 mm before at 550 nm, but see below), we have managed to take advantage of the optics of the capillary itself to refocus the light beam and produce an exit beam that is sufficiently collimated (Fig. 2) to allow collection of the light by the detector and removes the need for any collecting optics after the capillary holder. The distance from the capillary to the detector

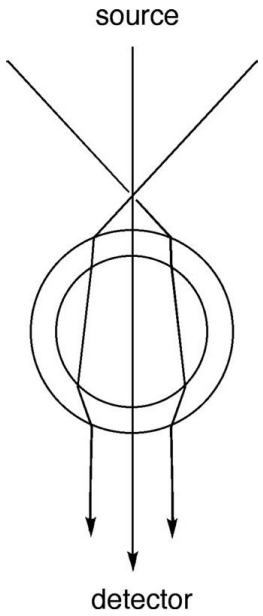

Fig. 2. The path of light through the capillary showing a slightly divergent beam incident on the capillary (top) exiting the capillary as a more collimated beam.

was kept as small as possible. This situation contrasts with the early phases of this work (which were undertaken with the larger Jasco sample compartment) where the distance from capillary to detector was longer and a post-sample collecting lens was required.

The choice of where to place the focal point of the 10 cm lens was made empirically to obtain the best data over the wavelength range (in the sense of matching standard cuvette data). The combination of DCX lens and the lensing effect of the loaded capillary have an attractive advantage of significantly reducing the effect of the chromatic aberration (wavelength dependence of the focal length of a lens) from the first lens. We found the focal point of the 10 cm lens was within experimental error its nominal value down to 400 nm, but below this point gradually reduced to 8 cm at 225 nm. However, even at 225 nm the post capillary light beam was only 2.5 mm at 1.5 cm after the capillary, that is, only twice the size of the beam at 550 nm.

The lens and capillary holder have been designed to enable the sample to be inserted reproducibly into the light beam of a Jasco spectrophotometer (illustrated in Fig. 1). The size of aperture of the light (*i.e.* the front masking) for the capillary holder is 1.2 mm, with a 1 mm gap between the aperture and the capillary itself. The capillary is also back masked with a 1.2 mm wide slit. This design of caCD cell unit is now commercially available. As empirically shown by the data below, this lens/capillary arrangement, together with the masking to ensure only light passing through the sample is collected, is sufficient

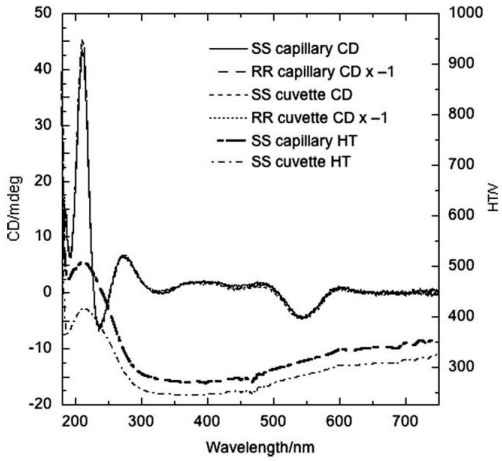

Fig. 3. CD spectra, with HT traces overlaid, of $Na[Co(EDDS)].H_2O$ (0.55 mM in water) in a cuvette (1 mm path length) and capillary (1.12 mm path length, data divided by 1.12 to facilitate comparison). The RR spectra have been multiplied by minus 1.

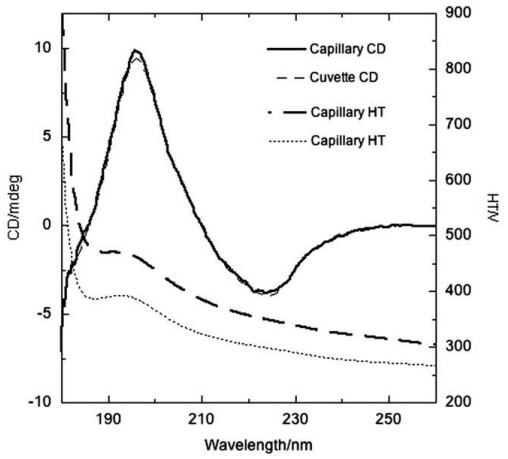

Fig. 4. CD spectra, with HT traces overlaid, of concanavalin A (0.10 mg/ml) in a cuvette (1 mm path length) and capillary (1.19 mm path length, data divided by 1.19 to facilitate comparison).

to enable good quality data to be collected. The quality of data is significantly affected by one's patience in initially ensuring the lens is aligned "perfectly" and the beam exiting a loaded capillary is as small as possible. Once established for a given instrument, this does not have to be changed until the lamp or mirrors are changed, in which case the system may need minor adjusting.

In terms of data collection, the accuracy of the baseline spectrum is as important as the sample spectrum. The orientation of the capillary should be kept the same for the sample and the baseline spectra. In practice, the variation between 500 nm and 200 nm is in fact only ~0.3 mdeg when the capillary is rotated by 90° turns. As this is less than the sample to sample variation often observed with reloading a normal cuvette, it may or may not be important in a given application. In any case, the capillaries used in this work were marked to ensure identical orientation from experiment to experiment.

Circular Dichroism Spectra

A representative selection of CD spectra are shown in Figures 3–6. Three independent repeats of each type of spectrum were collected. The data all overlaid to within the noise envelope of the spectra. Data from caCD and standard cuvettes have been overlaid to illustrate the quality of data that can be produced using quartz capillaries. In each case, the capillary data have been scaled to be equivalent to a 1 mm path length to facilitate comparison. In each case, the HT recorded by the spectrophotometer was kept below 600 V (see below for further discussion of this).

We have recently developed CoEDDS, (EDDS = *N*,*N*-enthylenediaminedisuccinic acid) as a multiple wavelength standard for CD spectroscopy.[3] Both enantiomers are available and it has proved to be an extremely rigorous test of instrument quality both in our laboratory and elsewhere. The spectra in Figure 3 show that the caCD spectra overlay the standard cuvette spectra fairly well over the whole wavelength region for both enantiomers, once path length differences have been accounted for. To make it obvious that both enantiomers give equal magnitude and opposite signed spectra, the RR spectra have been multi-

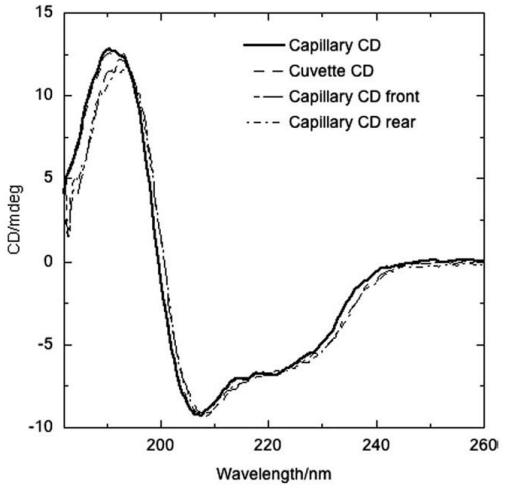

Fig. 5. CD spectra, of lysozyme (0.10 mg/ml) in a cuvette (1 mm path length) and capillary (1.16 mm path length, data divided by 1.16 to facilitate comparison), capillary CD front, denotes CD measured in a cuvette located before a water-filled capillary filled. Similarly, capillary CD rear, denotes a spectrum measured in a cuvette placed after the light beam has passed through a water-filled capillary.

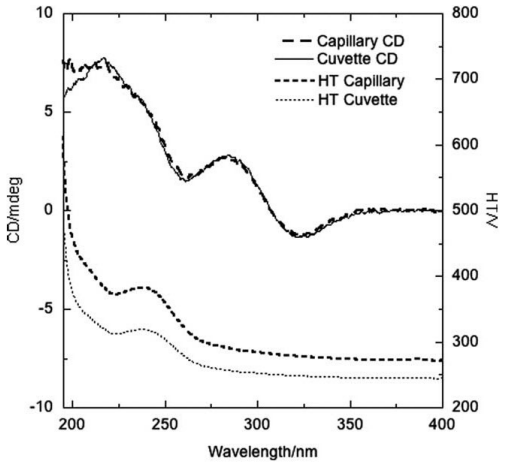

Fig. 6. CD spectra, with HT traces overlaid, of progesterone (0.10 mg/ml) in a cuvette (1 mm path length) and capillary (1.16 mm path length, data divided by 1.16 to facilitate comparison).

plied by −1. The magnitudes of the CoEDDS spectra follow the Beer-Lambert law (data not shown) with a 0.275 mM solution giving signals of half the magnitude of the ones illustrated.

The CD spectra for the largely β-sheet protein concanavalin A 2 are shown in Figure 4. The caCD spectrum is very similar to the standard cuvette data down to 180 nm.

Figure 5 shows a similar situation for the mixed α-helical and β-sheet protein lysozyme. Literature data can be found in references.[5,6] In this case, the data collected in cuvettes but with the capillary unit present and filled with water are also overlaid. The attenuation of these spectra below 190 nm compared with the normal cuvette spectrum coincides with the HT going above 600 V (due to the extra components in the light path). So, these spectra give one confidence that the capillary unit is not significantly distorting spectra at moderate HT voltages.

The spectra for progesterone (Fig. 6) suggest that sharp rises in the HT at low wavelength render the capillary data less reliable.[7] In each case the HT voltage with the capillary is higher than for the cuvette, which does reduce the concentration ranges that can be studied.

CONCLUSION

The aim of this work was to expand the utility of circular dichroism spectroscopy through a reduction of the sample volume required. This reduction has been achieved through the use of extruded quartz capillaries as a means of holding the sample within the light beam. A DCX lens was employed to focus 550 nm light ~1.5 mm in front of the front face of the center of the capillary. This position was used for all wavelengths. The sample-filled capillary acts as a further net focusing lens, resulting in better performance than might be expected given the variation in focal length of the lens with the wavelength of light. The entire ensemble has been designed to fit to an aluminium base-plate suitable for use in a Jasco J-815 spectrophotometer, though could easily be adapted for other spectrometers.

At this stage, our conclusion is that we can collect meaningful caCD data over the accessible wavelength range of our spectrometer (750–180 nm) as long as the sample absorbance is not too high. Any "problem regions" correlate with regions of very high-absorbance where the 600 V "rule" on the photomultiplier tube voltage may give us a false sense of security. Care does need to be taken to ensure data are collected within the validity of the Beer-Lambert law. The capillaries are easier to clean than normal cuvettes as cleaning solutions can be flowed through them.

It has been shown that caCD lowers the sample requirements for CD spectroscopy by a significant margin: 3 μL of 0.1 mg/ml protein samples yield spectra with signal to noise of the same quality as standard flat-faced cuvettes. Less volume could be used but great care is required to ensure that the entire incident light beam goes through the sample.

In addition, the relatively low-cost of the quartz capillary opens up the possibility for single-shot applications, especially for potentially dangerous samples, such as amyloid fibers and other pathogens, and for high throughput methodologies. For such an application, it is possible to load the sample into one end of a capillary and load the solution to be used for the baseline in the other end. The baselines of both ends of a capillary are very similar if not identical. A possibility here is to have the achiral potassium chromate as the baseline solution and use the CD machine absorbance conversion to determine the absorbance of the chromate, and hence the path length of the capillary. This would restrict the available wavelength range of the baseline to being above ~190 nm.

ACKNOWLEDGMENTS

A preliminary account of this work was presented at the 12th International Conference on Circular Dichroism and 5th Interdisciplinary Symposium on Biological Chirality (CD-ISBC 2009) hosted at the University of Brescia, Italy. All CD spectra were acquired at the University of Warwick. This work was generously supported by the Engineering and Physical Sciences Research Council (EPSRC). The assistance of Dr David Josey and Mr Rhoderick Mortimore with engineering and design are gratefully acknowledged. The extremely helpful comments from the referees have significantly improved this article.

LITERATURE CITED

1. Hennessey JP, Johnson CW. Information content in the circular dichroism of proteins. Biochemistry 1981;20:1085–1094.
2. Whitmore L, Wallace BA. DICHROWEB: an online server for protein secondary structure analyses from circular dichroism spectroscopic data. Nucleic Acids Res 2004;32:W668–W673.

3. Damianoglou A, Crust EJ, Hicks MR, Howson SE, Knight AE, Ravi J, Scott P, Rodger A. A new reference material for UV-visible circular dichroism spectroscopy. Chirality 2008;20:1029–1038.
4. Haupt GW. An alkaline solution of potassium chromate as a transmittancy standard in the ultraviolet. J Res Natl Bur Stand 1952;48:414–423.
5. Tanaka F, Forester LS, Pal PK, Rupley JA. The circular dichroism of Lysozyme. J Biol Chem 1975;250:6977–6982.
6. Miles AJ, Wallace BA. Synchrotron radiation circular dichroism spectroscopy of proteins and applications in structural and functional genomics. Chem Soc Rev 2006;35:39–51.
7. Barrett MW, Farrant RD, Kirk DN, Marsh JD, Sanders JKM, Duax WL. The solution conformation of 17-acetoxy-6-methylprogesterone (medroxyprogesterone acetate): use of circular dichroism, nuclear overhauser effect difference and two-dimensional J spectroscopy. J Chem Soc Perkin transactions II 1982;105–110.

Appendix 2- Mohs scale of hardness

The Mohs scale of hardness is a measure of scratch resistance, based on ten naturally occurring minerals. Created in 1812 by a German mineralogist Friedrich Mohs, the hardness of a given material is calculated by finding the hardest mineral that the mineral can scratch, as well as the softest mineral that can scratch the material.

Mineral	Mohs Hardness	Absolute Hardness	Image
Talc **$H_4Mg_3Si_4O_{10}(OH)_2$**	1	1	
Gypsum **$CaSO_4.2H_2O$**	2	3	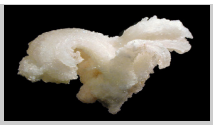
Calcite **$CaCO_3$**	3	9	
Fluorite **CaF_2**	4	21	
Apatite **$Ca_5(PO_4)_3(OH\text{-}, Cl\text{-}, F\text{-})$**	5	48	
Orthoclase Feldspar **$KAlSi_3O_8$**	6	72	
Quartz **SiO_2**	7	100	
Topaz **$Al_2SiO_4(OH\text{-}, F\text{-})_2$**	8	200	
Corundum **Al_2O_3**	9	400	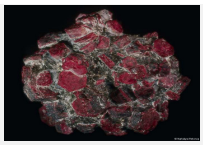
Diamond **Carbon Allotrope**	10	1600